THESIS APPROVAL

GRADUATE SCHOOL, KASETSART UNIVERSITY

Doctor of Engineering (Chemical Engineering)

DEGREE

Chemical Engineering | Chemical Engineering

FIELD | **DEPARTMENT**

TITLE: Production of L-Phenylalanine from Glycerol by a Recombinant *Escherichia coli*

NAME: Mr. Methee Khamduang

THIS THESIS HAS BEEN ACCEPTED BY

THESIS ADVISOR

(Associate Professor Penjit Srinophakun, Ph.D.)

THESIS CO-ADVISOR

(Assistant Professor Kanoktip Packdibamrung, Ph.D.)

THESIS CO-ADVISOR

(Assistant Professor Jarun Chutmanop, D.Eng.)

DEPARTMENT HEAD

(Associate Professor Phungphai Phanawadee, Ph.D.)

APPROVED BY THE GRADUATE SCHOOL ON _____

DEAN

(Associate Professor Gunjana Theeragool, D.Agr.)

THESIS

PRODUCTION OF L-PHENYLALANINE FROM GLYCEROL BY A RECOMBINANT *Escherichia coli*

METHEE KHAMDUANG

A Thesis Submitted in Partial Fulfillment of
the Requirements for the Degree of
Doctor of Engineering (Chemical Engineering)
Graduate School, Kasetsart University
2009

Methee Khamduang 2009: Production of L-Phenylalanine from Glycerol by a Recombinant *Escherichia coli*. Doctor of Engineering (Chemical Engineering), Major Field: Chemical Engineering, Department of Chemical Engineering. Thesis Advisor: Associate Professor Penjit Srinophakon, Ph.D. 152 pages.

L-phenylalanine was produced by *Escherichia coli* BL21(DE3) using glycerol as a substrate. This work can be divided into two parts, the investigation of the composition of the major nutrients and the operational variables effect in the stirred-tank bioreactor. Statistical method (central composite design) was used to design the optimal nutrient composition for the biomass and L-phenylalanine productions. It was found that the optimum medium for the biomass production comprised of 10 g/L glycerol and $(NH_4)_2SO_4$, 0.98 g/L $MgCl_2$, 2.94 g/L K_2HPO_4 and KH_2PO_4, 0.878 g/L yeast extract and 0.0878 g/L thiamine-HCL at the maximum biomass weight of 5.0 g DCW/L. While as 10 g/L glycerol, 100 g/L $(NH_4)_2SO_4$, 0.64 g/L $MgCl_2$, 1.91 g/L K_2HPO_4 and KH_2PO_4, 0.823 g/L yeast extract and 0.0823 g/L thiamine-HCl was the optimum medium for the L-phenylalanine production which gave the highest L-phenylalanine weight of 6.2 g/L.

The stirred-tank bioreactor (2.0 L working volume) was used to investigate the effect of the operational variables on the biomass and L-phenylalanine productions. Fermentations were carried out at 37 °C, pH 7.4, using a defined medium at the agitation speeds of 300-500 rpm and the aeration rates of 2-8 L/min. Under the optimum operating condition at 400 rpm agitation rate, 4 L/min aeration rate, the highest L-phenylalanine productivity of 0.198 g/L.h was produced. While the highest biomass productivity of 0.428 g/L.h was produced at 8.0 L/min. Finally, the fed-batch fermentation was performed to obtain the biomass and L-phenylalanine productions. It was found that the highest biomass and L-phenylalanine concentrations occurred at 72 hour (11.33 g/L) and 60 hour (6.5 g/L), respectively.

_____ / / _____

Student's signature Thesis Advisor's signature

ACKNOWLEDGEMENTS

I would sincerely like to acknowledge the efforts of many people who have contributed to this work. This thesis could not be achieved without their following assistance, my thesis advisor Associate Professor Dr. Penjit Srinophakun for her generous advice, skillful assistance, technical helps, guidance, encouragement, supports and stimulated discussions through the period of my study.

Sincere thanks and appreciation are due to Assistant Professor Dr. Jarun Chutmanop and Assistant Professor Dr. Kanoktip Packdibamrung who are served as the members of the doctoral thesis committees, their helpful suggestions and comments.

I also would like to thank Professor Dr. Yusuf Chisti, School of Engineering, Massey University, Palmerston North, New Zealand for sharing fruitful experiences and discussion.

I would link to extend my heart-felt thank to my parents for their love and support during the years of my education, and I would like to thank all of my friends for their help particularly during my experiment. I also would like to thank Miss Paweena Aramrattana for her great help, taking care, understanding and encouragement.

Finally, I would like to thank the scholarship and financial support from Kasetsart University Research Development Institute, and the Center of Excellence for Petroleum, Petrochemicals and Advanced Materials, S&T Postgraduate Education and Research Development Office (PERDO).

Methee Khamduang

June 2009

TABLE OF CONTENTS

Page

TABLE OF CONTENTS i
LIST OF TABLES ii
LIST OF FIGURES iv
LIST OF ABBREVIATIONS xi
INTRODUCTION 1
OBJECTIVES 4
LITERATURE REVIEW 5
MATERIALS AND METHODS 48
Materials 48
Methods 50
RESULTS AND DISCUSSION 60
Screening experiments by one-factor-at-a-time technique 60
Optimization of fermentation media by RSM 64
Optimization of agitation and aeration rates in batch fermentation 79
The study of fed-batch fermentation 102
CONCLUSIONS AND RECOMMENDATIONS 106
LITERATURE CITED 108
APPENDICES 126
Appendix A Media formula 127
Appendix B Assay methods 130
Appendix C Standard graphs 133
Appendix D HPLC chromatogram of the L-phenylalanine 137
Appendix E Bioreactor and instruments 139
Appendix F Raw data 142
CURRICULUM VITAE 152

LIST OF TABLES

Table		Page
1	Physiological functions of the principal elements	12
2	Typical variables in a Fermentation	17
3	Advantages and disadvantages of RSM	18
4	The exponent on P_g / V varied with scale	35
5	Levels of variables used in the experimental design	53
6	Experimental plan of the optimization design	54
7	Experimental plan of the optimization design with the experimental and predicted values for the biomass and L-phenylalanine production of recombinant *E.coli* BL21(DE3) cells in different media	65
8	Model coefficient estimated by multiplies linear regression	67
9	ANOVA for full quadratic model	69

Appendix Table

A1	Luria-Bertani (LB) medium	128
A2	Basal salts, trace salts and vitamins solution	128
A3	Biomass fermentation medium	129
A4	L-phenylalanine fermentation medium	129
C1	Biomass concentration calibration data	134
C2	L-phenylalanine concentration calibration data	135
C3	Glycerol concentration calibration data	136
F1	Raw data of screening experiments by one-factor-at -a-time technique (Effect of glycerol concentration)	143
F2	Raw data of screening experiments by one-factor-at -a-time technique (Effect of $(NH4)_2SO_4$ concentration)	143
F3	Raw data of screening experiments by one-factor-at -a-time technique (Effect of pH)	144

LIST OF TABLES (Continued)

Appendix Table		Page
F4	Raw data of screening experiments by one-factor-at -a-time technique (Effect of temparature)	144
F5	Raw data of optimization of fermentation media by RSM	145
F6	Raw data of optimization for agitation rate in batch fermentation (Aeration rate was fixed at 4.0 L/min.)	146
F7	Raw data of optimization for aeration rate in batch fermentation (Agitation rate was fixed at 400 rpm.)	148
F8	Raw data comparison of biomass and L-phenylalanine production during batch fermentation under optimized medium by RSM and basal medium	150
F9	Raw data of fed-batch fermentation	151

LIST OF FIGURES

Figure		Page
1	Basic scheme for biodiesel production	6
2	Transesterification reaction of a triglyceride	6
3	Sample of one-variable-at-a-time approach (contour plot of yield)	15
4	Characteristic growth curve of a microorganism in batch culture	19
5	Growth associated product formed during the period of active culture growth	21
6	Nongrowth associated product formed during the period of nonculture growth (stationary phase)	21
7	Different feeding regimes in fed-batch processes	26
8	The film theory for mass transfer	31
9	The effect of air-flow rate on the k_La of an agitated aerated vessel	35
10	Different patterns of gas bubble dispersion in a stirred-tank reactor	36
11	Mechanism of uptake and initial enzymatic reactions in the microbial metabolism of glycerol	38
12	Fermentative patterns of glycerol dissimilation dependent on 1,3-PDO formation	40
13	Overview of some possible end products for different microorganisms during glycerol degradation	42
14	Chemical structure of L-phenylalanine	45
15	Catabolism in *E. coli*	47
16	Schematic of experimental set up	57
17	Effect of glycerol concentration on cell growth at 20 g/L $(NH_4)_2SO_4$	61
18	Effect of ammonium sulfate concentration on cell growth at 80 g/L glycerol	61
19	Effect of temperature on cell growth	62
20	Effect of pH on cell growth	63

LIST OF FIGURES (Continued)

Figure		Page
21	Effect of pH changed during batch fermentation on recombinant *E. coli* BL21(DE3) growth at 37 °C and 200 rpm on bioreactor 3.3 litter	64
22	Compared plot between predicted biomass (a) and L-phenylalanine concentration (b) (Equation 13 and 14) and experimental data (Table 7)	68
23	Response surface and contour plot of glycerol, $(NH_4)_2SO_4$ and biomass production at constant salts and vitamins concentrations	71
24	Response surface and contour plot of glycerol, salts and biomass production at constant $(NH_4)_2SO_4$ and vitamins concentrations	71
25	Response surface and contour plot of salts, vitamins and biomass production at constant glycerol and $(NH_4)_2SO_4$ concentrations	72
26	Response surface and contour plot of $(NH_4)_2SO_4$, vitamins and biomass production at constant glycerol and salts concentrations	72
27	Response surface and contour plot of $(NH_4)_2SO_4$, salts and biomass production at constant glycerol and vitamins concentrations	73
28	Response surface and contour plot of glycerol, vitamins and biomass production at constant $(NH_4)_2SO_4$ and salts concentration	73
29	Response surface and contour plot of glycerol, $(NH_4)_2SO_4$ and L-phenylalanine production at constant at constant salts and vitamins concentration	74
30	Response surface and contour plot of glycerol, vitamins and L-phenylalanine production at constant salts and $(NH_4)_2SO_4$ concentration	75
31	Response surface and contour plot of glycerol, salts and L-phenylalanine production at constant vitamins and $(NH_4)_2SO_4$ concentration	75

LIST OF FIGURES (Continued)

Figure		Page
32	Response surface and contour plot of $(NH_4)_2SO_4$, vitamins and L-phenylalanine production at constant glycerol and salts concentration	76
33	Response surface and contour plot of $(NH_4)_2SO_4$, salts and L-phenylalanine production at constant glycerol and vitamins concentration	77
34	Response surface and contour plot of salts, vitamins and L-phenylalanine production at constant glycerol and $(NH_4)_2SO_4$ concentration	78
35	Time course of recombinant *E. coli* BL21(DE3) biomass and L-phenylalanine productions during batch fermentation comparing of optimized (RSM) and basal media	79
36	Biomass, L-phenylalanine, glycerol, $(NH_4)_2SO_4$ and dissolved oxygen profiles during culture of recombinant *E. coli* BL21(DE3) at the agitation rate of 200 rpm, and constant at 4.0 L/min aeration rate and pH 7.4	80
37	Biomass, L-phenylalanine, glycerol, $(NH_4)_2SO_4$ and dissolved oxygen profiles during culture of recombinant *E. coli* BL21(DE3) at the agitation rate of 300 rpm, and constant at 4.0 L/min aeration rate and pH 7.4	81
38	Biomass, L-phenylalanine, glycerol, $(NH_4)_2SO_4$ and dissolved oxygen profiles during culture of recombinant *E. coli* BL21(DE3) at the agitation rate of 400 rpm, and constant at 4.0 L/min aeration rate and pH 7.4	82

LIST OF FIGURES (Continued)

Figure		Page
39	Biomass, L-phenylalanine, glycerol, $(NH_4)_2SO_4$ and dissolved oxygen profiles during culture of recombinant *E. coli* BL21(DE3) at the agitation rate of 500 rpm, and constant at 4.0 L/min aeration rate and pH 7.4	84
40	Comparison of biomass production during culture of recombinant *E. coli* BL21(DE3) at different agitation rates of 200 rpm, 300 rpm, 400 rpm and 500 rpm and constant at 4.0 L/min aeration rate and pH 7.4	85
41	Comparison of L-phenylalanine production during culture of recombinant *E. coli* BL21(DE3) at different agitation rates of 200 rpm, 300 rpm, 400 rpm and 500 rpm and constant at 4.0 L/min aeration rate and pH 7.4	86
42	Comparison of dissolved oxygen during culture of recombinant *E. coli* BL21(DE3) at different agitation rates of 200 rpm, 300 rpm, 400 rpm and 500 rpm and constant at 4.0 L/min aeration rate and pH 7.4	87
43	Comparison of biomass productivities during culture of recombinant *E. coli* BL21(DE3) at different agitation rates of 200 rpm, 300 rpm, 400 rpm and 500 rpm and constant at 4.0 L/min aeration rate and pH 7.4	88
44	Comparison of L-phenylalanine productivities during culture of recombinant *E. coli* BL21(DE3) at different agitation rates of 200 rpm, 300 rpm, 400 rpm and 500 rpm and constant at 4.0 L/min aeration rate and 7.4 pH	90
45	Specific growth rate of cell at various impeller agitation rates at a fixed aeration rate of 4.0 L/min	91

LIST OF FIGURES (Continued)

Figure		Page
46	Biomass, L-phenylalanine, glycerol, $(NH_4)_2SO_4$ and dissolved oxygen profiles during the culture of recombinant *E. coli* BL21(DE3) at 2.0 L/min aeration rate, and constant at 400 rpm agitation rate and pH 7.4	92
47	Biomass, L-phenylalanine, glycerol, $(NH_4)_2SO_4$ and dissolved oxygen profiles during the culture of recombinant *E. coli* BL21(DE3) at 4.0 L/min aeration rate, and constant at 400 rpm agitation rate and pH 7.4	93
48	Biomass, L-phenylalanine, glycerol, $(NH_4)_2SO_4$ and dissolved oxygen profiles during the culture of recombinant *E. coli* BL21(DE3) at 6.0 L/min aeration rate, and constant at 400 rpm agitation rate and pH 7.4	94
49	Biomass, L-phenylalanine, glycerol, $(NH_4)_2SO_4$ and dissolved Oxygen profiles during the culture of recombinant *E. coli* BL21(DE3) at 8.0 L/min aeration rate, and constant at 400 rpm agitation rate and pH 7.4	95
50	Comparison of biomass production during culture of recombinant *E. coli* BL21(DE3) at different aeration rates of 2.0 L/min, 4.0 L/min, 6.0 L/min and 8.0 L/min and constant at 400 rpm agitation rate and pH 7.4	97
47	Biomass, L-phenylalanine, glycerol, $(NH_4)_2SO_4$ and dissolved oxygen profiles during the culture of recombinant *E. coli* BL21(DE3) at 4.0 L/min aeration rate, and constant at 400 rpm agitation rate and pH 7.4	93

LIST OF FIGURES (Continued)

Figure		Page
51	Comparison of L-phenylalanine production during culture of recombinant *E. coli* BL21(DE3) at different aeration rates of 2.0 L/min, 4.0 L/min, 6.0 L/min and 8.0 L/min and constant at 400 rpm agitation rate and pH 7.4	98
52	Comparison of dissolved oxygen during culture of recombinant *E. coli* BL21(DE3) at different aeration rates of 2.0 L/min, 4.0 L/min, 6.0 L/min and 8.0 L/min and constant at 400 rpm agitation rate and pH 7.4	99
53	Comparison of biomass productivities during culture of recombinant *E. coli* BL21(DE3) at different aeration rates of 2.0 L/min, 4.0 L/min, 6.0 L/min and 8.0 L/min and constant at 400 rpm agitation rate and pH 7.4	100
54	Comparison of L-phenylalanine productivities during culture of recombinant *E. coli* BL21(DE3) at different aeration rates of 2.0 L/min, 4.0 L/min, 6.0 L/min and 8.0 L/min and constant at 400 rpm agitation rate and pH 7.4	101
55	Specific growth rate of biomass at various aeration rates. All data were obtained at a fixed agitation rate of 400 L/min	102
56	Biomass, L-phenylalanine, glycerol, $(NH_4)_2SO_4$ and dissolved oxygen profiles during fed-batch fermentation of recombinant *E. coli* BL21(DE3) at aeration rate of 8.0 L/min (0-12 h and 60-72 h) and 4.0 L/min (12-60 h), and constant at 400 rpm agitation rate and pH 7.4	104
57	Biomass and L-phenylalanine productivities during fed-batch fermentation of recombinant *E. coli* BL21(DE3) at aeration rate of 8.0 L/min (0-12 h and 60-72 h) and 4.0 L/min (12-60 h), and constant at 400 rpm agitation rate and pH 7.4	105

LIST OF FIGURES (Continued)

Appendix Figure		Page
C1	Biomass concentration calibration curve	134
C2	L-phenylalanine concentration calibration curve	135
C3	Glycerol concentration calibration curve	136
D4	HPLC chromatogram of the L-phenylalanine production from recombinant *E. coli* BL21(DE3) at 0.7 mL/min flow rate	138
D1	HPLC chromatogram of the L-phenylalanine production from recombinant *E. coli* BL21(DE3) at 1.0 mL/min flow rate	138
E1	3.3 L BioFio III reactor (New Brunswick Scientific, USA) with controller	140
E2	Air pump	141
E3	Water cooler	141

LIST OF ABBREVIATIONS

ANOVA	=	analysis of variance
° C	=	degree Celsius
CCD	=	central composite design
cm	=	centimeter
D_i	=	diameter of impeller
DCW	=	dry cell weight
DNA	=	deoxyribonucleic acid
DO	=	dissolved oxygen
D_T	=	diameter of tank
DW	=	deionized water
G	=	glycerol
GN	=	glycerol interaction with $(NH_4)_2SO_4$
GS	=	glycerol interaction with salts
GV	=	glycerol interaction with vitamins
g	=	gram
h	=	hour
HPLC	=	high performance liquid chromatography
ID	=	identical diameter, centimeter
L	=	liter
LB	=	Luria-Bertani
µg	=	microgram
µm	=	micrometer
µl	=	microliter
µmol	=	micromole
M	=	mole per liter (molar)
mg	=	milligram
min	=	minute
ml	=	milliliter
N	=	$(NH_4)_2SO_4$

LIST OF ABBREVIATIONS (Continued)

NS	=	$(NH_4)_2SO_4$ interaction with salts
NV	=	$(NH_4)_2SO_4$ interaction with vitamins
ng	=	nanogram
nm	=	nanometer
rpm	=	round per minute
RSM	=	response surface method
S	=	salts
SV	=	salts interaction with vitamins
OD	=	optical density
UV	=	ultraviolet
V	=	vitamins
v/v	=	volume by volume
w/w	=	weight by weight

Subscripts

i, *j*	=	Component index

PRODUCTION OF L-PHENYLALANINE FROM GLYCEROL BY A RECOMBINANT *Escherichia coli*

INTRODUCTION

Since the world has been searching for alternative energy instead of petroleum, with its increasing price, Thailand is one of the countries that has responded to this trend. Biodiesel was selected to be the first alternative energy because it is an abundant resource within the country. Presently, hundreds of thousands of liters of biodiesel are daily produced, not only for commerce, but also for household consumption. In the production process of transesterification, which is a popular dominant reaction, 10-25 percent of the byproduct glycerol is produced, depending on the perfection of the reaction. While comparing the amount produced from this reaction to the amount produced from daily biodiesel production, glycerol is produced more than three to four hundred thousand liters per day (The Department of Alternative Energy Development and Efficiency (DEDE), 2009).

The study of glycerol utilization as an alternative source of carbon in microbial fermentation has become one of the glycerol consumption and interesting value-added methods (Barbiorato *et al*., 1997). Microbial conversion of glycerol has been investigated recently with particular focus on the production of bio-molecules which can be used in medicine, cosmetics and food industries (Paula da Silva *et al*., 2009). The fermentation of glycerol producing amino acid has been studied using *Escherichia coli* groups. The genetically modified *Escherichia coli* BL21(DE3), a high L-phenylalanine producer that can convert various carbohydrates to L-phenylalanine was applied as the model of this study. During the course of the studies, it was found that the recombinant *E. coli* mainly produced L-phenylalanine when glycerol was used as the substrate (Packdibamrung *et al*., 2007).

Generally, statistical experimental design of L-phenylalanine production in the batch fermentation was performed in this study to optimize the medium formulas. Response surface methodology (RSM), which is a collection of statistical techniques for designing experiments, building models, evaluating the effects of factors and searching for the optimum conditions have been successfully used in the optimization of bioprocesses (Nikerel *et al*. 2006; Kwak *et al*. 2006). RSM mainly consists of the central composite design, box-behnken design, one-factor design, D-optimal design, user-defined design, and historical data design. The central composite design (CCD) and the box-behnken design (BBD) are the most popular of response surface design methods, which has 5 levels and 3 levels, respectively for one-numeric factor (Zheng *et al*. 2008; Zain *et al*. 2007; Imandi *et al*. 2006).

Mass transfer processes have a major impact on the growth of microorganisms in industrial fermentations. Nutrients must be continuously replenished in the liquid layers closest to the microorganisms since the microorganisms are constantly consuming them. Nutrients such as glucose or ammonia, presenting as low as 1 mol/L in the fermentation media can cause mass transfer problem (McNeil and Harvey, 2008). For aerobic fermentations, oxygen is required as one of the nutrients. At 30 °C the solubility of oxygen in pure water is 0.236 mmol/L, and the presence of salts and other nutrients (required for the growth of any organism) reduces its solubility (Stanbury *et al*., 1999). Thus, the achievement of high oxygen mass transfer rate is a major challenge in aerobic fermentation.

Oxygen supply is known as an important parameter in aerobic amino acid fermentation (Akashi *et al*., 1979; Ensari and Kim, 2003; Hirose and Shibai, 1980; Hua *et al*., 1998). When organisms are cultured in low dissolved oxygen (DO) of their growth stage, their metabolic activities often differ from those under fully aerobic and anaerobic conditions, due to the changes in their respiration mechanism. These alterable organisms usually possess respiratory enzymes such as dehydrogenases and oxydases and the expression and composition of these enzymes were influenced substantially by environmental dissolved oxygen (Unden and Bongaerts, 1997). The DO concentration or oxygen supply profile were also reported as one of the crucial

factors in optimally regulating metabolic distribution or activities in other fermentation processes such as organic acid (Hua and Shimizu, 1999), bio-polymer (Wang and Inoue, 2001) and polysaccharide productions (Huanga *et al.*, 2006; Tang and Zhong, 2003). Thus, in microbial fermentation, it is crucial to optimize the DO concentration or oxygen supply.

In the present study of CCD methods, RSM was adopt to optimize the levels of medium components that affected the L-phenylalanine production and biomass growth of the recombinant *E. coli* in the batch fermentation. The optimum aeration rate and the agitation rates were investigated for the batch fermentation process aiming to achieve the maximum L-phenylalanine and biomass productions. Based on the results of the optimal aeration and agitation rates, an oxygen supply strategy will be suggested to successfully utilize the substrate and enhance L-phenylalanine production.

OBJECTIVES

1. To optimize the glycerol concentration for culture of *Escherichia coli* BL21(DE3) harboring gene encoding phenylalanine dehydrogenase from *Acinetobacter lwoffii* using statistical methods

2. To study the optimal conditions for L-phenylalanine production in laboratory scale

LITERATURE REVIEW

1. Biodiesel production

Biodiesel is an alternative fuel for diesel engines that is produced chemically from vegetable oils or animal fat and alcohol such as methanol. The reaction requires a catalyst, usually a strong base, such as sodium or potassium hydroxide, and produces new chemical compounds called methyl esters. These esters have come to be known as biodiesel. As its primary feedstock is a vegetable oil or animal fat, biodiesel is generally considered to be renewable. Since the carbon in the oil or fat originated mostly from carbon dioxide in the air from plant photosynthesis, biodiesel is considered to much less contribute to the global warming than fossil fuels.

Diesel engines operated on biodiesel have lower emissions of carbon monoxide, unburned hydrocarbons, particulate matter, and air toxics than when operated on petroleum-based diesel fuel. A scheme of the flow chart of the biodiesel process is given in Figure 1. As can be seen in Figure 1, methanol and KOH are mixed to form methoxide. Then the mixture is transferred to the reactor where transesterrification reaction (Figure 2) between vegetable oils and methoxide are taken place. In Figure 2, the transesterification reaction of a triglyceride with three moles ethanol is utilized NaOH as a catalyst and rendering three moles of biodiesel (ethyl ester) and one mole of glycerol. After completing the reaction, crude biodiesel and crude glycerin are separated at the purification units while methanol dissolving in the crude biodiesel and crude glycerin is recovery and used in the next reaction.

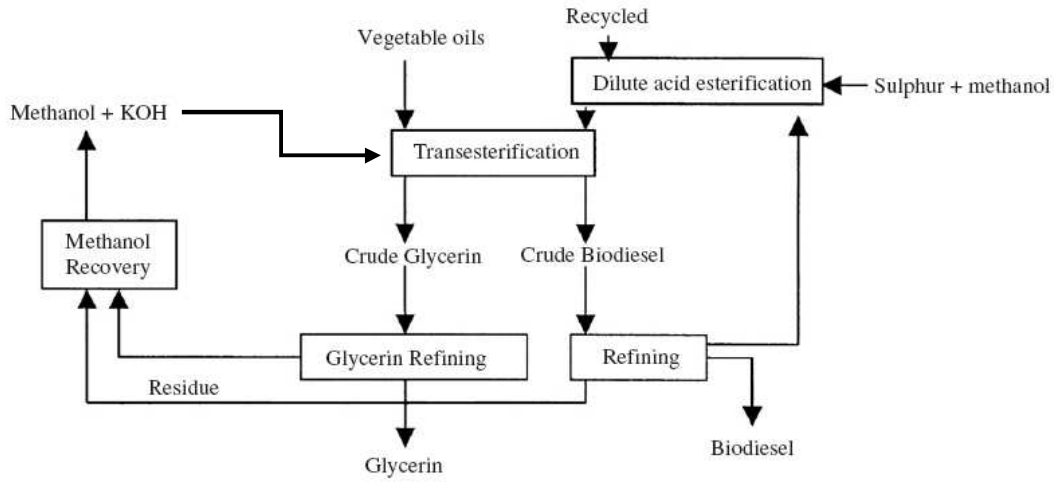

Figure 1 Basic scheme for Biodiesel production

Source: Marchetti *et al.* (2007)

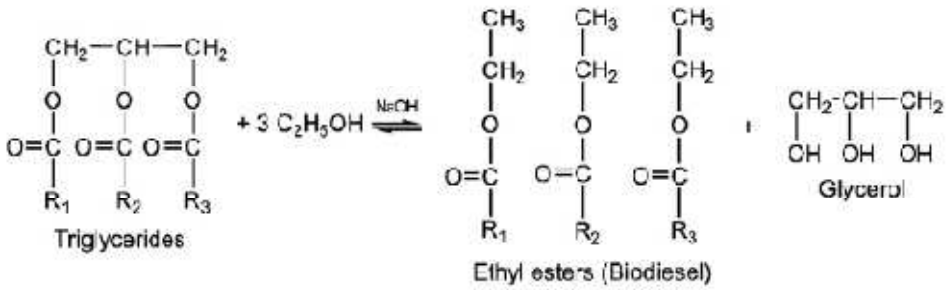

Figure 2 Transesterification reaction of a triglyceride with ethanol (alcoholysis), utilizing NaOH as a catalyst and rendering biodiesel (mixture of fatty acid ethyl esters) and glycerol

Source: Paula da Silva *et al.* (2009)

1.1 Glycerol from biodiesel production

Glycerol can be produced either by microbial fermentation or chemical synthesis from petrochemical feedstock. It can also be recovered from soap manufacturing. In the traditional process of the soap production, glycerol is released as a by-product during the hydrolysis of fats. This process is currently of less importance, since soap has been largely replaced by detergents (Wang *et al*., 2001).

Thailand is one of the countries that has responded to this trend. Biodiesel was selected to be the first alternative energy because of the abundant resources within the country. Biodiesel is produced from vegetable oils and animal fats through transesterification with, for instance, ethanol or methanol (alcoholysis). Generally the reaction is catalyzed by NaOH or KOH and glycerol represents 10% (v/v) of the ester production. (González-Pajuelo *et al*., 2004; Mu *et al.*, 2006; Papanikolaou *et al.*, 2002). Europe mainly uses rapeseed oil for biodiesel production. However, in Brazil, oils from soybean, sunflower, African oil palm (*Elaeis guineensis*), castor oil and *Jatropha curcas* are used. Therefore, in some European countries, the production of glycerol has increased significantly due to biodiesel production. As a consequence, the price of glycerol has fallen and the majority of companies that chemically produced glycerol have been shut down because of the excess glycerol and glycerol price reduction (Deckwer, 1995; Dharmadi *et al*., 2006).

In Europe, some biodiesel companies have severe problems getting rid of the excess glycerol, and disposal cost is quite expensive. The collapse of glycerol prices causes major problems to these companies (Dharmadi *et al*., 2006; Willke and Vorlop, 2004). It is reported that approximately 75–95% of the final costs of biodiesel arise from the cost of raw materials (Yuste and Dorado, 2006). Biodiesel is now widely accepted as a renewable fuel and a major goal for biodiesel production the future will be the one possibility is to use inexpensive or low-cost raw materials, such as vegetable waste cooking oil. (Yuste and Dorado, 2006). The tax exemption for biofuels is another important approach.

Considering the increasing need for renewable fuels throughout the world and the increasing demand and production of biodiesel, an excess of glycerol will be surplus. Since glycerol can be used as a carbon source in industrial microbiology, this by-product adds value to the product chain of the biodiesel industry, and contributes to their competitiveness. Glycerol is presented in many applications in the cosmetic, paint, automotive, food, tobacco, pharmaceutical, pulp and paper, leather and textile industries. It is also used as a feedstock for the production of various chemicals (Wang *et al*., 2001). Glycerol has also been considered as a feedstock for new industrial fermentations in the future (Wang *et al.*, 2001). Thus, one of the many promising applications for the use of glycerol is its bioconversion to high value compounds through microbial fermentation. Glycerol is not only cheap and abundant, but its higher degree of reduction than sugars offers the opportunity to obtain reduced chemicals, such as succinate, ethanol, xylitol, propionate, hydrogen, etc. at higher yields than those obtained from sugars (Dharmadi *et al.*, 2006).

1.2 Thailand biodiesel production

In Thailand, the consumption of crude and petroleum oil, in the year 2000, were around 92 million liter/day (50.57% of total commercially energy consumption); whereas, local crude oil production could supply only 9.2 million liters /day (10% of total consumption of crude and refined oil). Nevertheless, imported crude petroleum oil was around 102 million liters /day worth Bt 285,862 million per annum which is 86% of total commercial energy import. With of the total petroleum energy consumption produced from crude oil, diesel fuel consumption was around 41 million liters /day, which was 49% of total petroleum products (The National Energy Policy Office (NEPO), 2001).

Thailand was the first country to launch biodiesel as a national program on July 10, 2001. It was reported that the work was initiated by the Royal Chitralada Project, a royal sponsored project to help rural farmers. International co-operation among ASEAN country was also starting by the Renewable Energy Institute of Thailand and Asia-Pacific Roundtable for Sustainable consumption. The primary aims

of the project in Thailand are: an alternative output for excess agricultural production and substitution of diesel imports. In 2007, several biodiesel plants were operating in Thailand using the excess palm oil/palm stearin and in some cases, waste vegetable oil as raw materials. The production capacity was about 1 million liter/day and should reach 2 million liter by early 2008. In 2008, about 400 petrol stations are now distributing B5 (5% biodiesel with 95% diesel) in Chiangmai and Bangkok (The Department of Alternative Energy Development and Efficiency (DEDE), 2009). The national biodiesel standard has been developed based on the European and American standard. The target of the Government was to mandate B2 by April 2 2008 and to increase to B5 by 2011 which will require almost 4 million liters/day of biodiesel. Raw material or potential feedstock for biodiesel production in Thailand are palm oil, coconut oil, soy bean oil, ground nut oil, castor oil, sesame oil, sunflower oil and jatropha oil (The Department of Alternative Energy Development and Efficiency (DEDE), 2009).

2. Fermentation processes

The origins of fermentation are lost in ancient history, perhaps even in prehistory. The ancient Egyptians and Sumerians both had knowledge of the techniques used to convert starchy grains alcohol. For most of history these processes, or similar ones based on fruit juice conversion, have represented the most commonly accepted interpretation of the word ‘fermentation’. However, fermentation’ has many different and distinct meanings for differing groups of individuals. In the present context it seems to mean the use of submerged liquid culture of selected strains of microorganisms, plant or animal cells, for the manufacture of some useful products, or to gain insights into the physiology of these cell types. This is a relatively narrow definition, but would include the ‘traditional’ fermentations described above. By contrast, the modern fermentation industry, which is a large product of the Twentieth century, is dominated by aerobic cultivations intended to make a range of higher value products than simple ethanol (McNeil and Harvey, 2008).

2.1 Medium formulation

Not only a source of energy, organisms require a source of materials for biosynthesis of cellular matter and products in cell operation, maintenance and reproduction. These materials must supply all elements necessary to accomplish this. Some microorganisms utilize elements in the form of simple compounds, others require more complex compounds, usually related to the form in which they are ultimately incorporated in the cellular material. The four predominant types of polymeric cell compounds are the lipids (fats), the polysaccharides (starch, cellulose, etc.), the information-encoded polydeoxyribonucleic acid and polyribonucleic acids (DNA and RNA), and proteins (Stanbury *et al*., 1999). Lipids are essentially insoluble in water and can thus be found in the non-aqueous biological phases, especially the plasma and organelle membranes. Lipids also constitute portions of more complex molecules, such as lipoproteins and liposaccharides. Lipids also serve as the polymeric biological fuel storage (McNeil and Harvey, 2008).

Natural membranes are normally impermeable to highly charged chemical species such as phosphorylated compounds. This allows the cell to contain a reservoir of charged nutrients and metabolic intermediates, as well as maintaining a considerable difference between the internal and external concentrations of small cations, such as H^+, K^+ and Na^+. Vitamins A, E, K and D are fat-soluble and water-insoluble (Stanbury *et al*., 1999). Sometimes they are also classified as lipids.

Typically 30-70% of the cell's dry weight is protein. All proteins contain C, H, N, and O. Sulfur contributes to the three-dimensional stabilization of almost all proteins. Proteins show great diversity of biological functions. The building blocks of proteins are the amino acids. The predominant chemical elements in living matter are: C, H, O, and N, and they constitute approximately 99% of the atoms in most organisms (Vogel, 1997). Carbon, an element of prehistoric discovery, is widely distributed in nature. Carbon is unique among the elements in the vast number and variety of compounds it can form. There are upwards of a million or more known carbon compounds, many thousands of which are vital to organic and life processes.

Hydrogen is the most abundant of all elements in the universe, and it is thought that the heavier elements were, and still are, being built from hydrogen and helium. It has been estimated that hydrogen makes up more than 90% of all atoms or three quarters of the mass of the universe (Went, 1979). Oxygen makes up 21 and nitrogen 78 volume percent of the air. These elements are the smallest ones in the periodic system that can achieve stable electronic configurations by adding one, two, three or four electrons respectively (Stanier *et al*., 1976; Bennett and Frieden, 1967). This ability to add electrons, by sharing them with other atoms, is the first step in forming chemical bonds, and thus, molecules. Atomic smallness increases the stability of molecular bonds and also enhances the formation of stable multiple bonds.

The biological significance of the main chemical elements in microorganisms is given in Table 1 (Bennett and Frieden, 1967; Stanier *et al*., 1976). Ash composes of approximately *5* percent of the dry weight of biomass with phosphorus and sulfur accounting, for respectively 60 and 20 percent. The remainder is usually made up of Mg, K, Na, Ca, Fe, Mn, Cu, Mo, Co, Zn and Cl (Stanier *et al*., 1976). The predominant atomic constituents of organisms, C, H, N, O, P, and S, go into making up the molecules of living matter. All living cells on earth contain water as their predominant constituent. The remainder of the cell consists of large proteins, nucleic acids, lipids, and carbohydrates, along with a few common salts. A few smaller compounds are very ubiquitous and function universally in bioenergetics, e.g., ATP for energy capture and transfer, and NAD in biochemical dehydrogenation. Microorganisms share similar chemical compositions and universal pathways. They all have to accomplish energy transfer and conversion, as well as synthesis of specific and patterned chemical structures (Stanier *et al*., 1976).

The microbial environment is largely determined by the composition of the growth medium. Using pure compounds in precisely defined proportions yields a defined or synthetic medium. This is usually preferred for researching specific requirements for growth and product formation by systematically adding or eliminating chemical species from the formulation. Defined media can be easily reproduced, have low foaming tendency, show translucency and allow easy product

recovery and purification (McNeil and Harvey, 2008). Complex or natural media such as molasses, corn steep liquor, meat extracts, etc., are not completely defined chemically, however, they are the media of choice in industrial fermentations. In many cases the complex or natural media have to be supplemented with mainly inorganic nutrients to satisfy the requirements of the fermenting organism. The objective in media formulation is to blend ingredients rich in some nutrients and deficient in others with materials possessing to achieve the proper chemical balance at the lowest cost and easy processing (Vogel, 1997). Fermentation nutrients are generally classified as sources of carbon, nitrogen, sulfur, minerals and vitamins.

Table 1 Physiological functions of the principal elements

Element	Symbol	Atomic	Physiological function
Hydrogen	H	1	Constituent of cellular water and organic cell materials
Carbon	C	6	Constituent of organic cell materials
Nitrogen	N	7	Constituent of proteins, nucleic acids and coenzymes
Oxygen	O	8	Constituent of cellular water and organic materials, as 0, electron acceptor in respiration of aerobes
Sodium	Na	11	Principal extracellular cation
Magnesium	Mg	12	Important divalent cellular cation, inorganic cofactor for many enzymatic reactions, incl. those involving ATP; functions in binding enzymes to substrates and present in chlorophylls
Phosphorus	P	15	Constituent of phospholipids, coenzymes and nucleic acids

Table 1 (Continued)

Element	Symbol	Atomic	Physiological function
Sulfur	S	16	Constituent of cysteine, cystine, methionine and proteins as well as some coenzymes as CoA and cocarboxylase
Chlorine	Cl	17	Principal intracellular and extracellular anion
Potassium	K	19	Principal intracellular cation, cofactor for some enzymes
Calcium	Ca	20	Important cellular cation, cofactor for enzymes as proteinases
Manganese	Mn	25	Inorganic cofactor cation, cofactor for enzymes as proteinases
Iron	Fe	26	Constituent of cytochromes and other heme or non-heme proteins, cofactor for a number of enzymes
Cobalt	Co	27	Constituent of vitamin B_{12} and its coenzyme derivatives
Copper	Cu	29	
Zinc	Zn	30	Inorganic constituents of
Molybdenum	Mo	42	Special enzymes

Source: Vogel (1997)

2.2 Statistical methods for fermentation optimization

A common problem for a biochemical engineer is to hand a microorganism and be told to take six months to design a plant to produce the new fermentation product. Although this seems to be a formidable task, with the proper

approach this task can be reduced to a manageable level. There are many ways to approach the problem of optimization and design of a fermentation process, one could determine the nutritional requirements of the organism and design a medium based upon the optimum combination of each nutrient, i.e., glucose, amino acids, vitamins, minerals, etc. This approach has two drawbacks. First, it is very time-consuming to study each nutrient and determine its optimum level, let alone its interaction with other nutrients. Secondly, although knowledge of the optimal nutritional requirements is useful in designing a media, this knowledge is difficult to apply when economics dictate the use of commercial substrates such as corn steep liquor, soy bean meal, etc., which are complex nutrients (Vogel, 1997).

2.2.1 Traditional one-variable-at-a-time method

The traditional approach to the optimization problem is the one-variable-at-a-time method (Nikerel *et al.*, 2006). In this process, at each condition one parameter is varied while others are kept constant. Using this optimization, the second variable's optimum is found, etc. This process works if, and only if, there is no interaction between variables. In the case shown in Figure 3, the optimum found using the one-variable-at-a-time approach was 85%, far from the real optimum of 90% (Vogel, 1997). Because of the interaction between the two nutrients, the one-variable-at-a-time approach failed to find the true optimum. In order to find the optimum conditions, it would have been necessary to repeat the one-variable-at-a-time process at each step to verify that the true optimum was reached. This requires numerous sequential experimental runs, a time-consuming and ineffective strategy, especially when many variables need to be optimized. Because of the complexity of microbial metabolism, interaction between the variables is inevitable, especially when using commercial substrates which are a complex mixture of many nutrients. Therefore, since it is both time-consuming and inefficient, the one-variable-at-a-time approach is not satisfactory for fermentation development. Fortunately, there are a number of statistical methods which will find the optimum quickly and efficiently (Stanbury *et al.*, 1999).

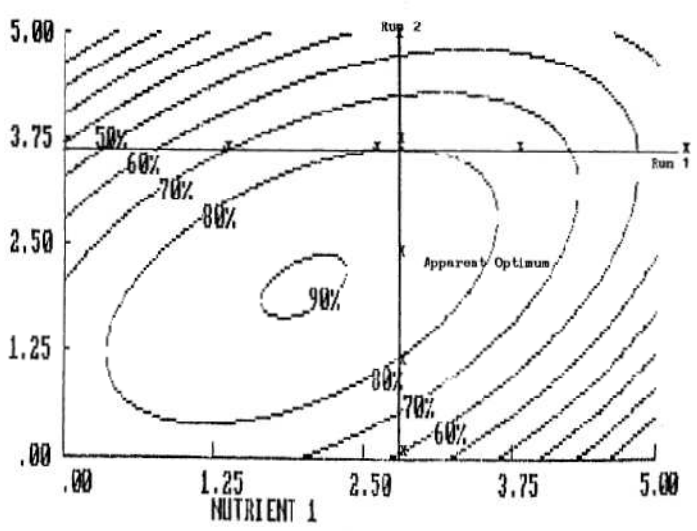

Figure 3 Sample of one-variable-at-a-time approach (contour plot of yield).

Source: Vogel (1997)

2.2.2 Response surface methodology

The best method for process optimization is response surface methodology (RSM). This process will not only determine the optimum conditions, but also give the information necessary to design a process. Response surface methodology (RSM) is a method of optimization using statistical techniques based upon the special factorial designs of Box and Behenkin and Box and Wilson. It is a scientific approach to determine the optimum conditions which combines special experimental designs with the Taylor first and second order equations. The RSM process determines the *surface* of the Taylor expansion curve which describes the *response* (yield, impurity level, etc.) The Taylor equation, which is the heart of the RSM method, has the following form:

$$\text{Response} = A + B.X1 + C.X2 + \ldots H.X1^2 + I.X2^2 + \ldots M.Xl.X2 + N.Xl.X3 + \ldots \quad (1)$$

where A,B,C,. . . are the coefficients of the terms of the equation, and

X1 = linear term for variable 1

X2 = linear term for variable 2

.

.

.

$X1^2$ = nonlinear squared term for variable 1

$X2^2$ = nonlinear squared term for variable 2

.

.

.

X1.X2 = interaction term for variable 1 and variable 2

Xl.X3 = interaction term for variable 1 and variable 3

.

.

.

The Taylor equation is named after the English mathematician Brook Taylor who proposed that any continuous function can be approximated by The power series. It is used in mathematics for approximating a wide variety of continuous functions (Lazic, 2004). The RSM protocol, therefore, uses the Taylor equation to approximate the function which describes the response in nature, coupled with the special experimental designs for determining the coefficients of the Taylor equation.

The use of RSM requires that certain criteria must be met (Lazic, 2004; McNeil and Harvey, 2008; Vogel, 1997). These are as following.

(i) The factors which are critical for the process are known.

RSM programs are limited in the number of variables that they are designed to handle. As the number of variables increases, the number of experiments required by the designs increases exponentially. Therefore, most RSM programs are limited to 4 to 5 variables. Fortunately, for the scale up of most fermentation the number of

variables to be optimized are limited. Some of the more important variables are listed in Table 2.

Table 2 Typical Variables in a Fermentation

Aeration rate	Agitation rate
Temperature	Carbon/Nitrogen ratio
Phosphate level	Magnesium level
Back pressure	Sulfer level
Carbon source	Nitrogen source
pH	Dissolved oxygen level
Power input	

Source: McNeil and Harvey (2008); Vogel (1997)

(ii) The factors must vary continuously over the experimental range tested. For example, the variables of pH, aeration rate, and agitation rate are continuous and can be used in an RSM model. Variables such as carbon source (potato starch and corn syrup) or nitrogen source (cotton seed meal and soy bean meal) are non-continuous and cannot be optimized by RSM. However, level of corn syrup or level of soy bean meal are continuous and can be optimized.

(iii) There exists a mathematical function which relates the response to the factors.

The difficult and time-consuming nature of these calculations have inhibited the wide spread use of RSM. Fortunately, numerous computer programs are available to perform this chore. They range from the expensive and sophisticated, such as SAS™, to inexpensive, PC based programs, SPSS™, E-Chip™, X- STAT™, MINITAB™ and Statistica™ (Lazic, 2004; McNeil and Harvey, 2008; Vogel, 1997). The availability of these programs, however, has led to a “black box” approach to

RSM. This approach can lead to many problems if the user does not have a thorough understanding of the process or the meaning of the results.

2.2.3 Advantages and disadvantages of RSM

The response surface methodology approach has many advantages and disadvantages over other optimization procedures. These are listed in Table 3.

Table 3 Advantages and Disadvantages of RSM

Advantages of RSM	Disadvantages of RSM
1. Greatest amount of information from experiments. 2. Forces you to plan. 3. Know how long project will take. 4. Gives information about the interaction between variables. 5. Multiple responses at the same time. 6. Gives information necessary for design and optimization of a process.	1. Tells what happens, not why. 2. Notoriously poor for predicting outside the range of study.

Source: McNeil and Harvey (2008); Vogel (1997)

2.3 Modes of fermentor operation

2.3.1 Batch culture

Batch fermentation is the simplest mode of operation, and is often used in the laboratory to obtain substantial quantities of cells or products for further analysis. A batch fermentation is a closed system, where all of the nutrients required

for the organism's growth and product formation are contained within the vessel at the start of the fermentation process (Stanbury *et al.*, 1999). The vessel can take the form of a shake flask, single use disposable system, or, for tighter control of parameters such as oxygen transfer, pH, agitation, etc., or a bioreactor can be used. Historically, these processes would have involved non-sterile systems with self-selecting or natural inoculants. However, nowadays nearly all fermentation processes involve inoculation of a selected and specially bred strain of microbe, plant or animal cell into a sterile medium held within a sterile fermenter vessel. After medium sterilization, the organism is inoculated into the vessel and allowed to grow. The fermentation is terminated when one or more of the following has been reached: (i) microbial growth has stopped due to the depletion of the nutrients or the build of toxic compounds; (ii) after a fixed predetermined period of time; (iii) the concentration of desired product has been achieved (McNeil and Harvey, 2008).

When cells are grown in a batch culture, they will typically proceed through a number of distinct phases (Figure 4).

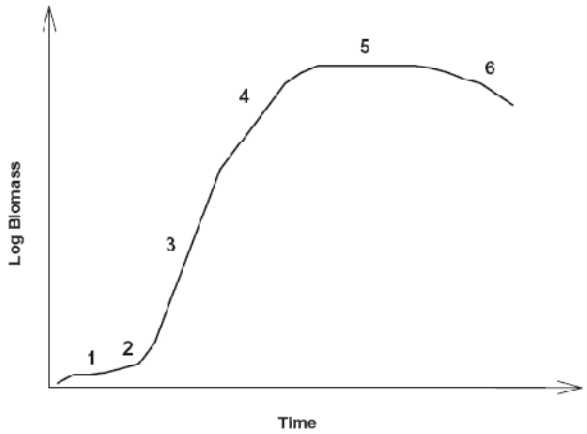

Figure 4 Characteristic growth curve of a microorganism in batch culture. 1, Lag phase (not always present); 2, transient acceleration phase; 3, exponential phase; 4, deceleration phase; 5, stationary phase; 6, death phase

Source: McNeil and Harvey (2008)

The lag phase, which may or may not be present, is described as 'little or no growth at the beginning of the fermentation due to the physiochemical equilibrium between the microorganism and the environment following inoculation'. The lag phase can be time consuming and costly and so it is highly desirable to minimize this phase. This can be achieved by growing the inoculums in comparable medium to the bioreactor and under similar growth conditions (pH, temperature, etc.). A minimum of 5% by volume should be used for inoculation. Once the cells have adapted to the new conditions of growth, they enter the exponential phase. Then, key to minimizing the length of the lag phase lies in making sure that the culture being transferred undergoes the minimum levels of stress possible. In practical terms, this implies keeping the environments in the two fermentation systems as similar as possible. In reality, this is sometimes very difficult, e.g. a late exponential stage shake flask culture will typically exist in an environment where substrate levels are reduced, oxygen levels low, and carbon dioxide levels elevated, pH may also be very different from the process start point. Clearly, the transfer of such a culture to a fully charged fermenter with fresh medium, is highly aerated, low CO_2 environment. Inoculation of fermenters to minimize lag phase is something of a compromise and often involves empiricism and experience of that particular culture character (McNeil and Harvey, 2008).

Nutrient depletion and the formation of inhibitors (typically excreted products such as ethanol, lactic acid, acetic acid, methanol, and aromatic compounds) have the effect on decelerating cell growth (Zheng *et al*., 2008), and the cells then enter the stationary phase where the rate of cell growth equals that of cell death. Eventually, the cells enter death phase and this is characterized by a drop in optical density and biomass levels in most cultures.

The batch culture growth curve gives a good indication of when to stop the fermentation. Growth-associated products (primary metabolites) are produced during the exponential phase with their formation decreasing when growth ceases. Typically the rate of product formation directly relates to the rate of growth (Figure 5). The fermentation can be terminated at the end of the exponential growth phase

before the cell enters stationary phase. This growth phase is sometimes referred to as the trophophase. Nongrowth-associated products (e.g., classic secondary metabolites) have a negligible rate of formation during active cell growth. These secondary metabolites are produced when the cells enter stationary phase (Figure 6) (McNeil and Harvey, 2008).

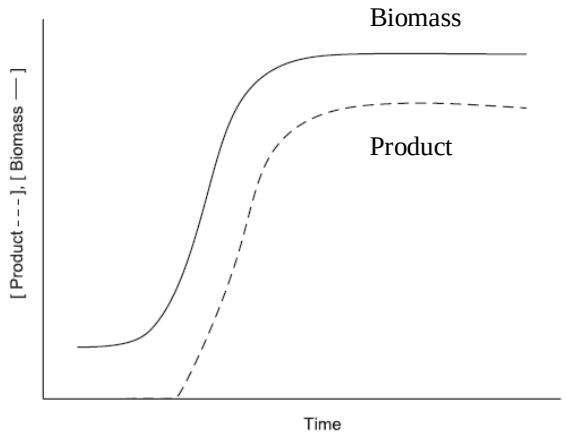

Figure 5 Growth associated product formed during the period of active culture growth.

Source: McNeil and Harvey (2008)

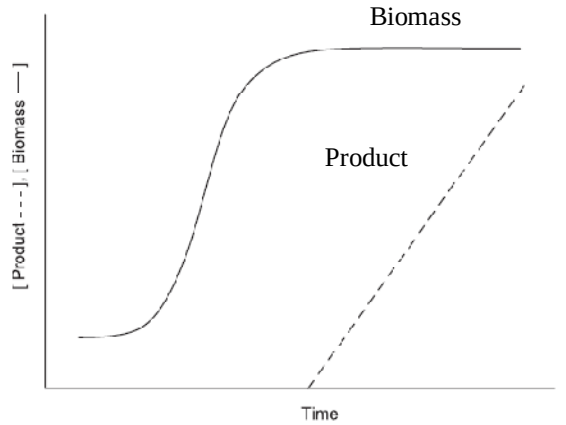

Figure 6 Nongrowth associated product formed during the period of nonculture growth (stationary phase).

Source: McNeil and Harvey (2008)

2.3.1.1 Kinetics of batch culture

The batch culture is a simple, well controlled vessel in which the concentration of nutrients, cells and products vary with time as the growth of the microorganism proceeds. Material balance in the reactor may assist the biochemical reactions occurring in the media. In the batch fermentation, living cells propagate and many parameters of the media go through sequential changes with time as the cells grow. The following parameters are monitored while the batch process continues: cells and cell by-product, concentration of nutrients, desirable and undesirable products, inhibition, pH, temperature, and substrate concentration etc. The objective of a good process design is to minimize the lag phase period and maximize the length of exponential growth phase (Najafpour, 2007).

The substrate balance in a batch culture for component *i* in the culture volume of V_R and change of molar concentration of C_i is equal to the rate of formation of product in Equation 2.

$$\frac{d}{dt}(V_R \cdot C_i) = V_R \cdot r_{fi} \tag{2}$$

where V_R is the culture volume, assumed to be constant while no liquid media is added or removed, C_i is the molar concentration of component *i*, and r_{fi} is the rate of product formation. Then (Equation 2) is reduced to Equation 3.

$$\frac{dC_i}{dt} = r_{fi} \tag{3}$$

The rate of product formation, r_{fi}, depends upon the state of the cell population, environmental condition, temperature, pH, media composition and morphology with cell age distribution of the microorganism. A similar balance can be formulated for microbial biomass and cell concentration. The exponential phase of the microbial growth in a batch culture is defined by Equation 4.

$$\frac{dX}{dt} = \mu X \quad (4)$$

There is no cell removal from the batch vessel and the cell propagation rate is proportional to the specific growth rate, μ (1/h), using the differential growth equation the cell concentration with respect to the time is (Stanbury *et al.*, 1999):

$$X(t) = X_0 e^{\mu t} \quad (5)$$

2.3.1.2 Advantages of the batch culture (McNeil and Harvey, 2008; Stanbury *et al.*, 1999; Vogel, 1997)

(i) Simplicity of use: A batch culture can be easily readied, depending on the microorganism used, and can be finished in less than 24 hours.

(ii) Operability and reliability: less likely to have instrument failure on short batch runs

(iii) Production of secondary metabolites that are not growth-related (i.e., produced when the organism enters stationary phase);

(iv) Fewer possibilities of contamination: all of the materials required for the bioprocess are present in the vessel and sterilized before the run starts. The only material added (with the exception of the inoculum at the beginning of the bioprocess) and removed during the course of a batch fermentation are the gas exchange, and if using a bioreactor, sterile a antifoam and pH control solutions.

(v) It is easy to assign a unique batch number to each run, generating high confidence in the history of each batch of product. This is critically important in a highly regulated environment.

2.3.1.3 Disadvantages of the batch culture (McNeil and Harvey, 2008; Stanbury *et al.*, 1999; Vogel, 1997)

(i) Culture ageing, and more importantly differentiation, can be a specific problem, especially so with growth-related products;

(ii) Build up of toxic metabolites can restrict the cell growth and product formation;

(iii) Initial substrate concentrations may have to be limited due to problems with inhibition and repression effects, therefore, affecting the amount of product that can be obtained from such simple systems;

(iv) Batch-to-batch variability;

(v) The use of batch cultures in industrial systems can lead to an increased nonproductive period due to down time required for cleaning, resterilisation, filling and cooling of equipment;

(vi) If using the organism from one bioprocess to seed another culture, degeneration or differentiation may occur, which could affect the bioprocess and product formation;

(vii) Cellular autolysis may occur during the decline and stationary phase, affecting the amount of product, its composition and potentially adding to downstream processing challenges due to release of autolytic breakdown products, activation of proteases;

(viii) From a physiological viewpoint the use of batch cultures actually contributes greatly to the complexity of the experiments since the cell population is heterogeneous and constantly changing. This makes the use of such systems for clearly identifying cause and effect relationships in cell physiology rather unattractive.

2.3.2 Fed-batch culture

Fed-batch culture is essentially similar to the batch culture, and most fed-batches begin life with a straightforward batch phase. However, unlike batch these cultures do not operate as closed systems. At a given point during the fed-batch

process, one or more substrates, nutrients, and/or inducers are introduced into the bioreactor. Fed-batch cultures can be run in different ways, e.g. at a fixed volume where at a certain time point, a portion of the fermenter contents (consisting of spent medium, cells, product, and unused nutrients) is drawn off and replaced with an equal volume of fresh medium and nutrients (withdraw and fill), or at a variable volume where nothing is removed from the bioreactor during the time course of the process, with the cells and product remaining within the vessel until the end of the fermentation period, and the addition of fresh medium and nutrients has the effect of increasing the culture volume. This feeding strategy allows the organism to grow at the desired specific growth rate, minimize the production of unwanted by-products, and to allow the achievement of high cell densities and product concentrations. The addition of the feed can be over a short or long period, starting immediately after inoculation or at a predetermined point during the run. The feeding strategy can be continuous over a long period of time or incremental, with the addition of fixed volumes at given time points (Figure 7). All are determined either from past fermentation data allowing the process operator to permit the same predetermined feed, or from the organism's physiology and the concentrations of key metabolites within the fermentation broth (McNeil and Harvey, 2008).

Escherichia coli, when grown aerobically with excess glucose present excretes copious amounts of acetate (Park *et al.*, 1992; Snay *et al.*, 1989), as the ready availability of substrate exceeds the oxidative capacity of the bacterial cells. This can lead to culture inhibition, and slow fermentations. Carbon dioxide can also affect cell growth in high cell density culture. High partial pressure of carbon dioxide decreases growth rate and stimulates acetate formation. Therefore, the increase of the pressure in a fermenter enhances both oxygen transfer and the detrimental effect of carbon dioxide (Lee, 1996).

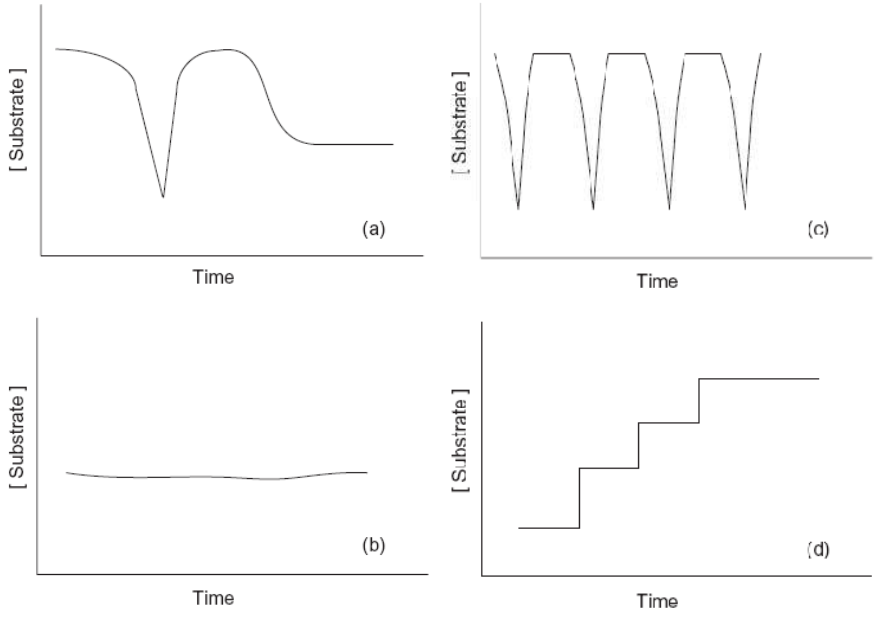

Figure 7 Different feeding regimes in fed-batch processes, (a) Variable feeding regime; (b) continuous feeding regime; (c) intermittent feeding regime; (d) incremental feeding regime

Source: McNeil and Harvey (2008)

Formation of acetate in *E. coli* cultures not only occurs under fully aerobic conditions with an excess carbon source, but it also forms under anaerobic conditions. These two mechanisms are often referred to as the overflow metabolism and the mixed-acid fermentation, respectively. When *E. coli* is grown under fully aerobic conditions, the formation of acetate typically takes place at high growth rates and/or high glucose uptake rates (Akesson *et al*., 1999).

High cell density culture is an attractive means of achieving high product concentration. However, researchers cannot obtain high cell density (greater than 10 g/l) with batch culture alone, because the cells suffer from substrate inhibition and catabolite inhibition. It is well documented that catabolic acid by-products will accumulate in the fermentation broth during the batch culture, and they will inhibit cell growth and recombinant protein production (Yee and Blanch, 1993b). In order to

attain high cell densities by the use of glucose as carbon source, fed-batch culture is preferred to minimize acetate production and to eliminate substrate inhibition (Yee and Blanch, 1993a).

In fed-batch cultures, in order to restrict the formation of the acetate, the feed rate for glucose should be controlled. In the early stage of cultivation, the cell density is rather low, so the glucose feed rate is low due to the low glucose consumption rate. In this period, no acetate is formed. As the cells grow, the feed rate and oxygen consumption can be increased and finally the oxygen consumption exceeds the maximum oxygen transfer capacity even when the stirrer speed is at its maximum, and an anaerobic condition will occur, so the feed rate should be reduced (Akesson *et al*., 2001). Many other researchers used air and/or pure oxygen to maintain dissolved oxygen concentration greater than 20% of air saturation to avoid anaerobic condition during the later part of the high cell density culture (DeLisa *et al*., 1999; Vuolanto *et al*., 2001; Yee *et al*., 1993a,b).

When the anaerobic condition is avoided, acetate present in the media can also be reassimilated by the cells (Akesson *et al*., 2001; vande Walle and Shiloach, 1998). With the decrease of growth rate at the later stage of aerobic culture, the pH in the broth starts to increase due to the accumulation of ammonia, depletion of amino acid and the consumption of acetate. Robbins and Taylor (1989) hypothesized that ammonia was produced by the extensive deamination of amino acids (Jensen and Carlsen, 1990; Robbins and Taylor, 1989).

High cell density cultures producing a recombinant protein or metabolite have only been reported since 1975. Many feeding strategies have been developed to avoid substrate inhibition and the accumulation of acetate. There are two principal strategies for the control of the nutrient feed: the open-loop (feed forward) control and the closed-loop (feedback) control (Luli, 1988).

2.3.2.1 Advantages of fed-batch culture (McNeil and Harvey, 2008; Stanbury *et al.*, 1999; Vogel, 1997)

(i) Controlling the concentration of the limiting substrate prevents the repressive effects of high substrate concentration and avoids catabolite repression.

(ii) By careful feeding strategy the organism's growth rate and subsequent oxygen demand can be controlled. This was one of the original aims of developing a bakers' yeast fed-batch process: to balance the oxygen transfer rate of a given fermenter with the rate of nutrient feeding in order to minimize substrate flow to the ethanol.

(iii) High cell density (up to ten times greater) can be achieved by use of fed-batch over batch culture. Batch culture limits the final cell growth due to no extra carbon being added during the run, and the carbon that is presented at the beginning of the bioprocess results in catabolite repression and inhibition of growth. Using fed-batch with a careful feeding strategy, *E. coli* and *Pichia* can achieve very high cell densities of over 100 g/L.

(iv) Increased production of non-growth-related secondary metabolites. Many secondary metabolites are produced from intermediates and end products of primary metabolism. Others are formed after introduction of key precursors after the growth phase, as is seen in penicillin production with phenylacetic acid or phenoxyacetic acid, precursors of penicillins G and V respectively, being added prior to the stationary phase to allow the formation of penicillin.

(v) Reduction of broth viscosity. This is particularly important in filamentous fungal fermentations, or where the product is highly viscous, such as the polysaccharide products of *Sphingomonas elodea* - gellan gum; and *Xanthomonas campestris* - xanthan gum. The addition of fresh medium during the fermentation run, leads to the broth being 'diluted', and a brief viscosity drop, allowing better aeration and agitation within the system.

2.3.2.2 Disadvantages of fed-batch culture (McNeil and Harvey, 2008; Stanbury *et al.*, 1999; Vogel, 1997)

(i) Detailed knowledge of the organism's growth and product formation pattern is required, especially when no feedback loop is used.

(ii) Deficiency of reliable online sensors for accurate substrate determination in near real time.

(iii) Without feedback control, the feed is predetermined and therefore does not allow for any fluctuations within the bioprocess. This can potentially lead to mismatches between feed rates and culture metabolism, in turn leading substrate levels to become depleted or rise to undesirable levels.

(iv) The process operator must be fully trained and highly skilled.

2.4 Aeration and agitation in aerobic fermentation

The majority of fermentation processes is aerobic, and therefore, requires the provision of oxygen. If the stoichiometry of respiration is considered, then the oxidation of glucose may be represented as:

$$C_6H_{12}O_6 + 6O_2 = 6H_2O + 6CO_2 \quad (6)$$

Thus, 192 grams of oxygen are required for the completed oxidation of 180 grams of glucose. However, both components must be in solution before they are available to the microorganism. Oxygen is approximately 6000 times less soluble in water than glucose, thus, it is not possible to provide a microbial culture with all the oxygen it will need for the completed oxidation of the glucose (or any other carbon source) in one addition. Therefore, a microbial culture must be supplied with oxygen during growth at a rate sufficient to meet the organisms' demand (Bartholomew, 1960).

The oxygen demand of an industrial fermentation process is normally satisfied by aerating and agitating the fermentation broth. However, the productivity

of many fermentations is limited by oxygen availability, therefore, it is important to consider the factors which affect a fermenter's efficiency in supplying microbial cells with oxygen.

2.4.1 Oxygen requirements of fermentations

The analysis of the stoichiometry of respiration gives an appreciation of the problem of oxygen supply. However, it gives no indication of an organism's true oxygen demand as it does not take into account the carbon that is converted into biomass and products. A number of workers (Darlington, 1964; Johnson, 1964; Mateles, 1971) have used the incorporation of oxygen, carbon, and nitrogen into biomass to predict the oxygen demand for fermentation. They found that a culture's demand for oxygen is very much dependent on the source of carbon in the medium. Thus, the more reduced the carbon source, the greater will be the oxygen demand. Darlington (1964) and Johnson (1964) demonstrated that 100 grams of biomass from hydrocarbon requires approximately three times the amount of oxygen to produce the same amount of biomass from carbohydrate. Later, product formation and biomass production by oxygen conversion were calculated (Cooney, 1979; Righelato *et al*., 1968).

2.4.2 Oxygen transfer in the fermenter

During fermentation, the transfer of oxygen from air to the cell occurs in a number of steps (Bartholomew *et al*., 1960):

(i) The transfer of oxygen from an air bubble into solution.

(ii) The transfer of the dissolved oxygen through the fermentation medium to the microbial cell.

(iii) The uptake of the dissolved oxygen by the cell.

The simplest theory involved in mass transfer across an interface is film theory, as shown in Figure 8. In this model, the gas (CO) is transferred from the gas phase into the liquid phase and it must reach the surface of the growing cells.

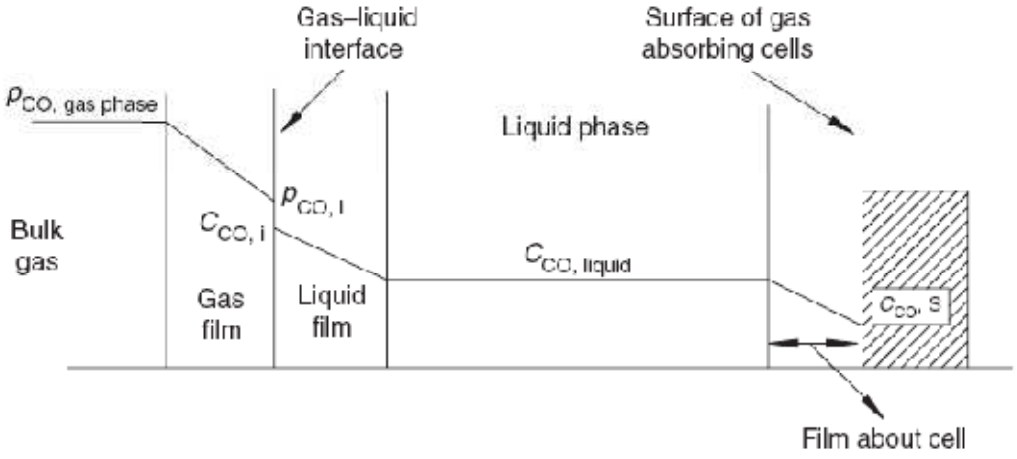

Figure 8 The film theory for mass transfer.

Source: Najafpour (2007)

It was demonstrated in a *Streptomyces griseus* fermentation that the limiting step in the transfer of oxygen was the transfer of oxygen into solution. The findings have been shown to be correct for non-viscous fermentations, but it has been demonstrated that oxygen transfer may be limited by either of the other two stages in some highly viscous fermentations.

The rate of oxygen transfer from air bubble to the liquid phase may be described by the equation:

$$\frac{dC_L}{dt} = k_L a(C^* - C_L) \tag{7}$$

where C_L = concentration of dissolved oxygen in fermentation broth (mmoles/dm^3)

t = time (h)

dC_L/dt = change in oxygen concentration over a time period, i.e. the oxygen transfer rate (mmoles O_2 dm^3/h)

k_L = liquid-phase mass transfer coefficient (cm/h)

a = gas-liquid interface area per liquid volume (cm^2/cm^3)

C* = saturated dissolved oxygen concentration (mmols /dm^3)

From the Equation 7, it is clear that three parameters are involved in the oxygen transfer rate: the liquid-phase mass transfer coefficient (k_L), the gas-liquid interfacial area per liquid volume (a), and the concentration driving force (C*-C). It is extremely difficult to measure both 'k_L' and 'a' during fermentation and, therefore, the two terms are generally combined in the term $k_L a$, the volumetric mass-transfer coefficient, having units of reciprocal time (1/h).

The volumetric mass-transfer coefficient is used as a measure of aeration capacity of a fermenter. The larger $k_L a$, the higher the aeration capacity of the system. The $k_L a$ value will depend upon the design and operating conditions of the fermenter and will be affected by such variables as aeration rate, agitation rate, and impeller design. These variables affect 'k_L' by reducing the resistances to transfer and affect 'a' by changing the number, size, and residence time of air bubbles (Rao, 2005).

2.4.3 Factors affecting $k_L a$ values

A number of factors have been demonstrated to affect the $k_L a$ value achieved in a fermentation vessel. Such factors include the bubble size, the degree of agitation, the air flow rate, the rheological properties of the culture broth, and the presence of antifoam agents.

2.4.3.1 Bubble size

The value of $k_L a$ is strongly affected by the bubble characteristics in the liquid medium. The size of air bubbles is the most important variable (Motarjemi and Jameson, 1978). Small air bubbles have more interfacial area than large air bubbles, which cause increased $k_L a$ value. Small bubbles have other important characteristics such as slow rising velocity and high gas hold-up. Slow

rising velocities keep air bubbles in the liquid longer, allow more time for the oxygen to dissolve. Small bubbles create high gas hold-up, defined as the fraction of the fluid volume in the reactor occupied by gas:

$$\varepsilon = \frac{V_G}{V_L + V_G} \quad (8)$$

where ε = Gas hold-up

V_G = volume of gas bubbles in the reactor (m^3), and

V_L = volume of liquid in the reactor (m^3)

The total interfacial area for oxygen transfer depends on the total volume of gas in the system as well as on the average bubble size. High gas hold-up gives a high oxygen transfer rate because the total volume of the air bubbles in the fermenter is greater. Decreased bubble size largely increases total interfacial area of the gas bubbles. Kaster *et al*. (1990) demonstrated that a microbubble dispersion increased oxygen transfer rate in aerobic fermentation of yeast. A given volume of gas dispersed into many small bubbles rather than a few large ones provides more interfacial area. Since the efficiency of oxygen transport is approximately proportional to the ratio of the bubble surface area to the bubble volume, the smaller size bubbles increase oxygen transfer rate in the fermenter.

2.4.3.2 Degree of agitation

The degree of agitation has been demonstrated to have a profound effect on the oxygen-transfer efficiency of an agitated fermenter. Banks (1977) reported that agitation assisted oxygen transfer in the following ways:

(i) Agitation increases the area available for oxygen transfer by dispersing the air in the culture fluid in the form of small bubbles.

(ii) Agitation delays the escape of air bubbles from the liquid.

(iii) Agitation prevents coalescence of air bubbles.

(iv) Agitation decreases the thickness of the liquid film at the gas-liquid interface by creating turbulence in the culture fluid.

The degree of agitation may be measured by the amount of power consumed in stirring the vessel contents. A large number of empirical relationships have been developed between k_La, power consumption, and superficial air velocity which can be generally expressed as:

$$k_La = k\,(P_g / V)^{x} V_S^{y} \qquad (9)$$

where P_g = power absorption in an aerated system

V = liquid volume in the vessel

V_S = superficial air velocity

k, x and y = empirical factors specific to the system under investigation.

Bartholomew (1960) demonstrated that the relationship depended on the size of the vessel and the exponent on the term P_g / V varied with scale (Table 4). In a laboratory scale fermenter, the k_La value was almost directly proportional to the gassed power consumption per unit volume, and the relationship was scale-dependent. Van't (1979) summarized the various correlations for coalescing air-water dispersion systems as falling within 20-40% of: k = 0.026, x = 0.4 and y = 0.5. The common feature of these relationships is that the values of x and y are less than unity.

Table 4 The exponent on P_g / V varied with scale

Scale	Value of exponent on P_g / V
Laboratory	0.95
Pilot plant	0.67
Production plant	0.5

Source: Bartholomew (1960)

2.4.3.3 Air flow rate (Aeration rate)

The effect of air flow rate on k_La values in conventionally agitated systems is illustrated in Figure 9. The air flow rate employed rarely falls outside the range of 0.5-1.5 volumes of air per volume of medium per minute, and this rate tends to be maintained constant on scale-up. If the impeller is unable to disperse the incoming air, then extremely low oxygen transfer rates may be achieved due to the impeller becoming 'flooded'.

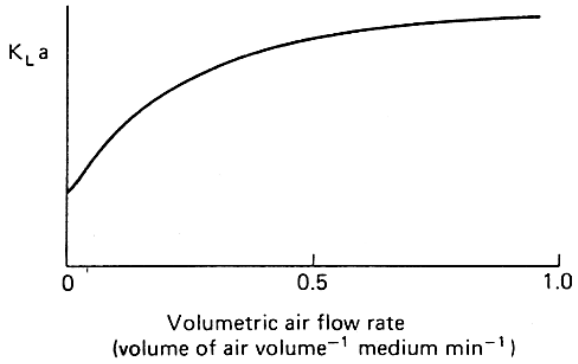

Figure 9 Effect of air-flow rate on the k_La of an agitated aerated vessel.

Source: Stanbury (1999)

A schematic representation of air flow rate (aeration) and impeller speed (agitation) is shown in Figure 10. Flooding is the phenomenon where the air-flow dominates the flow pattern due to an inappropriate combination of high air-flow rate and low speed of agitation (Figure 10 a). As the impeller speed increases, gas is captured behind the agitator blades and is dispersed into the liquid. Figure 10 (b) shows the minimum stirrer speed required to completely disperse the gas. With further increases in stirrer speed, small recirculation pattern starts to emerge as indicated in Figure 10 (c) and (d). The desired dispersion pattern is shown in Figure 10 (e).

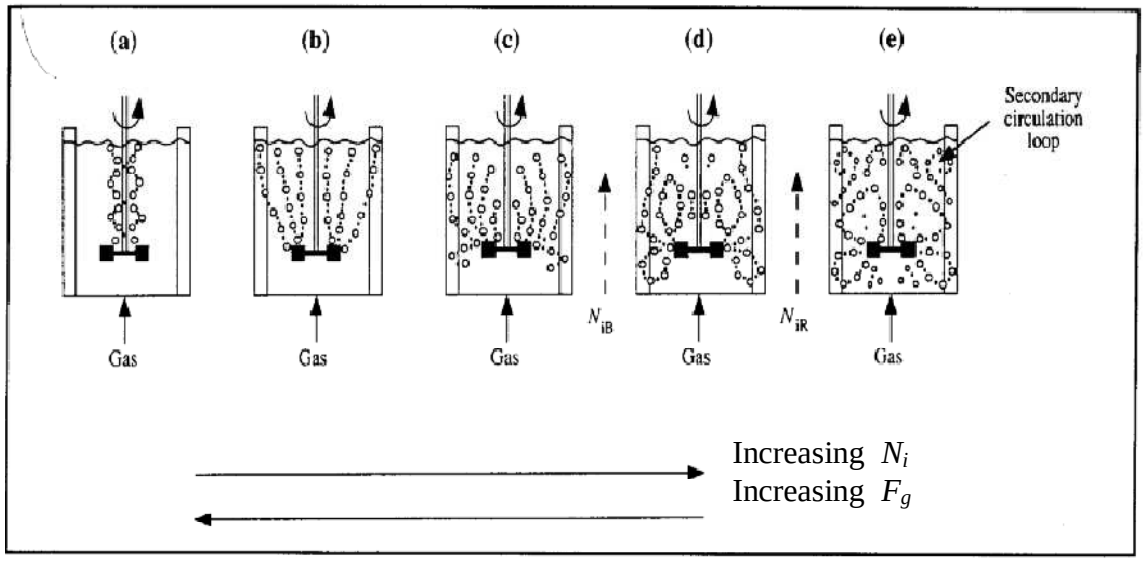

Figure 10 Different patterns of gas bubble dispersion in a stirred-tank reactor.

Source: Doran (1995)

2.4.3.4 Medium rheology

A Newtonian liquid has a constant viscosity regardless of shear, so that the viscosity of a newtonian fermentation broth will not vary with agitation rate. However, a non-newtonian liquid does not obey Newton's law of viscous flow and does not have a constant viscosity. Thus, the viscosity of a non-Newtonian fermentation broth will vary with agitation rate and is described as an

apparent viscosity (μ_a). Buckland *et al*. (1988), using different agitator systems, reported that the k_La was inversely proportional to the square root of the broth viscosity, i.e.:

$$k_L a \propto 1/\sqrt{Viscosity} \quad (10)$$

A fermentation broth consists of the liquid medium in which the organism grows, the microbial biomass, and product secreted by the organism. Thus, the rheology of the broth is affected by the composition of the original medium and its modification by the growing culture, the concentration and morphology of the biomass and the concentration and rheological properties of the microbial products. Therefore, fermentation broths vary widely in their rheological properties and significant changes in broth rheology may occur during a fermentation, which may have marked influence on the relationship between k_La and the degree of agitation.

2.4.3.5 Antifoam agents

The high degree of aeration and agitation required in a fermentation, frequently gives rise to the undesirable phenomenon of foam formation. In extreme circumstances, the foam may overflow from the fermenter via the air outlet or sample line resulting in the loss of medium and product, as well as increasing the risk of contamination. The presence of foam may also have an adverse effect on the oxygen-transfer rate. Thus, antifoams need to be added to break down the foam.

All antifoams are surfactants and may, themselves, be expected to have some effect on oxygen transfer. The observed predominant effect is that antifoams tend to decrease the oxygen-transfer rate (Rao, 2005). Antifoams cause the collapse of bubbles in foam but they may favor the coalescence of bubbles within the liquid phase, resulting in larger bubbles with reduced surface area to volume ratios and hence a reduced rate of oxygen transfer (Van't and Sonsberg, 1992). Thus, a balance must be struck between the necessity for foam control and the deleterious

effects of the controlling agent. Van't and Sonsberg (1992) observed that, above a critical liquid height, the k_La value decreases dramatically due to the excessive use of antifoams.

2.5 Glycerol using as carbon and energy source for microbial fermentation

2.5.1 Glycerol uptake and metabolism

Like other small uncharged molecules, glycerol can cross the cytoplasmic membrane through passive diffusion. However, cells limited to passive uptake have a growth disadvantage at low concentrations of substrate. Glycerol uptake is frequently cited as the only example of transport mediated by facilitated diffusion across the *Escherichia coli* inner membrane (Voegele *et al.*, 1993). Facilitated diffusion is achieved by an integral membrane protein, the glycerol facilitator GlpF (Darbon *et al.*, 1999; Heller *et al.*, 1980; Voegele *et al.*, 1993) (Figure 11).

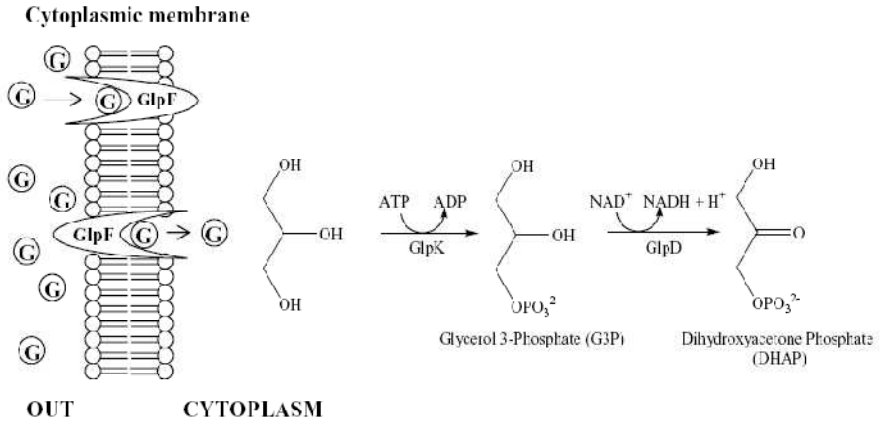

Figure 11 Mechanism of uptake and initial enzymatic reactions in the microbial metabolism of glycerol (G). *Note:* The gene products GlpF, GlpK, GlpD correspond to a glycerol facilitator protein, glycerol kinase, and glycerol 3 - phosphate dehydrogenase, respectively.

Source: Hou and Shaw (2008)

Intracellular glycerol is subsequently converted to glycerol-3-phosphate by glycerol kinase (GlpK). Glycerol-3-phosphate remains being trapped in the cell until it is further metabolized because it is not a substrate for the glycerol facilitator (Braun *et al*., 2000; Darbon *et al*., 1999; Voegele *et al*., 1993). GlpF acts as a highly selective channel, also conducting polyalcohols and urea derivatives, for which it is stereo-selective and enantio-selective (Braun *et al*., 2000; Fu *et al*., 2000). All these channels are strictly selective for non-ionic compounds, including hydroxide and hydronium ions, thus preventing the dissipation of the membrane potential (Braun *et al*., 2000; Fu *et al*., 2000). The influx of glycerol mediated by GlpF is 100- to 1000-fold greater than expected for a transporter and is non-saturable at a glycerol concentration of >200 mM (Fu *et al*., 2000). In *Saccharomyces cerevisiae*, the flow of glycerol across the plasma membrane is controlled either by passive diffusion, a channel protein or an active uptake mechanism (Wang and Inoue, 2001).

2.5.2 Glycerol bioconversion in industrial microbiology

A number of microorganisms are able to grow anaerobically on glycerol as the sole carbon and energy source, such as *Citrobacter freundii* (Daniel *et al*., 1995; Homann *et al*., 1990; Seifert *et al*., 2001), *Klebsiella pneumoniae* (Biebl *et al*., 1998; Forage and Foster, 1982; Menzel *et al*., 1997; Németh *et al*., 2003; Tong *et al*., 1991), *Clostridium pasteurianum* (Biebl, 2001; Luers *et al*., 1997; Macis *et al*.,1998), *Clostridium butyricum* (Abbad-Andaloussi *et al*., 1995; Biebl, 1991; Biebl *et al*., 1992; Colin *et al*., 2001; Himmi *et al*., 1999; Malaoui and Marczak, 2001), *Enterobacter agglomerans* (Barbirato *et al*.,1996; Barbirato and Bories,1997; Barbirato *et al*., 1997), *Enterobacter aerogenes* (Ito *et al*., 2005) and *Lactobacillus reuteri* (Talarico *et al*., 1990). In Klebsiella, Citrobacter, Clostridium and Enterobacter, glycerol is metabolized both oxidatively and reductively (Zhu *et al*., 2002). In the oxidative pathway, the NAD^+-dependent glycerol dehydrogenase (EC 1.1.1.6) catalyzes the conversion of glycerol to dihydroxyacetone and the glycolytic enzyme dihydroxyacetone kinase (EC 2.7.1.29) phosphorylates the latter product (Daniel *et al*., 1995; Luers *et al*., 1997; Macis *et al*., 1998), which is then funneled to glycolysis. The reducing pathway is catalyzed by coenzyme B12-dependent glycerol

dehydratase (EC 4.2.1.30) and related diol dehydratases (EC 4.2.1.28) (Forage and Foster, 1982; Toraya *et al*., 1978), converting glycerol to 3- hydroxypropionaldehyde (Seifert *et al*., 2001; Tong *et al*., 1991; Toraya *et al*., 1980), and by the $NADH^{+}H^{+}$-dependent 1,3-propanediol dehydrogenase (1,3-propanediol-oxydoreductase, EC 1.1.1.202), reducing 3-hydroxypropionaldehyde to 1,3-propanediol and regenerating NAD+ (Ahrens *et al*.,1998; Macis *et al*.,1998; Németh *et al*., 2003; Skraly *et al*.,1998; Veiga da Cunha and Foster, 1992) (Figure 12).

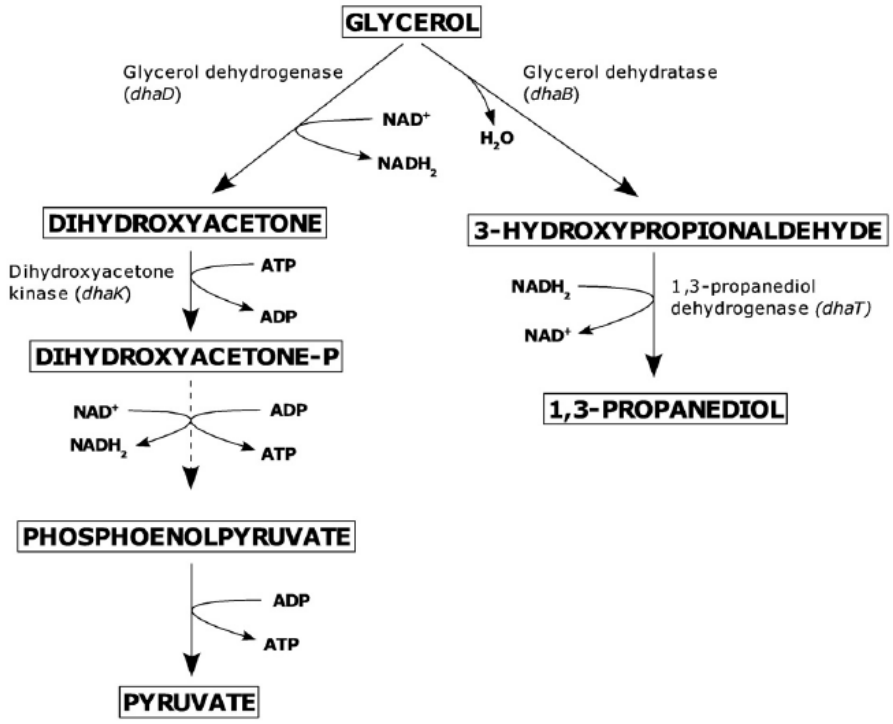

Figure 12 Fermentative patterns of glycerol dissimilation dependent on 1,3-PDO formation. The key enzymes of the dha regulon and respective genes related to glycerol metabolism are shown. Pyruvate will be reduced to different organic compounds dependent on microorganism and fermentation conditions, regenerating NAD+.

Source: Paula da Silva *et al*. (2009)

The final 1, 3-propanediol (1,3-PDO) product is highly specific for glycerol fermentation and cannot be obtained from any other anaerobic conversion (Deckwer, 1995; Homann *et al*., 1990). In *K. pneumoniae* (Forage and Lin, 1982) and *C. freundii*, the genes encoding the functionally linked activities of glycerol dehydratase (dhaB), 1,3-PDO dehydrogenase (dhaT), glycerol dehydrogenase (dhaD), and dihydroxyacetone kinase (dhaK) are encompassed by the dha regulon (Zhu *et al*., 2002) (Figure 12). The 1, 3-PDO operon of *C. butyricum* is composed of three genes, a different type of glycerol dehydratase (dhaB1), its activator protein (dhaB2) and dhaT (Raynaud *et al*., 2003). In this bacterium, glycerol dehydratase is extremely oxygen sensitive, strongly associated with the cell membrane and vitamin-B12 independent (González-Pajuelo *et al*., 2004, 2005a,b, 2006; Raynaud *et al*., 2003; Saint-Amans *et al*., 2001). In *S. cerevisiae* and a number of other yeasts, glycerol is degraded via dihydroxyacetone or via glycerol-3-phosphate (Wang and Inoue, 2001). In the latter, glycerol is converted to glycerol-3-phosphate through glycerol kinase (EC 2.7.1.30), which can be used either as a precursor for lipid biosynthesis or conversion to dihydroxyacetone phosphate and can then either be transformed to glyceraldeyde-3-phosphate by triose phosphate isomerase (EC 5.3.1.1) in glycolysis or can serve as a substrate for the synthesis of other metabolites (Wang *et al*., 2001). Similar pathways for glycerol oxidation (glp regulon) are present in *K. pneumoniae* (Ruch *et al*., 1974; Forage and Lin, 1982), *Gluconobacter oxydans* (Bories *et al*., 1991; Claret *et al*., 1994) and *C. acetobutylicum* (González-Pajuelo *et al*., 2006) (Figure 13).

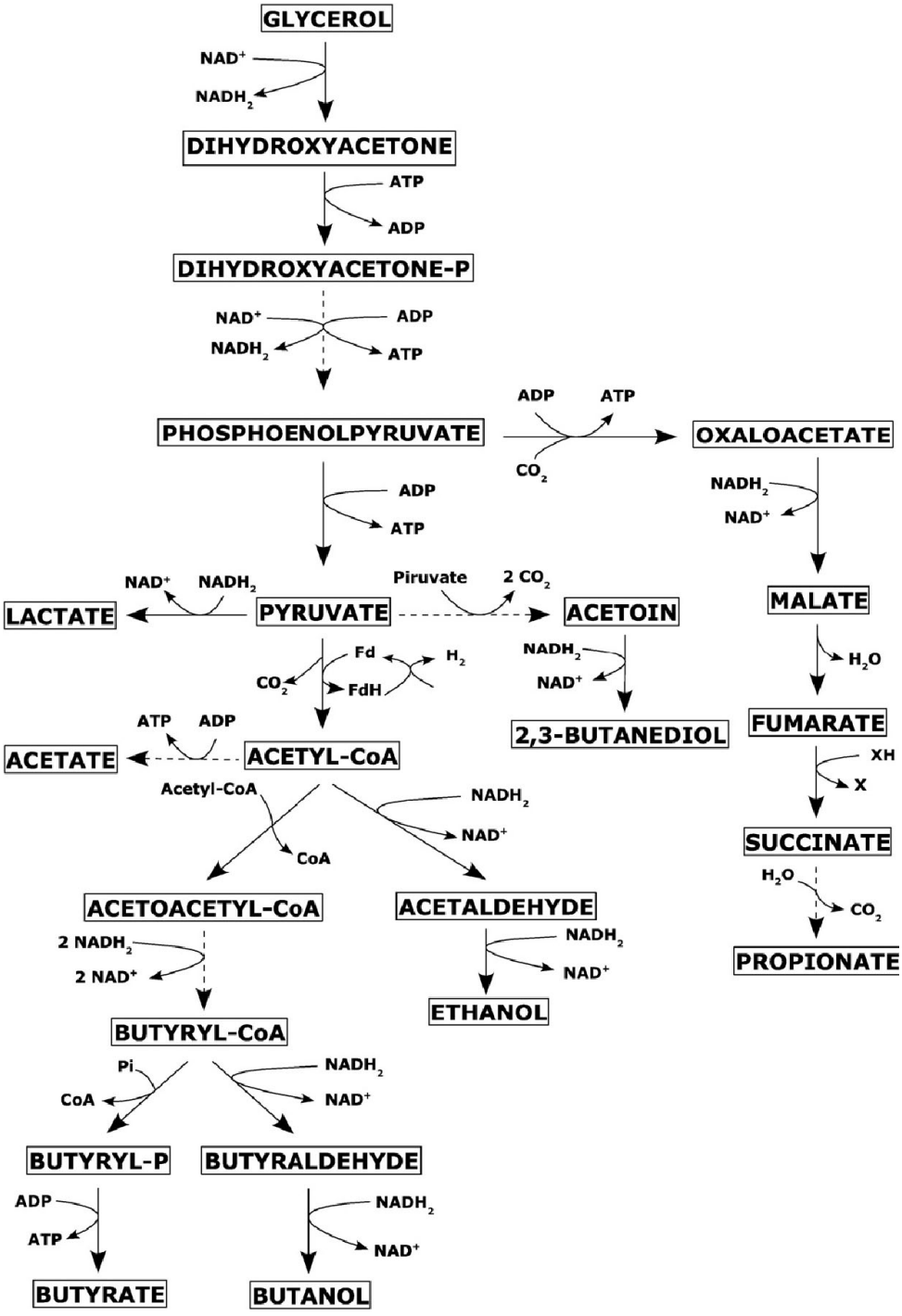

Figure 13 Overview of some possible end products for different microorganisms during glycerol degradation.

Source: Paula da Silva *et al*. (2009)

According to Ruch *et al*. (1974), the glycerol-3-phosphate pathway is responsible for the aerobic degradation of glycerol in *K. pneumonia* (formerly *K. aerogenes*), while the dihydroxyacetone pathway is responsible for the anaerobic degradation of this substrate. Fermentation from glycerol to ethanol or butanol by *C. pasteurianum* does not depend on the formation of by-products (Biebl, 2001), since hydrogen carriers are completely regenerated in the pathway (Biebl *et al*.,1998). Another example of a redox-balanced process is the conversion of glycerol into succinic acid. Although the pathways for ethanol and succinate are equivalent regarding the overall redox balance, the energetic contribution of the ethanologenic pathway is much higher, as 1 ATP is produced per each molecule of glycerol converted into ethanol, while production of energy in the succinate pathway is limited to the potential generation of a proton motive force by fumarate reductase (Dharmadi *et al*., 2006).

3. Amino acid fermentation

Amino acids are biomolecule found in all organisms. They can be classified into two groups by ability of the polarized light plane rotation: L-formed and D-formed. L-amino acids play important role in all life by serving as building block of enzyme, hormone, antibody and protein. Furthermore, they can also balance buffering capacity in blood and often function as chemical messengers in cell communication (Holum, 1982). In contrast, D-formed amino acid is rarely found. The optically active amino acids have been extensively studied. They are commonly occurring moiety in the rational design of chiral drugs such as anticancer compounds and viral inhibitors (Taylor *et al*., 1998).

3.1 L-amino acids

L-amino acids have stimulated the research on various methods for their synthesis such as chemical reaction, extraction from protein hydrolysates and fermentation (Hummel *et al*., 1987). However, the products contain both D-formed and L-formed amino acids. Therefore, some researchers have attempted to produce

L-amino acid by enzymatic method e.g. L-amino acid transaminase, amino acid racemase (Berberich *et al.*, 1968), L-aminopeptidase (Kamphuis *et al.*, 1992), and L-amino acid-β-decarboxylase (Yamamoto *et al.*, 1980). These methods lead to enantiomerically pure compounds. A recent alternative method is the enzymatic reductive amination of α-keto acid by amino acid dehydrogenase, a route which has the advantage of complete enantioselectivity and up to 100% towards selectivity of desired product. The enzymatic reaction is performed in a single reaction step, and allows synthesis of non-proteinogenic L-amino acids are not available through hydrolysis or fermentation (Kamphuis *et al.*, 1992).

Production of L-aromatic amino acids and derivative compounds is considerable industrial importance (Bongaerts *et al.*, 2001). Recently, the using of L-amino acids for many compounds synthesis are spread widely in animal nutrition, human medicine and the pharmaceutical industries. For example, L-leucine, L-valine, L-isoleucine are used as food and feed activities (Gu and Chang, 1990) while L-alanine is used as the precursor in drug production and can be also used as food additive due to its sweet taste (Suye *et al.*, 1992). L-phenylalanine, another interesting L-amino acid, is one of the essential starting materials for an artificial sweetener, aspartame (L-aspartate-L-phenylalanine-1-methyl ester, or Nutrasweet) (Chao *et al.*, 2000). In addition, non-natural amino acids are increasing in demand by the pharmaceutical industry for single-enantiomer drugs. They are in demand as precursor to ligands for synthesis, however, they are very expensive (Busca *et al.*, 2004).

3.2 L-phenylalanine

L-phenylalanine is L-aromatic amino acid (Figure 14), which is essential for human nutrition. It was used as a component of amino acid infusions for medical purposes. L-phenylalanine is also a raw material utilized in the manufacture of a dipeptide sweetener known as aspartame. Its applications range from feed to food and pharmaceutical products. At present, L-phenylalanine biosynthesis genes have been

well characterized and the enzymology of L-phenylalanine biosynthesis has been extensively investigated (Ohshima and Soda, 1989).

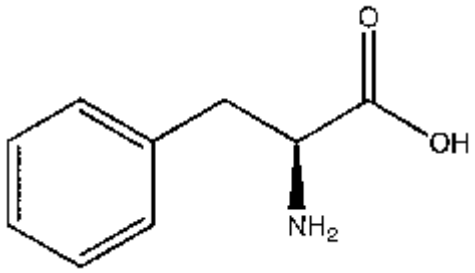

Figure 14 Chemical structure of L-phenylalanine

Various methods have been shown to achieve the production of L-phenylalanine. These include extraction from natural protein, chemical synthesis, fermentation and production from enzymatic method. Many enzymatic processes are known to produce L-phenylalanine from many substrate including *trans*-cinnamic acid (Yamada *et al.*, 1981), 5-banzylhydantoin and acetamidocinnamic acid (Nakamichi *et al*., 1989) by using L-phenylalanine amino-lyase, from phenylpyruvate by using L-phenylalanine dehydrogenase (Hummel and Kula, 1989) and from phenylpyruvate by using aminotransferase (Calton *et al*., 1986). The production method of L-phenylalanine from phenylpyruvate is very promising as a commercial process because it can be obtained at low cost and the productivity of L-phenylalanine is very high (Nakamichi *et al.*, 1989). L-phenylalanine is produced commercially mostly by fermentation involving recombinant *E. coli* and sucrose (Leuchtenberger *et al*., 2005). The yield of this amino acid on sucrose is about 0.20-0.25 g/g and the final concentration in the fermentation broth can be nearly 50 g/L (Leuchtenberger *et al*., 2005).

3.3 L-phenylalanine production by recombinant *Escherichia coli*

Theodor Escherich first described *E. coli* in 1885, as *Bacterium coli commune*, which he isolated from the feces of newborns. It was later renamed

Escherichia coli, and for many years the bacterium was simply considered to be a commensal organism of the large intestine. It was not until 1935 that a strain of *E. coli* was shown to be the cause of an outbreak of diarrhea among infants. *E. coli* and its relatives are known to microbiologists as "enteric bacteria", because they live in the intestinal tract of humans and other animals. The best known other enteric bacteria are *Salmonella*, which includes the agent of typhoid fever, and *Shigella*, which is the bacterial cause of dysentery. *E. coli* is in the bacterial family *Enterobacteriaceae*, which is made up of Gram-negative, nonsporeforming, rod-shaped bacteria that are often motile by means of flagella. The majority of strains grows well on the usual laboratory media in both the presence and absence of oxygen, and metabolism can be either by respiration or fermentation.

Physiologically, *E. coli* is versatile and well-adapted to its characteristic habitats. In the laboratory it can grow in media with glucose as the sole organic constituent. Wild-type *E. coli* has no growth factor requirements, and metabolically it can transform glucose or glycerol into all of the molecular components that make up the cell (Figure 15). The bacterium can grow in the presence or absence of O_2. Under anaerobic conditions, it will grow by means of fermentation, producing characteristic "mixed acids and gas" as end products. However, it can also grow by means of anaerobic respiration, since it is able to utilize NO_3 or fumarate as final electron acceptors for respiratory electron transport processes.

The research group of Department of Biochemistry, Faculty of Science, Chulalongkorn University has studied phenylalanine dehydrogenase from *Acinetobactor lwoffii* and this gene was cloned and expressed in *E. coli* BL21(DE3) host cell using expression vector, pET-17b (Sitthai, 2004). The expression of phenylalanine dehydrogenase by this strain was not affected by IPTG (isopropyl-β-D-thiogalactopyranoside) relative to control (Packdibamrung *et al.,* 2007; Sitthai, 2004). The recombinants *E. coli* were studied L-phenylalanine production on various carbon sources that was shown overproduction L-phenylalanine on glycerol as a carbon source (Packdibamrung *et al.,* 2007).

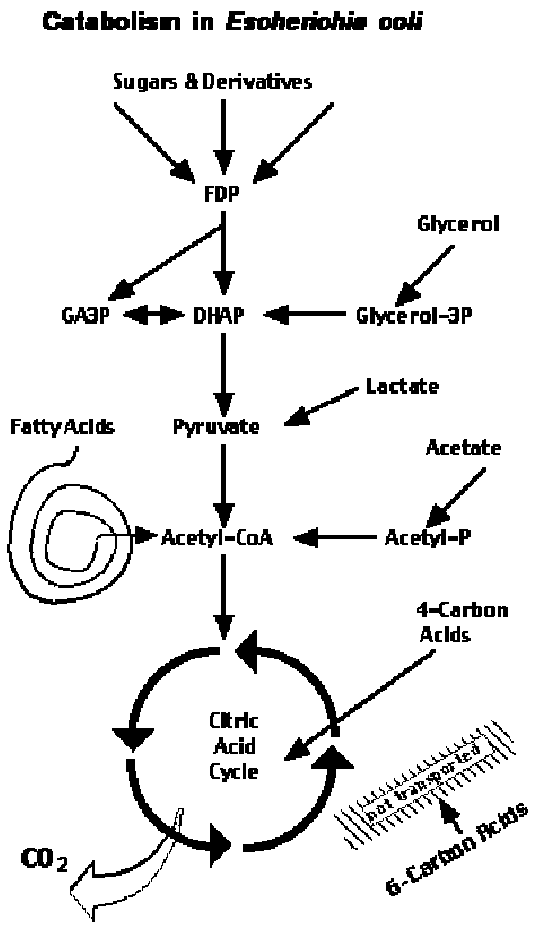

Figure 15 Catabolism in *E. coli*

Source: Clark (2002)

MATERIALS AND METHODS

Materials

1. Chemicals

1.1 Acetic acid: Merck, AR grade, Germany
1.2 Acetone: Merck, HPLC grade, Germany
1.3 Acetronitrile: Merck, HPLC grade, Germany
1.4 Acetylacetone: Merck, AR grade, Germany
1.5 Ager: commercial grade
1.6 Ampicillin: Sigma, AR grade, U.S.A.
1.7 Ammonium sulfate: commercial grade
1.8 Antifoam 1614: Dow Corning, AR grade, U.S.A.
1.9 Calcium chloride: commercial grade
1.10 Dabsyl-Cholride: Sigma, AR grade, U.S.A.
1.11 di-Potassium hydrogen phosphate anhydrous: commercial grade
1.12 Ethanol: Merck, HPLC grade, Germany
1.13 Glucose: commercial grade
1.14 Glycerol 99 % (for fermentation): commercial grade
1.15 Glycerol 99.5 % (standard preparation): Sigma, AR grade, U.S.A.
1.16 Hydrochloric acid: Merck, AR grade, Germany
1.17 Iron sulfate: commercial grade
1.18 Isopropanol: Merck, AR grade, Germany
1.19 L-phenylalanine: Merck, AR grade, Germany
1.20 Magnisium chloride: commercial grade
1.21 Manganise sulfate :commercial grade
1.22 Methyl red: Sigma, AR grade, U.S.A.
1.23 Peptone: Merck, AR grade, Germany
1.24 Potassium phosphate monobasic: commercial grade
1.25 Potassium phosphate monobasic: Merck, HPLC grade, Germany
1.26 2-propanol: Merck, HPLC grade, Germany

1.27 Sodium chloride: commercial grade

1.28 Sodium hydrogen carbonate: Merck, AR grade, Germany

1.29 Sodium hydroxide: Merck, AR grade, Germany

1.30 Sodium meta periodate: Merck, AR grade, Germany

1.31 Thiamine-HCl: Merck, AR grade, Germany

1.32 Yeast extracted: Merck, AR grade, Germany

1.33 Zinc sulfate: commercial grade

2. Equipments

2.1 Air pump (1.5 HP): model DR-115, Tong Cheng Iron works co., Ltd, Thailand

2.2 Autoclave: TAI CHANG medical instrument factory, Thailand

2.3 Autopipette: Pipetman, Galson, France

2.4 3.3 L BioFio III reactor and controller: New Brunswick Scientific, U.S.A.

2.5 Centrifuge: model PLC-012, Gemmy, Taiwan

2.6 Erlenmeyer flask

2.7 Glass plate

2.8 Glass tube

2.9 High Performance Liquid Chromatography (HPLC): Spectra SYSTEM, U.S.A.

2.10 HPLC Column: SUPEL COSIL^{TM} LC-DABS , 3µm , catalog#59137, U.S.A.

2.11 Hot air oven: Memmert air, model 500, Germany

2.12 Microcentrifuge tube

2.13 pH meter: ORION, model 420A, U.S.A.

2.14 Shaking Incubator: model SI2, China

2.15 Spectrophotometer: model Anthekie Advanced, Secomam, France

2.16 Syringe Filter: Pore size 0.2 µm, Whatman, U.S.A.

2.17 Vial glass: 2 mL

2.18 Vortex Mixer: model KMC-1300V, Scientific Industries, Inc, U.S.A.

2.19 Water cooler: model CB1D, Bosstech, Thailand

2.20 Balance: model BL210S, U.S.A.

Methods

1. Organism and Storage

Escherichia coli BL21(DE3) (genotype: F^- *omp*T *hsdS*$_B$ (r_B^- m_B^-) *gal dcm* (DE3)) was the host strain (Invitrogen Corporation, Carlsbad, CA, USA) used to express the phenylalanine dehydrogenase gene of *Acinetobacter lwoffii*. The phenylalanine dehydrogenase gene was cloned using pET-17b (Novagen; Merck KGaA, Darmstadt, Germany) as an expression vector. The plasmid contained an ampicillin resistance gene as the marker gene. This recombinant strain had been constructed at the Department of Biochemistry, Faculty of Science, Chulalongkorn University, Thailand (Sitthai, 2004) and was used throughout the study. The culture was maintained on Luria-Bertani (LB), pH 7.4 (Appendix Table A1) agar slant containing 50 mg/L ampicillin. The pH of the medium was adjusted to 7.4 and the culture was incubated at 37 °C for 24 hours. Sub-culturing was carried out once every 4 weeks and the culture was stored at 4 °C.

2. Inoculum preparation

Starter was prepared by transferring two loops of the stock culture into a 250 ml Erlenmeyer flask containing 50 ml of sterilized LB medium (Appendix Table A1) with 50 mg/L ampicillin, and incubated at 37 °C on a rotary platform shaker at 200 rpm for 16-18 hours to attain an optical density of 0.6-0.8 measured at 600 nm.

3. Screening experiments by one-factor at a time technique

The 50 ml medium working volume in a 250 ml Erlenmeyer flask was maintained on Basal salts, Trace salts and vitamins solution (Appendix Table A2) and containing 50 mg/L ampicillin. The medium flask was sterilized at 121 °C for 20 min.

The pH of the medium was adjusted to 7.4 and the culture was incubated at 37 °C for 32 hours at 200 rpm rotational speed and inoculum volume was 5 % (v/v) (from section 2) of the 50 mL working volume of the flask.

3.1. Effect of different C:N ratio between glycerol and ammonium sulfate

The effect of glycerol and $(NH_4)_2SO_4$ concentration ratio on biomass concentration was determined. The glycerol concentration was varied at 10, 20, 30, 40, 50, 60, 70, 80, 90 and 100 g/L while $(NH_4)_2SO_4$ was kept contant at 20 g/L. After that, the optimal glycerol concentration of biomass production was kept constant, and then the $(NH_4)_2SO_4$ concentration was varied at 10, 20, 30, 40, 50, 60, 70, 80, 90 and 100 g/L.

3.2. Effect of temperature and initial pH on growth

Recombinant *E. coli* BL21(DE3) was cultivated in 250 ml Erlenmeyer flasks containing a medium (Appendix Table A2) with optimal glycerol and $(NH_4)_2SO_4$ concentration from section 3.1) of 50 ml with 50 mg/L ampicillin. The temperatures (30, 37 and 45 °C) and pH (6.0, 6.5, 7.0, 7.4 and 8.0) were varied. The fermentation was incubated at 37 °C with a 200 rpm rotational speed for 32 hours.

4. Optimization of fermentation media by Response Surface Methodology (RSM)

Recombinant cells were cultivated in 250 ml Erlenmeyer flasks containing a medium of 50 ml with 50 mg/L ampicillin, of which the composition was specified according to the experimental design (Table 5 and 6), in an orbital shaker. The fermentation was incubated at 37 °C at a 200 rpm rotational speed for 32 hours and inoculum volume was 5 % (v/v) (from section 2) of the 50 mL working volume.

4.1 Fermentation medium

The basal culture media (Appendix Table A2) for L-phenylalanine production contained trace element solution (g/L): $FeSO_4$: 0.002; $MnSO_4$: 0.002; $CaCl_2$: 0.05; and $ZnSO_4$: 0.01. Glycerol and $(NH_4)_2SO_4$ were used as a carbon source and nitrogen sources. $MgCl_2$, KH_2PO_4 and K_2HPO_4 were used as salts (mixer of 14.30 % $MgCl_2$, 42.85 % KH_2PO_4 and 42.85 % K_2HPO_4). Yeast extract and thiamine-HCl were taken as vitamins (mixer of 90.91 % yeast extract and 9.09 % thiamine-HCl).

4.2 Experimental design

The growth medium contained carbon source (glycerol), inorganic nitrogen source ($(NH_4)_2SO_4$), salts ($MgCl_2$, K_2HPO_4 and KH_2PO_4) and vitamins (yeast extract and thiamine-HCl). The lowest and highest levels of glycerol, $(NH_4)_2SO_4$), salts, and vitamins are set as in Table 5.

Table 5 Levels of variables used in the experimental design.

Variables	Range and levels		
	-1	0	+1
G, Glycerol (gL^{-1})	10.0	55.0	100.0
N, $(NH_4)_2SO_4$ (gL^{-1})	10.0	55.0	100.0
S, Salts (gL^{-1})	1.750	4.375	7.000
V, Vitamins (gL^{-1})	0.550	1.375	2.200

A 2^4 full factorial central composite design (CCD) with eight star points and seven replicates at the center points leading to 31 runs was employed for the optimization of the culture conditions as given in Table 6. The variables were coded according to the following Equation (11) (Prakash *et al*., 2007).

$$x_i = \frac{(X_i - X_0)}{\Delta X} \; ; i = 1,2, \dots, k \qquad (11)$$

Where x_i = dimensionless value of a variable, X_i the real value of a variable, X_0 the value of X_1 at the center point, and ΔX the step change.

Table 6 Experimental plan of the optimization design

Runs	Concentration (gL^{-1})			
	Glycerol	$(NH_4)_2SO_4$	Salts[1]	Vitamins[2]
1	100.0	10.0	1.750	2.200
2	100.0	100.0	7.000	2.200
3	55.0	55.0	4.375	1.375
4	10.0	10.0	7.000	2.200
5	10.0	100.0	1.750	2.200
6	55.0	55.0	7.000	1.375
7	55.0	100.0	4.375	1.375
8	10.0	55.0	4.375	1.375
9	10.0	100.0	1.750	0.550
10	10.0	10.0	1.750	0.550
11	55.0	55.0	4.375	0.550
12	55.0	55.0	4.375	1.375
13	55.0	55.0	4.375	1.375
14	55.0	55.0	1.750	1.375
15	100.0	10.0	7.000	2.200
16	100.0	100.0	7.000	0.550
17	100.0	55.0	4.375	1.375
18	55.0	10.0	4.375	1.375
19	55.0	55.0	4.375	1.375
20	55.0	55.0	4.375	1.375
21	10.0	100.0	7.000	0.550
22	55.0	55.0	4.375	1.375
23	10.0	100.0	7.000	2.200
24	100.0	100.0	1.750	2200
25	10.0	10.0	7.000	0.550
26	10.0	10.0	1.750	2.200
27	100.0	10.0	7.000	0.550
28	100.0	10.0	1.750	0.550
29	55.0	55.0	4.375	2.200
30	55.0	55.0	4.375	1.375
31	100.0	100.0	1.750	2.200

[1] salts composes of 14.30 % $MgCl_2$, 42.85 % KH_2PO_4 and 42.85 % K_2HPO_4

[2] vitamins are the mixture of 90.91 % yeast extract and 9.09 % thiamine-HCl

The second-order polynomial, Equation (12), which includes all interaction terms, was used to calculate the predicted response (Prakash *et al*., 2007).

$$\hat{Y}_i = \beta_0 + \sum_{i=1}^{4} \beta_i x_i + \sum_{i=1}^{4} \beta_{ii} x_i^2 + \sum_{i.j=1}^{4} \beta_{ij} x_i x_j \quad (12)$$

Where $\hat{Y}_i$ is the predicted response, β_0 is the offset term, β_i is the linear effect, β_{ii} is the squared effect, β_{ij} is the interaction effect and $x_i, x_j$are independent variables.

The proportion of variance was explained by the polynomial models, which were given by the multiple coefficient of determination, R^2 and adjusted R^2 (sometimes written as $\bar{R}^2$). The adjusted R^2 is a modification of R^2 that adjusts for the number of explanatory terms in a model. Unlike R^2, the adjusted R^2 increases only if the new term would improve the model better than expected by chance. The adjusted R^2 can be negative, and will always be less than or equal to R^2 (Myers and Montgomery, 2002). Analysis of variance, (ANOVA) was performed using MINITAB software version 15.0 (Trial version).

5. Optimization of aeration and agitation rates in batch fermentation

The fermentation was conducted in a 3.3 L BioFio III reactor (New Brunswick Scientific, USA) of 2.0 L working volume. The vessel was under temperature and pH control. The pH probe was calibrated before sterilization. The entire reactor assembly was sterilized at 121 °C for 20 min in a sterilizer (Autoclave). After sterilization, the medium was cooled to room temperature, and both the dissolved oxygen (DO) and the pH probe were recalibrated.

5.1 Growth medium and culture conditions

The defined medium (mean values of Appendix Table A3 and A4) was used in the batch fermentation contained: 10 g/L glycerol; 50 g/L $(NH_4)_2SO_4$; 0.81 g/L $MgCl_2$; 2.43 g/L KH_2PO_4; 2.43 g/L K_2HPO_4; 0.085 g/L yeast extract; 0.0085 g/L

thiamine-HCl; 0.002 g/L $FeSO_4$; 0.002 g/L $MnSO_4$; 0.05 g/L $CaCl_2$; and 0.01 g/L $ZnSO_4$. The $MgCl_2$ solution was sterilized separately. The pH of the medium was adjusted and controlled at 7.4 until the end of the fermentation process. Foam was controlled by additing a sterilized silicon antifoaming reagent 1614 (Dow Corning).

Seed culture was cultivated in 250 mL Erlenmeyer flasks containing a medium of 50 mL with 50 mg/L ampicillin, of which the composition was specified according to the batch fermentation, in an orbital shaker. The seed culture was incubated at 37 °C at 200 rpm rotational speed and 5 % (v/v) to inoculum was used in the 2 liter fermentation broth working volume. Three molar of NaOH was applied to maintain the pH value of the broth.

5.2 Bioreactor configurations

All experimentation was carried out in a 3.3 L (2 L working volume) glass stirred tank baffled BioFio III reactor (New Brunswick Scientific, USA). The diameter D_T of the bioreactor is 13.8 cm equipped with a 12 mm polarographic dissolved Oxygen probe (InPro 6800 Series O_2 Sensors, METTLER -TOLEDO, Switzerland) and built in automatic feedback controller for temperature and agitation. The two –phase gas liquid dispersion ring with four small holes, were agitated with one six-blade Rushton turbine impeller (D_i = 6.2 cm) rotated on a 21.8 cm shaft. Aeration rate were controlled by a flow meter. The airflow was distributed at the bottom of the bioreactor. Four equally spaced baffles were used to enhance the mixing (Figure 16 and Appendix Figure E1).

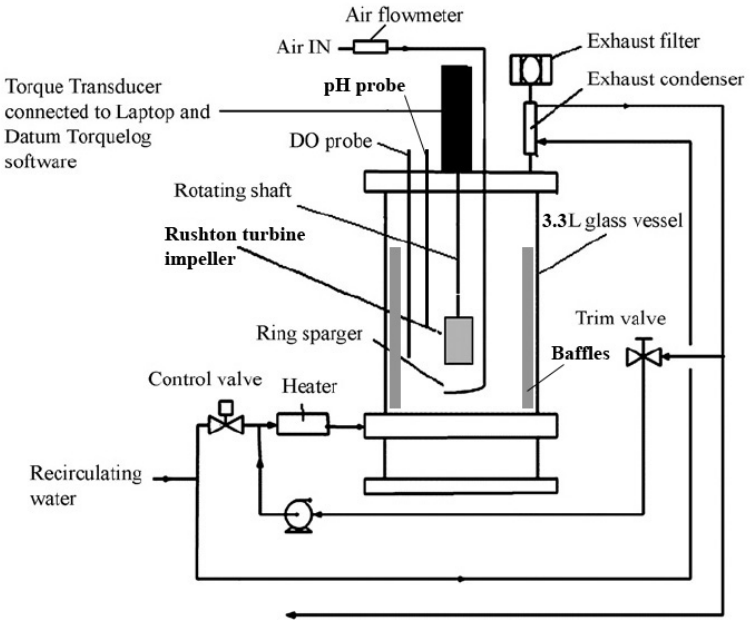

Figure 16 Schematic of experimental set up

Source: Modify from Boodhoo *et al.* (2008)

5.3 Fermentations

Recombinant *E. coli* BL21(DE3) fermentation was performed in the batch mode. Temperature was controlled at 37 °C. The effects of agitation and aeration on L-phenylalanine and biomass productions were investigated at the agitation speed of 200, 300, 400 and 500 rpm with fixed aeration rate at 4.0 L/min. Then aeration rate of 2.0, 4.0, 6.0 and 8.0 L/min was studied in the next steps with specific agitation rate at the optimal condition. The 0.2 mL/L antifoam 1614 (Dow Corning) was initially added to the fermenter. All experiments were carried out in triplicate.

6. The study of fed-batch fermentation

The fermentation medium (Appendix Table A3) was inoculated with 5 % (v/v) starter culture (biomass concentration about 1.4-1.6 g/L). Fermentation was carried

out at 37 °C, pH 7.4, atmospheric pressure. A constant pH was maintained by three molar sodium hydroxide solution. The experimental designs separated the fermentation into three phases. The first phase (0-12 hours) was conducted at agitation rate of 400 rpm and aeration rate was fixed at 8.0 L/min, 0.2 ml/L antifoam 1416 (Dow Corning) was initially added to the fermenter.

After 12 hours of the batch fermentation, the second phase (12-60 hour) was started by adding the glycerol pulse feeding (20 mL of 1000 g/L glycerol) every 12 hour till the end of the fermentation while the sterilization of 95 g/L solid $(NH_4)_2SO_4$ was started to add at the same time. However, $(NH_4)_2SO_4$ feeding was stopped after 12 hours. The second phase was conducted at the agitation rate of 400 rpm and aeration rate was fixed at 4.0 L/min. After 60 hours of fermentation, the last phase (60-72 hours) was started at the condition of the 400 rpm agitation rate and 8.0 L/min aeration rate. The experiment was carried out in triplicate and plotted the graph using mean value.

7. Assays

7.1 Cell concentration

Biomass concentration (grams of dry cell per liter) was determined from the optical density (OD) at 600 nm on a spectrophotometer. Five milliliter culture broth sample was diluted with deionized water (DW). After the OD values were measured, samples were transferred into 10 ml centrifuge tubes and centrifuged at 10,000 × g for 10 min. The cells were collected, washed, recentrifuged and collected again. The washed samples were dried at 80 °C for 24 hours or until a constant weighed. The OD and gravimetric data were used to develop a calibration curve (Appendix Figure C1) for all runs. The curve was linear within OD values of 0 to 1.2, with R^2 equal to 0.988. When OD values exceeded 1.0 absorbance unit, the samples were diluted to fit the calibration range and the corresponding cell mass concentration was multiplied by the dilution factor.

7.2 L-phenylalanine concentration

The concentration of L-phenylalanine in the fermentation broth was determined by high performance liquid chromatography (HPLC). A SUPELCO, LC-DABS HPLC column (15 cm× 4.6 mm ID, 3 µm particles) was used with a UV detector at 436 nm. The mobile phase A was 25 mM potassium dihydrogen phosphate, pH 6.8 and the mobile phase B was acetonitrile : 2- propanol, 75:25. Both mobile phases were mixing ratio 70:30 at a flow rate of 0.8-1.0 ml/min. Standard L-phenylalanine solutions were prepared at concentrations of 0.125, 0.25, 0.75, and 1.0 g/L. A 5 µl sample volume was injected into the column. The plot of L-phenylalanine concentration versus peak area was linear with R^2 equal to 0.918 (Appendix Figure C2). The culture samples were prepared by centrifugation at 10,000 x g for 10 min and the supernatant was collected, followed by filtration using nylon syringe filters (pore size 0.2 µm) and derivatization (Appendix B) of amino acid in supernatant with DABS-Cl (Stocchi *et al*., 1985). The L-phenylalanine and biomass productivities were then computed (Stanbury *et al*., 1999).

7.3 Glycerol concentration

The concentration of glycerol in the fermentation broth was determined by periodate method (Naviglio *et al*., 2007) which was determined from the optical density (OD) at 410 nm on a spectrophotometer (Appendix B). Standard glycerol solutions were prepared in concentrations of 0.0075, 0.015, 0.0225, 0.03, 0.0375, 0.045, 0.0525 and 0.06 g/L. The curve was linear within OD values of 0 to 1.4, with R^2 equal to 0.988. To determine the glycerol concentration in the fermentation broth, 10 ml sample was centrifuged at 10,000 × g for 10 min and the supernatant was collected. The glycerol content of the supernatant solution was calculated using the calibration curve (Appendix Figure C3) determined above. When glycerol concentrations exceeded 0.06 g/L, the samples were diluted to fit the calibration range and the corresponding glycerol concentration was multiplied by the dilution factor.

7.4 Ammonium sulfate ($(NH_4)_2SO_4$) concentration

The concentration of $(NH_4)_2SO_4$ in the fermentation broth was determined by method of Jeffery *et al.*, 1989 (Appendix B). This method was determined by titration with 0.1 M hydrochloric acid and use of methyl red was used of as an indicator. To determine the $(NH_4)_2SO_4$ concentration in the fermentation broth, 15 ml sample was centrifuged at 10,000 × g for 10 min and the supernatant was collected. The $(NH_4)_2SO_4$ content of the supernatant solution was calculated using the titration calculation method as shown in Appendix B. When $(NH_4)_2SO_4$ concentrations exceeded, the samples were diluted to low concentration range and the corresponding $(NH_4)_2SO_4$ concentration was multiplied by the dilution factor.

RESULTS AND DISCUSSION

1. Screening experiments by one-factor-at-a-time technique

These experiments were studied by varying the concentration of glycerol and ammonium sulfate and screening for the temperature and pH flexibility during fermentation.

1.1 Effect of different C:N ratio between glycerol and ammonium sulfate

The effects of initial glycerol and ammonium sulfate concentrations on the cell growth for recombinant *E. coli* BL21(DE3) were studied in the shake flask culture at 37 °C for 32 hours. As shown in Figure 17, the maximum biomass obtained from the shake flask fermentation was 0.947 g/L. The biomass concentration increased with the increasing of glycerol concentration at 10 g/L to 80 g/L. However, the biomass production decreased at the glycerol concentration higher than 80 g/L.

In Figure 18, this culture gave the maximum biomass concentration of about 1.785 g/L. Biomass increased with increasing of ammonium sulfate concentration. The biomass production decreased at the ammonium sulfate concentration higher than 80 g/L. However, the repression effect of high ammonium salt concentration on the recombinant *E. coli* growth was also observed by other authors (Thompson *et al*., 1985; Yee *et al*., 1993a). Thus, the medium containing 80 g/L glycerol and 80 g/L ammonium sulfate (C:N ratio 1:1) was used in the subsequent experiment.

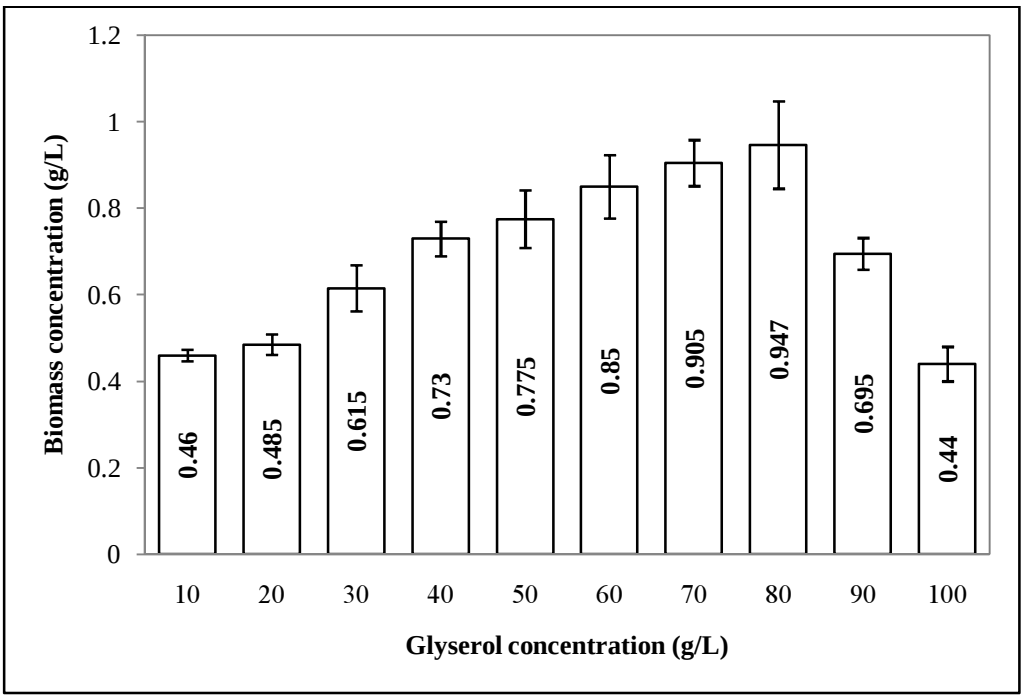

Figure 17 Effect of glycerol concentration on cell growth at 20 g/L $(NH_4)_2SO_4$

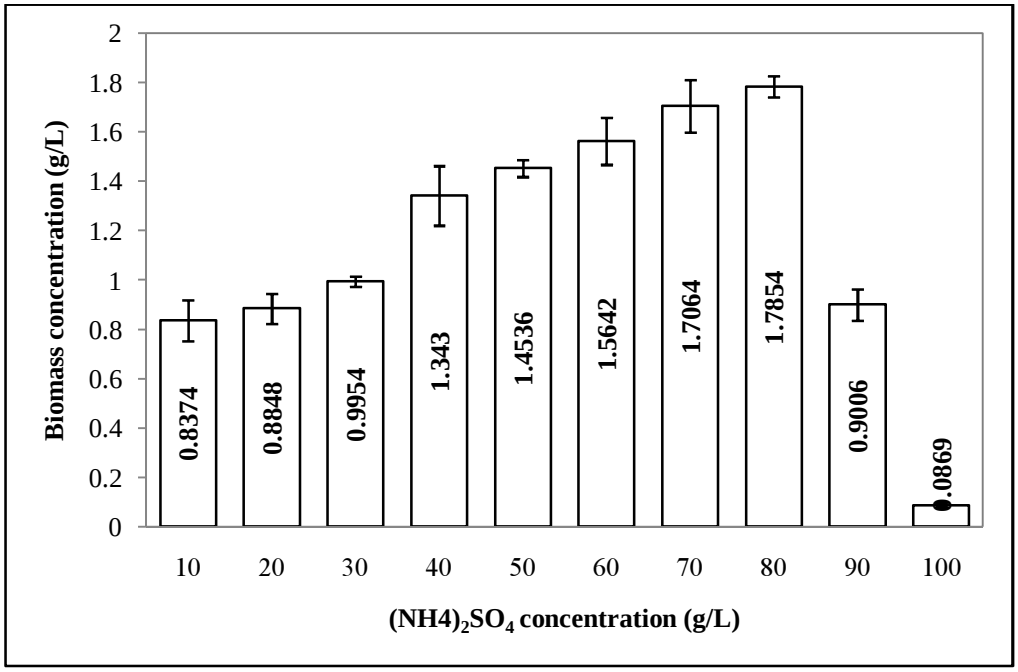

Figure 18 Effect of ammonium sulfate concentration on cell growth at 80 g/L glycerol

1.2 Effect of temperature and initial pH on cell growth

Recombinant *E. coli* BL21(DE3) was cultured in 80 g/L glycerol and 80 g/L ammonium sulfate media with shaking rate of 200 rpm at temperature range from 30 to 45 °C. It is shown that the highest biomass of recombinant *E. coli* is found at 37 °C (Figure 19). At the high temperature, the biomass concentration is low revealing the non-growth behavior. The investigation of the growth over the initial pH range 6.0-8.0 at the optimum temperature of recombinant *E. coli* was shown in Figure 20. When the initial pH level rose from 6.0 to 7.4-8.0, there was an increase in the biomass production from 1.205 to 1.715 g/L. The optimum initial pH values for biomass production was 7.4-8.0 for recombinant *E. coli* BL21(DE3). The results showed a significant effect of different temperature and initial pH values on the cell growth of recombinant *E. coli*. It implied that the temperature and pH control could stimulate the microorganism to produce bio-molecules (Stanbury *et al.*, 1999).

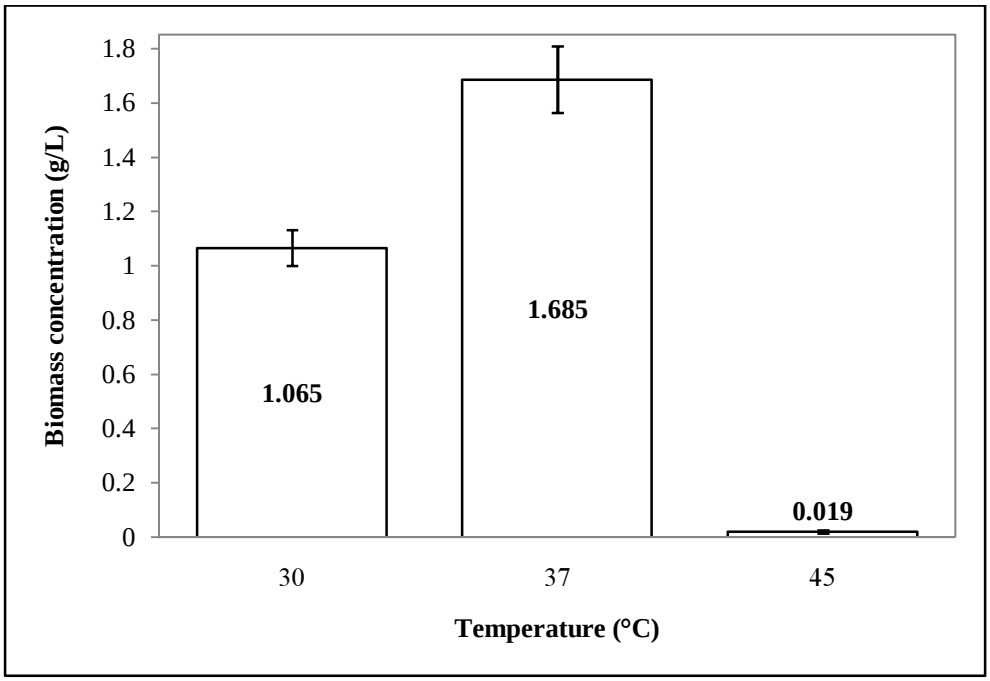

Figure 19 Effect of temperature on cell growth

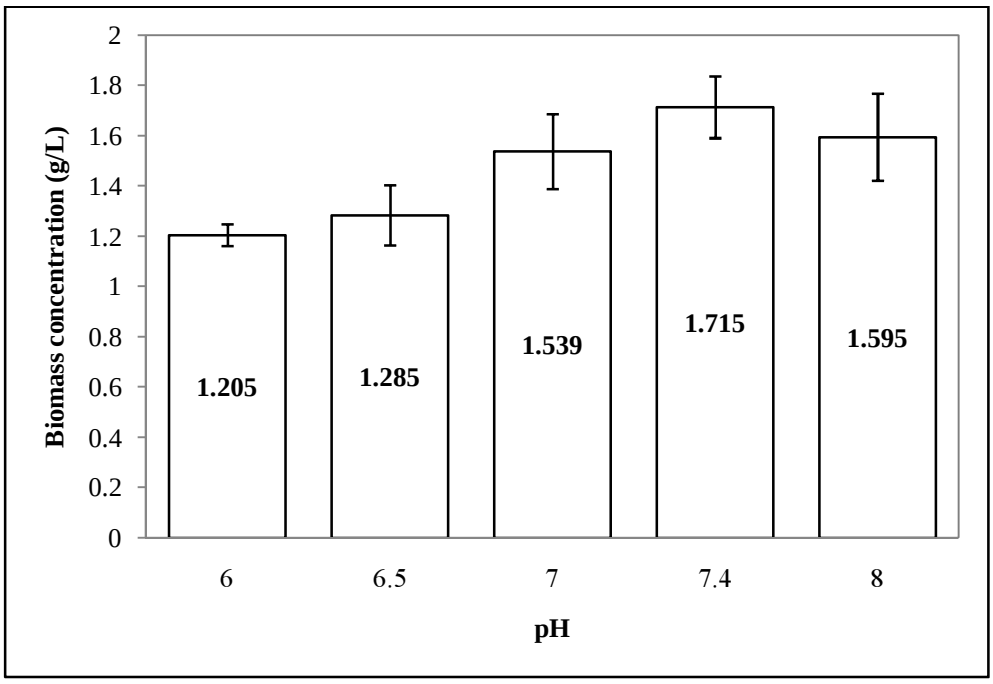

Figure 20 Effect of pH on cell growth

Figure 21 shows the time profile of the cell growth during a typical batch cultivation of recombinant *E. coli* BL21(DE3) in the optimum medium. The maximum value of the biomass production on initial pH 7.4 (not adjust during fermentation) of about 2.0 g/L was obtained and then the biomass was decreased rapidly after 48 hours. The maximum value of the biomass production of 2.91 g/L was obtained when pH was adjusted at 48 hours of fermentation and kept constant for the rest of the cultivation time. Concomitantly, significant decrease in pH value was observed during the phase of recombinant *E. coli* growth and it was reported that a decreasing of pH value would inhibit the cell growth (Mizutani *et al.*, 1986).

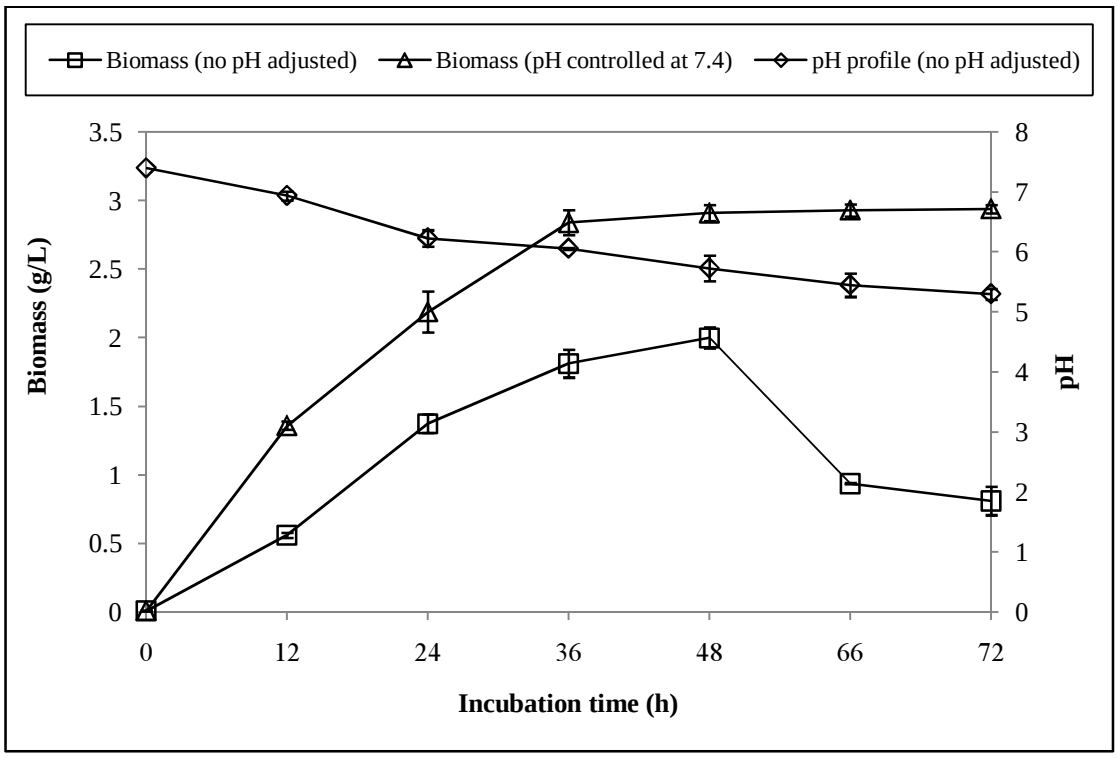

Figure 21 Effect of pH changed during batch fermentation on recombinant *E. coli* BL21(DE3) growth at 37 ℃ and 200 rpm on 3.3 liter bioreactor (2.0 liter working volume).

2. Optimization of fermentation media by Response Surface Methodology (RSM)

A factorial central composite design (CCD) was employed to analyze the interactive effect of those parameters and to obtain the optimum condition. A 2^4 full CCD with eight axial points and seven replications at the center points leading to 31 runs were employed for the optimization of the culture conditions as given in Table 7.

Table 7 Experimental plan of the optimization design with the experimental and predicted values for the biomass and L-phenylalanine production of recombinant *E.coli* BL21(DE3) cells in different media.

Runs	Concentration (gL^{-1})				Biomass (gL^{-1})			L-Phenylalanine (gL^{-1})		
	Glycerol	$(NH_4)_2SO_4$	Salts[1]	Vitamins[2]	Experimental	SD	Predicted	Experimental	SD	Predicted
1	100.0	10.0	1.750	2.200	4.350	0.082	4.341	1.020	0.023	1.038
2	100.0	100.0	7.000	2.200	4.445	0.072	4.494	3.466	0.094	2.761
3	55.0	55.0	4.375	1.375	4.305	0.070	4.438	3.248	0.281	3.674
4	10.0	10.0	7.000	2.200	4.897	0.095	5.000	4.090	0.235	3.597
5	10.0	100.0	1.750	2.200	4.659	0.052	4.736	5.979	0.585	5.812
6	55.0	55.0	7.000	1.375	4.504	0.053	4.542	2.542	0.154	3.218
7	55.0	100.0	4.375	1.375	4.504	0.036	4.291	3.777	0.160	4.342
8	10.0	55.0	4.375	1.375	4.798	0.046	4.721	5.007	0.413	5.504
9	10.0	100.0	1.750	0.550	4.038	0.061	4.153	5.731	0.649	5.554
10	10.0	10.0	1.750	0.550	4.794	0.052	4.746	2.169	0.223	2.465
11	55.0	55.0	4.375	0.550	4.397	0.018	4.360	3.141	0.219	3.280
12	55.0	55.0	4.375	1.375	4.440	0.056	4.438	4.180	0.302	3.674
13	55.0	55.0	4.375	1.375	4.452	0.055	4.438	3.405	0.423	3.674
14	55.0	55.0	1.750	1.375	4.452	0.055	4.354	3.468	0.228	3.204
15	100.0	10.0	7.000	2.200	4.487	0.018	4.390	0.931	0.076	1.414
16	100.0	100.0	7.000	0.550	4.073	0.026	4.158	3.320	0.246	3.592
17	100.0	55.0	4.375	1.375	4.288	0.086	4.304	3.528	0.159	3.443
18	55.0	10.0	4.375	1.375	4.383	0.036	4.536	2.278	0.173	2.124
19	55.0	55.0	4.375	1.375	4.340	0.036	4.438	4.489	0.202	3.674
20	55.0	55.0	4.375	1.375	4.366	0.044	4.438	3.983	0.469	3.674
21	10.0	100.0	7.000	0.550	4.469	0.020	4.480	5.632	0.609	5.206
22	55.0	55.0	4.375	1.375	4.383	0.036	4.438	3.703	0.226	3.674
23	10.0	100.0	7.000	2.200	4.987	0.036	4.915	5.876	0.519	6.219
24	100.0	100.0	1.750	2200	4.357	0.036	4.414	1.814	0.180	2.026
25	10.0	10.0	7.000	0.550	5.082	0.056	5.043	1.664	0.290	1.758
26	10.0	10.0	1.750	2.200	4.920	0.027	4.852	3.512	0.263	3.548
27	100.0	10.0	7.000	0.550	4.607	0.072	4.531	1.662	0.278	1.420
28	100.0	10.0	1.750	0.550	4.245	0.078	4.334	1.836	0.158	1.799
29	55.0	55.0	4.375	2.200	4.604	0.056	4.581	3.133	0.335	3.406
30	55.0	55.0	4.375	1.375	4.589	0.088	4.438	3.944	0.410	3.674
31	100.0	100.0	1.750	2.200	4.031	0.035	3.929	3.529	0.122	3.613

[1] salts composes of 14.30 % $MgCl_2$, 42.85 % KH_2PO_4 and 42.85 % K_2HPO_4

[2] vitamins are the mixture of 90.91 % yeast extract and 9.09 % thiamine-HCl

2.1 Construction of the models

The effects of four variables namely glycerol, $(NH_4)_2SO_4$, salts and vitamins on the L-phenylalanine and biomass productions were studied. The L-Phenylalanine and biomass productivities were selected as the response due to the different cycles of the runs. The experimental design matrix is presented in Table 7. Thirty one experiments were performed in triplicate.

By applying the multiple regression analysis on the experimentally determined data, the following second order polynomial equation was selected to represent the biomass and L-phenylalanine productions adequately. The coefficients of the calculated regression models (Equation 13 and Equation 14) are listed in Table 8, containing one constant, four linear, four quadratic and six interaction terms.

$$Y_{Biomass}\,(g/L) = 4.82395 - 0.08181G - 0.07404N + 0.01905S - 0.00723V + 0.00372G^2 - 0.00119N^2 + 0.00018S^2 + 0.00059V^2 + 0.00233GN - 0.00073GS - 0.00073GV + 0.00023NS + 0.00354NV - 0.00066SV \quad (13)$$

$$Y_{L\text{-}phe}\,(g/L) = 0.830645 - 0.436399G + 0.615735N + 0.136773S + 0.222248V + 0.039486G^2 - 0.021768N^2 - 0.00823S^2 - 0.005883V^2 - 0.015750GN - 0.002428GS - 0.013661GV + 0.002653NS - 0.00611NV - 0.003358SV \quad (14)$$

When the values of G, N, S and V were substituted in the above equations, the predicted dry cell weight ($Y_{Biomass}$) and L-phenylalanine ($Y_{L\text{-}phe}$) were obtained (Table 7).

The significance of each coefficient was determined by *p*-value, which is listed in Table 8. The smaller *p*-value ($p \leq 0.05$), the more significant is the corresponding coefficient. In Table 8, the experiment shows that the interaction effect of $(NH_4)_2SO_4$ and vitamins (NV) is significant for the biomass production, while for the L-phenylalanine production, the two first orders (G and N), one second order (G^2)

and two interactions (GN and GV) were also found to be significant. This indicates that they can act as limiting nutrients and small variations in their concentration can alter either the growth rate or the product formation rate or both to a considerable extent.

Table 8 Model coefficient estimated by multiplies linear regression

Parameters	Coefficient of biomass	Coefficient of L-phenylalanine	*P*-value of biomass	*P*-value of L-phenylalanine
constant	4.82395	0.830645	0.000	0.390
G	-0.08181	-0.436399	0.088	0.035
N	-0.07404	0.615735	0.120	0.005
S	0.01905	0.136773	0.594	0.368
V	-0.00723	0.222248	0.839	0.152
G^2	0.00372	0.039486	0.332	0.023
N^2	-0.00119	-0.021768	0.753	0.184
S^2	0.00018	-0.008230	0.892	0.164
V^2	0.00059	-0.005883	0.668	0.312
GN	0.00233	-0.015750	0.139	0.024
GS	-0.00073	0.002428	0.426	0.530
GV	-0.00073	-0.013661	0.426	0.002
NS	0.00023	0.002653	0.801	0.493
NV	0.00354	-0.006110	0.001	0.126
SV	-0.00066	0.003358	0.239	0.159

G = glycerol, N = $(NH_4)_2SO_4$, S = salts, V = vitamins

The parity plot showed a satisfactory correlation between the experimental and the predicted values of biomass and L-phenylalanine production (Figures 22). The points cluster around the diagonal line indicated the optimal fit of the models, since the deviation between the experimental and predicted values was minimal.

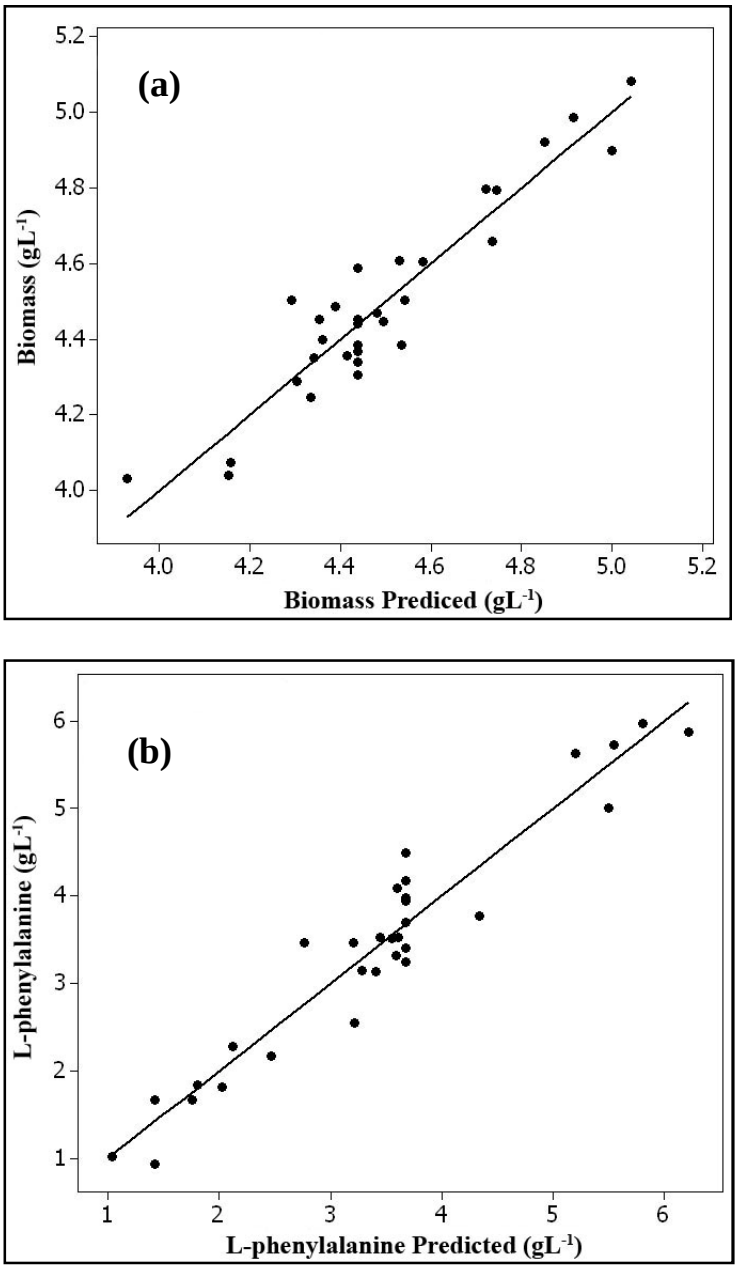

Figure 22 Compared plot between predicted biomass (a) and L-phenylalanine concentration (b) (Equation 13 and 14) and experimental data (Table 7)

The results of the second order response surface model in the form of the analysis of variance (ANOVA) were given in Table 9. The Lack of fit was tested by comparing the $F = MS_{lack\ of\ fit} / MS_{pure\ error}$ (Table 9) to a suitable upper percentage point of F (0.05, $DF_{lack\ of\ fit}$, $DF_{pure\ error}$) in the distribution table. The larger value of

F (in distribution table) showed the better fitted model (Box and Draper, 2007). In this case, *F*-value from the distribution table for the biomass and L-phenylalanine concentrations were 4.06 while the calculated values were 2.06 and 1.63. Therefore, the models are good fitted. In addition, the values of the adjusted determination coefficient (adjusted R^2 = 0.78 for biomass and R^2 = 0.86 for L- phenylalanine) are also good to advocate a good significance of the models. The high values of the correlation coefficient (R^2 = 0.89 for the biomass and R^2 = 0.93 for the L-phenylalanine) justified a good correlation between the independent variables (Nikerel *et al*., 2006; Prakash *et al*., 2007; Zheng *et al*., 2008).

Table 9 ANOVA for full quadratic model

Source	DF	SS	MS	*F*-value	*P*-value
Model *(Biomass)*	14	1.80347	0.128819	8.75	0.000
Residual Error *(Biomass)*	16	0.23542	0.014714		
Lack-of-Fit *(Biomass)*	10	0.18233	0.018233	2.06	0.195
Pure Error *(Biomass)*	6	0.05309	0.008849		
Total *(Biomass)*	30	2.03889			
Model *(L-phe)*	14	51.220	3.6586	14.01	0.000
Residual Error *(L-phe)*	16	4.178	0.2611		
Lack-of-Fit *(L-phe)*	10	3.052	0.3052	1.63	0.285
Pure Error *(L-phe))*	6	1.126	0.1877		
Total *(L-phe)*	30	55.398			

Biomass; R^2 = 0.89, adjusted R^2 = 0.78 and L-phenylalanine; R^2 = 0.93, adjusted R^2 = 0.86

2.2 Optimization of medium

The full quadratic model equation (Equation 13 and Equation 14) was optimized using Simultaneous Optimization Technique (Myers and Montgomery, 2002) that included in the Response Optimizer function in MINITAB program to

maximize biomass and L-phenylalanine concentrations. The optimum medium composition was found at 10 g/L glycerol, 10 g/L $(NH_4)_2SO_4$, 0.98 g/L $MgCl_2$, 2.94 g/L K_2HPO_4, 2.94 g/L KH_2PO_4, 0.878 g/L yeast extract and 0.0878 g/L thiamine-HCl with a prediction of 5.0 g DCW/L of biomass production and 10 g/L glycerol, 100 g/L $(NH_4)_2SO_4$, 0.64 g/L $MgCl_2$, 1.91 g/L K_2HPO_4, 1.91 g/L KH_2PO_4, 0.823 g/L yeast extract and 0.0823 g/L thiamine-HCl with a prediction of L-phenylalanine production of 6.2 g/L. Note that salts composed of $MgCl_2$, K_2HPO_4, and KH_2PO_4 and vitamins contained yeast extract and thiamine-HCl.

2.3 Identifying the affected factors

Figures 23 to 28 represent the response surface and contour plots for the optimization of medium constituents of the biomass and L-phenylalanine productions.

The effect of glycerol and $(NH_4)_2SO_4$ on the biomass production was shown in Figure 23. There was the optimum in the biomass production (more than 4.6 g/L) when low concentration of glycerol (10-15 g/L) and $(NH_4)_2SO_4$ (20-30 g/L) were used. The interaction effect of glycerol and salts on the biomass production was shown in Figure 24. An increased in the salt concentration to 2.2 g/L at the low concentration solution of glycerol (10-20 g/L) increased the biomass production to the maximum level (more than 4.6 g/L).

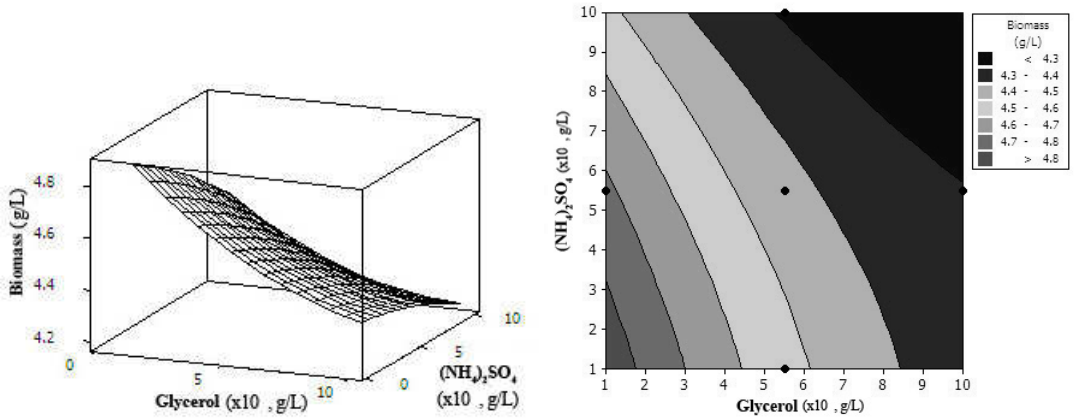

Figure 23 Response surface and contour plot of glycerol, $(NH_4)_2SO_4$ biomass production at constant salts and vitamins concentrations

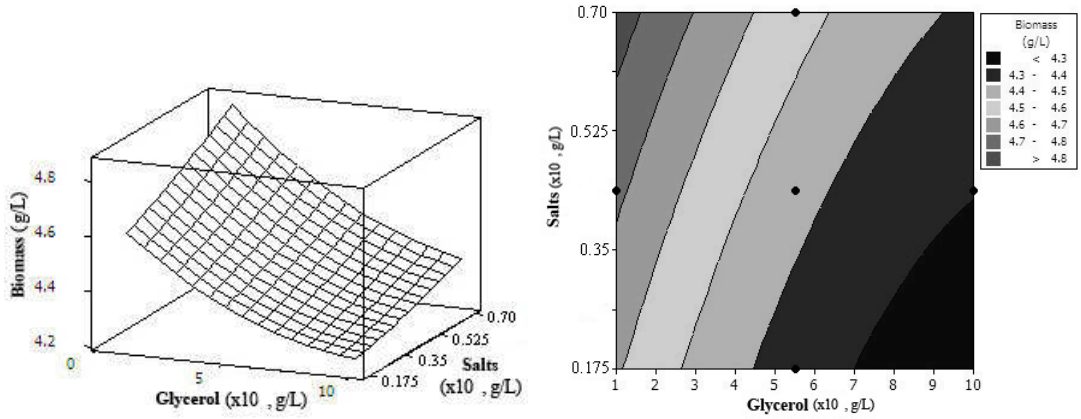

Figure 24 Response surface and contour plot of glycerol, salts and biomass production at constant $(NH_4)_2SO_4$ and vitamins concentrations

A similar effect of salt concentration on the biomass production was observed for the vitamin concentration (Figure 25). An increased in the salt concentration with vitamin added at the high concentration (7.0 and 2.2 g/L) increased the biomass production to more than 4.6 g/L. However, the trend was reversed at low salt (less than 5.25 g/L) and low vitamin (less than 1.90 g/L) concentrations.

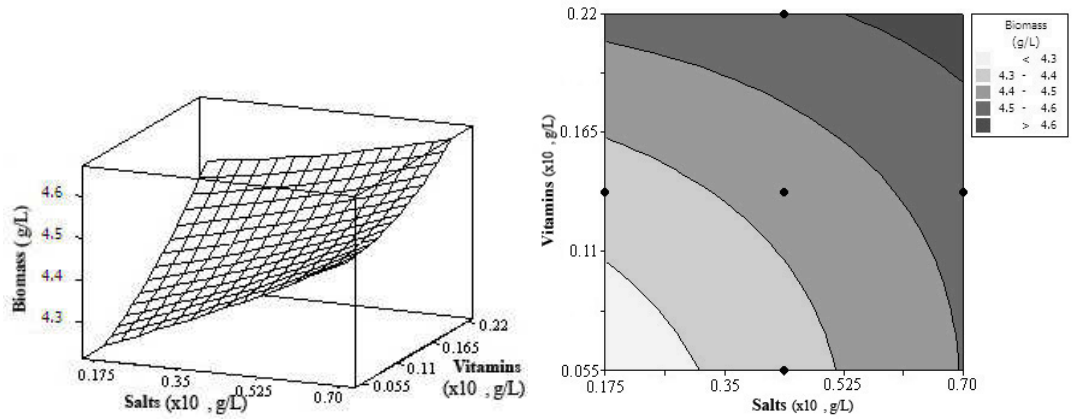

Figure 25 Response surface and contour plot of salts, vitamins and biomass production at constant glycerol and $(NH_4)_2SO_4$ concentrations

The interaction effect of $(NH_4)_2SO_4$ and vitamin concentrations on the biomass production in Figure 26 did not clearly indicate a proper combination of the biomass production. In Figure 27, an increased in the salt concentration to 7.0 g/L at low $(NH_4)_2SO_4$ concentration (10-30 g/L) increased the biomass production to the maximum level (more than 4.6 g/L).

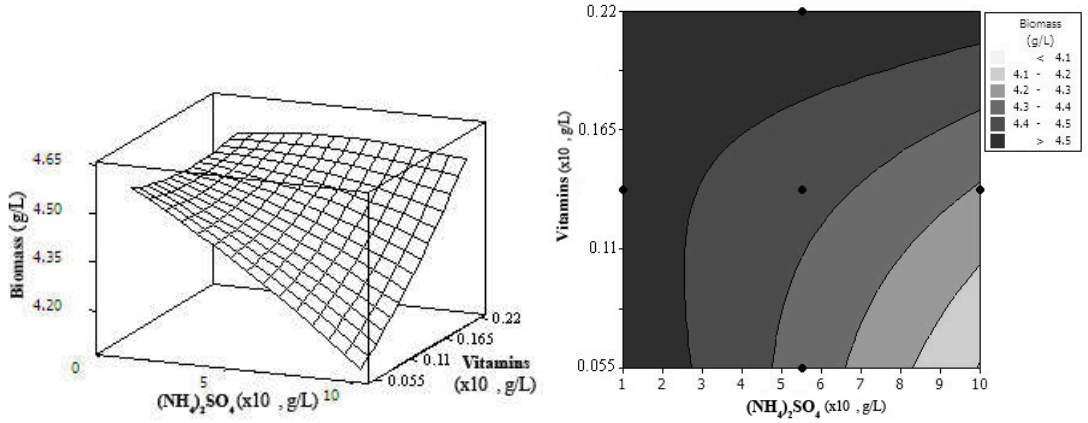

Figure 26 Response surface and contour plot of $(NH_4)_2SO_4$, vitamins and biomass production at constant glycerol and salts concentrations

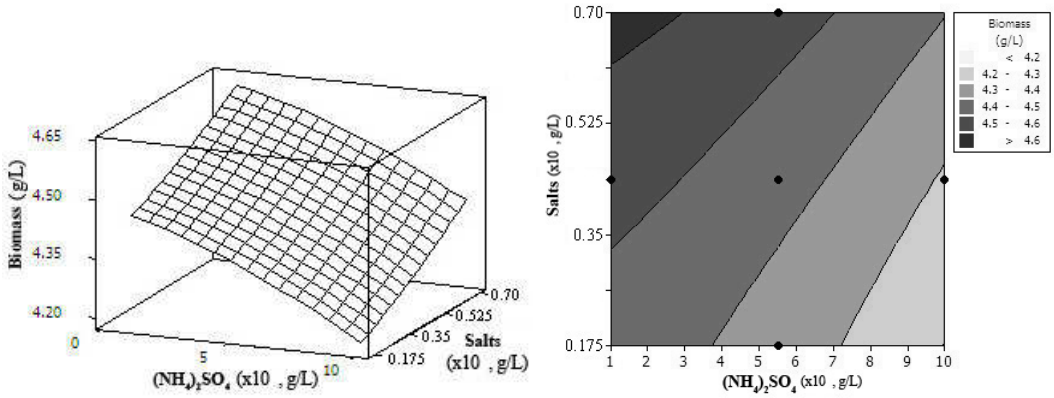

Figure 27 Response surface and contour plot of $(NH_4)_2SO_4$, salts and biomass production at constant glycerol and vitamins concentrations

The effect of glycerol and vitamin concentrations on the biomass production was shown in Figure 28. An increased in the vitamin concentration to 7.0 g/L at low glycerol concentration (10 g/L) increased the biomass production to the maximum value.

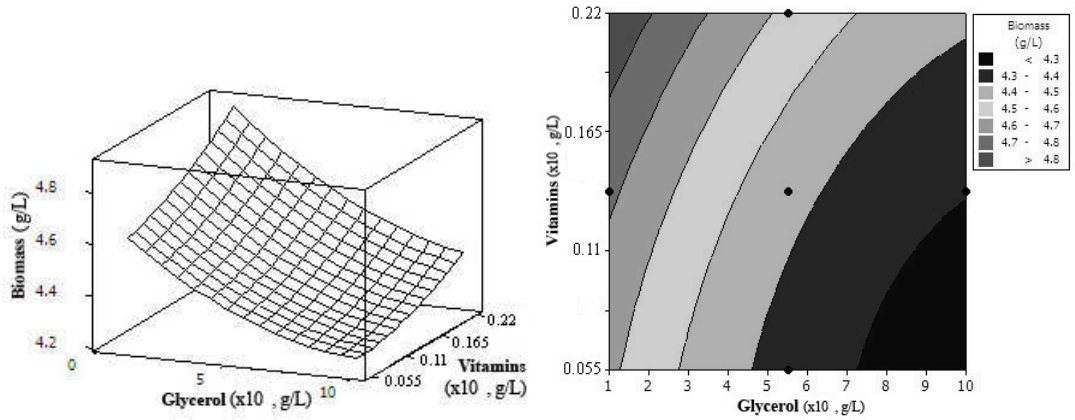

Figure 28 Response surface and contour plot of glycerol, vitamins and biomass production at constant $(NH_4)_2SO_4$ and salts concentration

Figure 29-34 represent the optimization of the medium constituents for the L-phenylalanine production. The RSM and contour plot represent the maximum L-phenylalanine production against glycerol and $(NH_4)_2SO_4$.

Figure 29, shows the maximum L-phenylalanine production (more than 6.0 g/L) at the concentrations of glycerol less than 20 g/L and $(NH_4)_2SO_4$ more than 75 g/L. However, the trend was decreased at high glycerol concentration (more than 20 g/L). The effect of glycerol as shown in Figure 30 and Figure 31 indicated that the increase of the glycerol concentration of above 10-20 g/L shows repressive effect, whereas at less than 15 g/L of glycerol concentration results of the L-phenylalanine production higher than 6.0 g/L.

From Figure 30, the maximum L-phenylalanine production (more than 6.0 g/L) occurred at 10-15 g/L glycerol concentration and 1.6-2.2 g/L vitamin concentration.

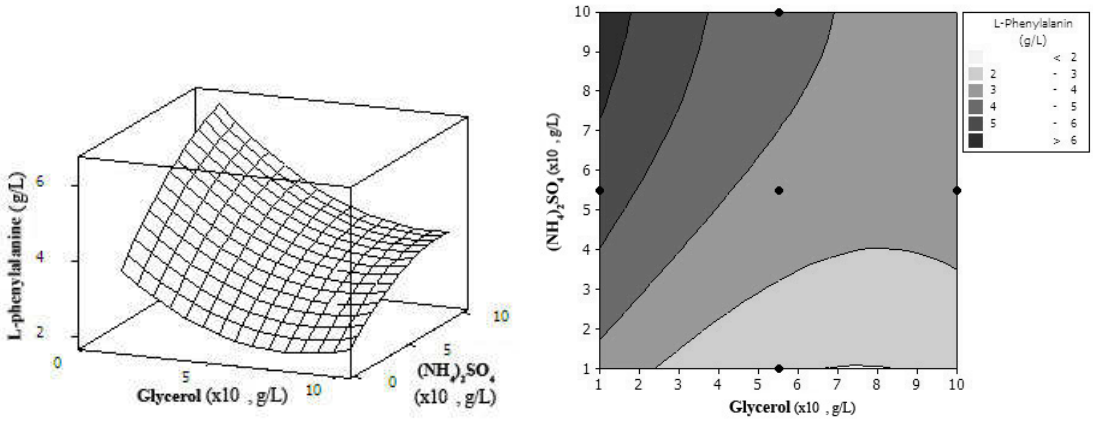

Figure 29 Response surface and contour plot of glycerol, $(NH_4)_2SO_4$ and L-phenylalanine production at constant at constant salts and vitamins concentration

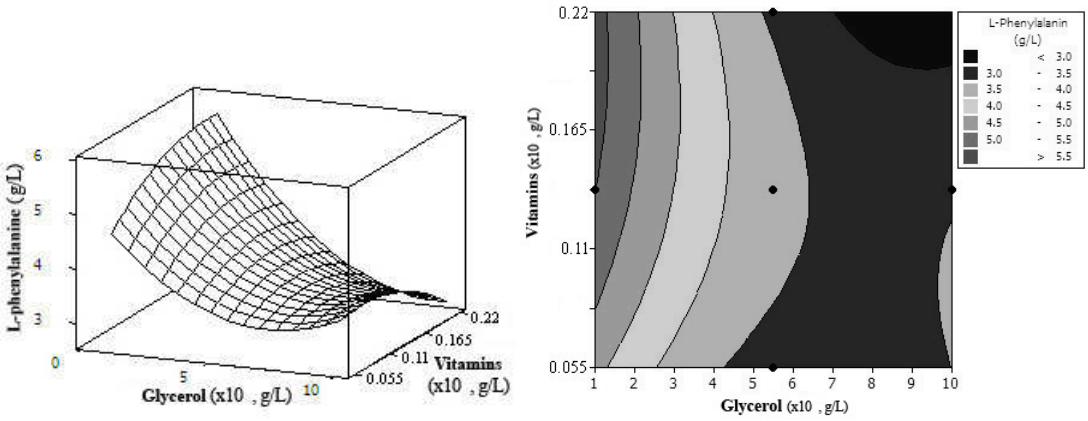

Figure 30 Response surface and contour plot of glycerol, vitamins and L-phenylalanine production at constant salts and $(NH_4)_2SO_4$ concentration

The effect of glycerol and salt concentrations on the L-phenylalanine production was shown in Figure 31. There was the optimum in L-phenylalanine production (more than 5.5 g/L) at low concentration of glycerol (10-15 g/L) and salt concentration (3.5-5.25 g/L).

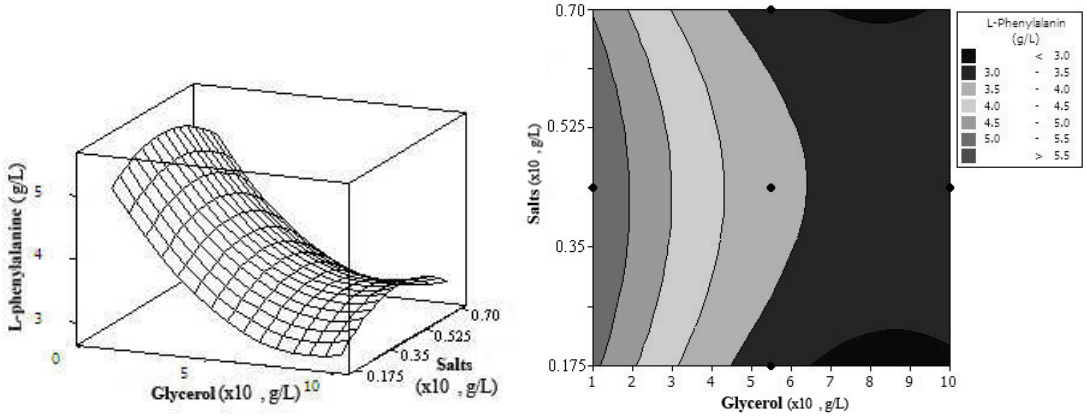

Figure 31 Response surface and contour plot of glycerol, salts and L-phenylalanine production at constant vitamins and $(NH_4)_2SO_4$ concentration

The interaction effect of $(NH_4)_2SO_4$ and vitamin concentrations on the L-phenylalanine production (Figure 32) indicated that the increasing of the concentration of $(NH_4)_2SO_4$ higher than 75-100 g/L showed the direct effect on the increasing of L-phenylalanine production. The 1.1-1.65 g/L vitamin concentration could increase the phenylalanine concentration to more than 4.0 g/L.

The effect of the $(NH_4)_2SO_4$ and salt concentrations on the L-phenylalanine production was shown in Figure 33. The L-phenylalanine production reached the maximum level at 4.0 g/L in 70-100 g/L $(NH_4)_2SO_4$ and 3.5-5.25 g/L salt concentration.

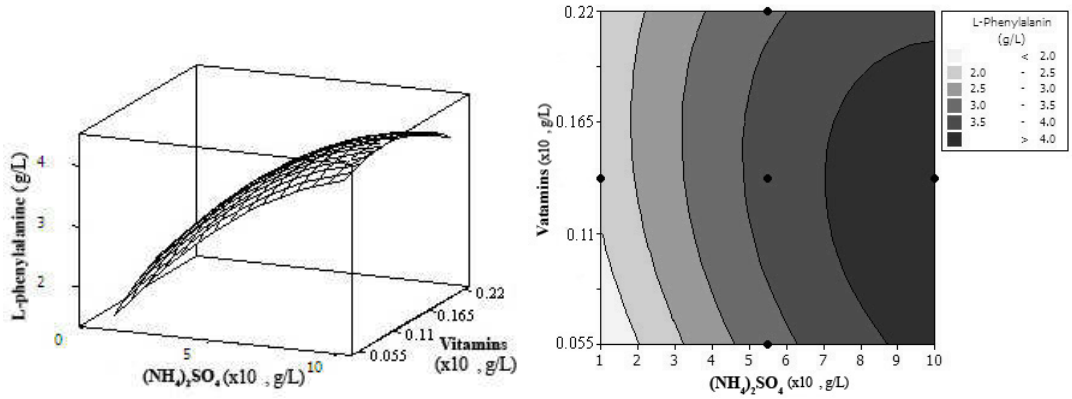

Figure 32 Response surface and contour plot of $(NH_4)_2SO_4$, vitamins and L-phenylalanine production at constant glycerol and salts concentration

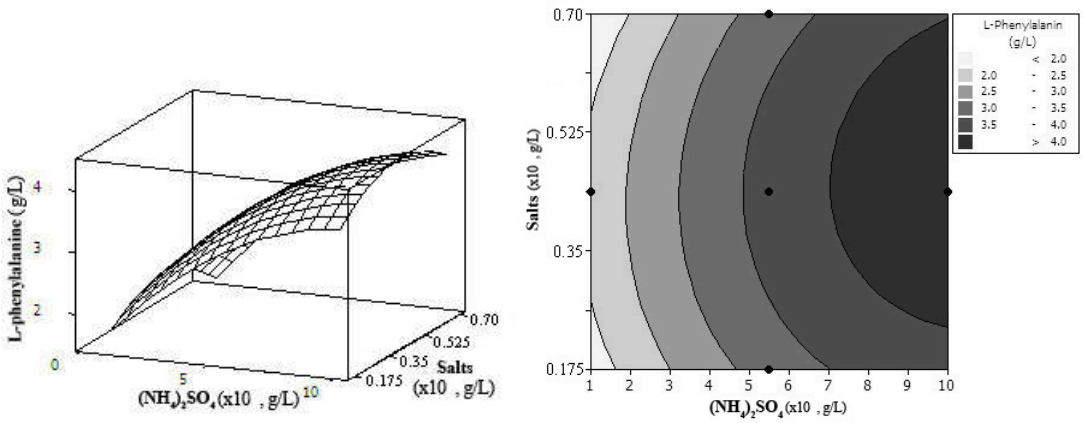

Figure 33 Response surface and contour plot of $(NH_4)_2SO_4$, salts and L-phenylalanine production at constant glycerol and vitamins concentration

A similar response effect as shown in figure 32 and 33 was observed at any level of the salt concentration. An increase in vitamin concentration up to 1.375 g/L with salt concentration up to 4.375 g/L increased the L-phenylalanine production to the maximum concentration of more than 3.6 g/L. Over the maximum concentration, increasing vitamin and salt concentrations decreased the L-phenylalanine production as show in Figure 34.

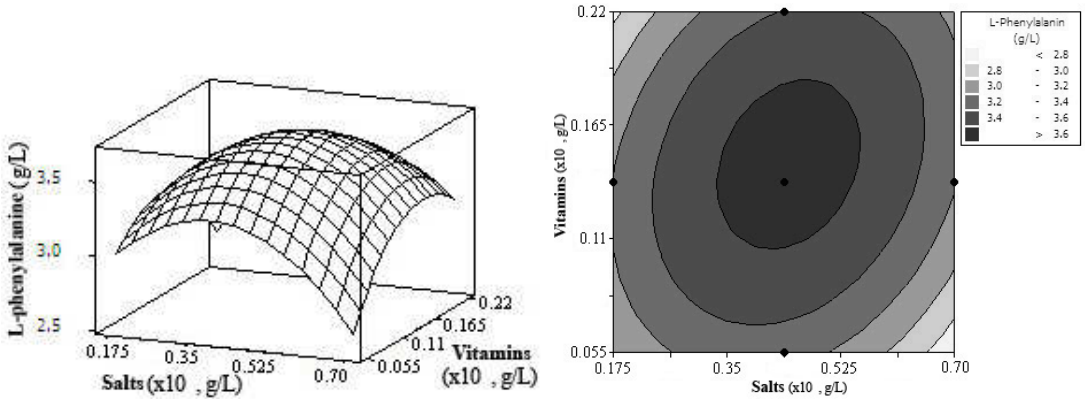

Figure 34 Response surface and contour plot of salts, vitamins and L-phenylalanine production at constant glycerol and $(NH_4)_2SO_4$ concentration

Figure 35 showed the biomass and L-phenylalanine productions using basal medium and optimized media. The basal medium is 80 g/L glycerol; 80 g/L $(NH_4)_2SO_4$; 1.0 g/L $MgCl_2$; 1.0 g/L KH_2PO_4; 1.0 g/L K_2HPO_4; 1.0 g/L yeast extract; 0.1 g/L thiamine-HCl; 0.002 g/L $FeSO_4$; 0.002 g/L $MnSO_4$; 0.05 g/L $CaCl_2$; and 0.01 g/L $ZnSO_4$ while the the optimum medium is 10 g/l glycerol; 50 g/l $(NH_4)_2SO_4$; 0.81 g/l $MgCl_2$; 2.43 g/l KH_2PO_4; 2.43 g/l K_2HPO_4; 0.085 g/l yeast extract; 0.0085 g/l thiamine-HCl; 0.002 g/l $FeSO_4$; 0.002 g/l $MnSO_4$; 0.05 g/l $CaCl_2$; and 0.01 g/l $ZnSO_4$. The biomass and L-phenylalanine productions were two times when the optimum medium was used instead of the basal medium.

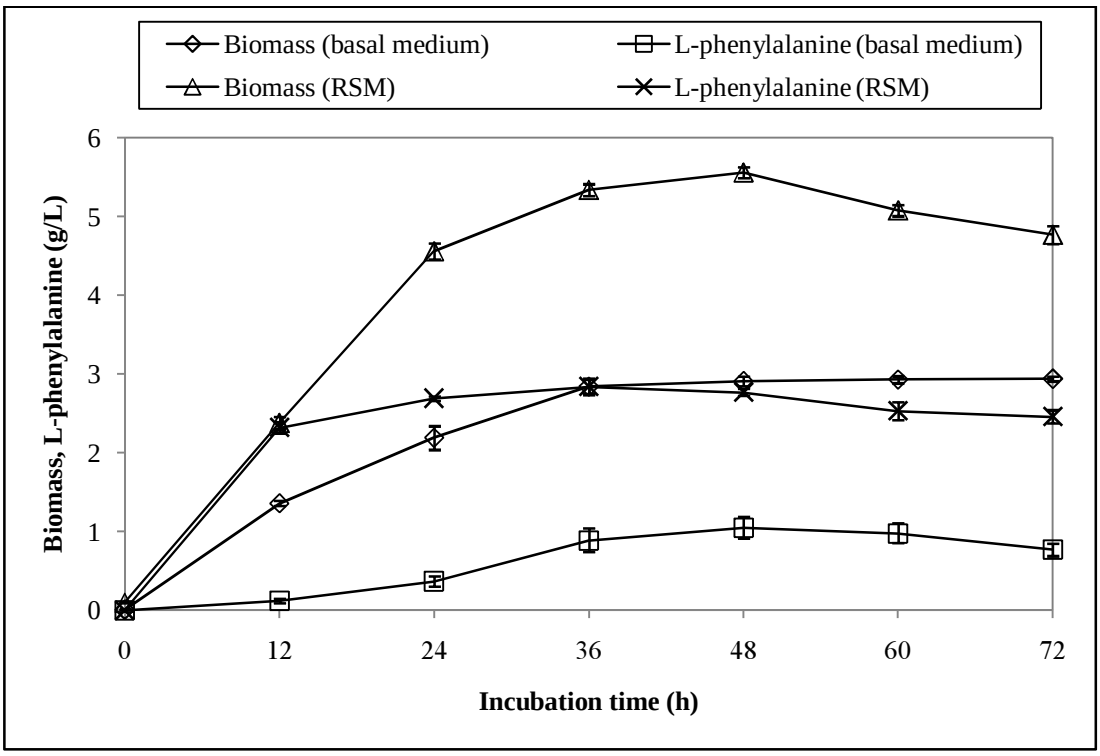

Figure 35 Time course of recombinant *E. coli* BL21(DE3) biomass and L-phenylalanine productions during batch fermentation comparing of optimized (RSM) and basal media

3. Optimization of agitation and aeration rates in batch fermentation

3.1 Agitation rate

The productions of L-phenylalanine and biomass were conducted in a 3.3 Liter STR with temperature and pH maintained at 37 °C and 7.4. The fermentation was carried out at 4.0 L/min aeration rate with various agitation rates (i.e. 200, 300, 400 and 500 rpm). Time courses of the L-phenylalanine and biomass productions were shown to relate with dissolved oxygen (DO) as in Figure 36 to 39.

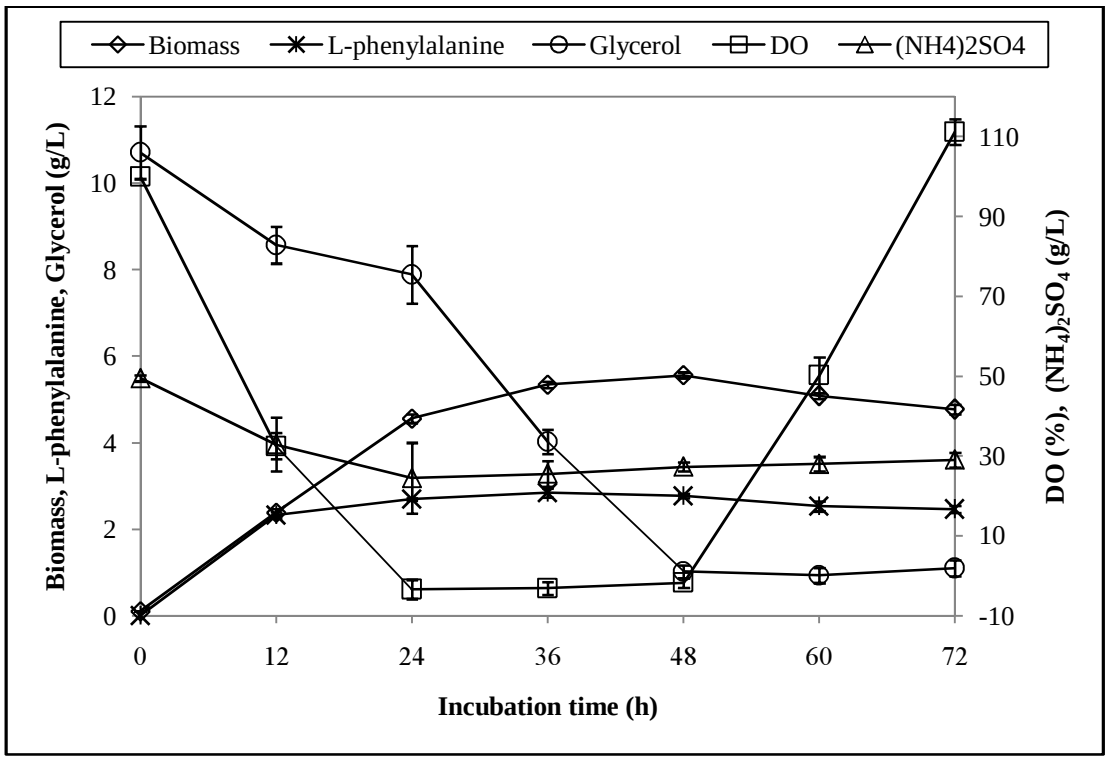

Figure 36 Biomass, L-phenylalanine, glycerol, $(NH_4)_2SO_4$ and dissolved oxygen profiles during culture of recombinant *E. coli* BL21(DE3) at the agitation rate of 200 rpm, and constant at 4.0 L/min aeration rate and pH 7.4

Figure 36 shows the cell growth, L-phenylalanine production, glycerol and $(NH_4)_2SO_4$ concentration and dissolved oxygen profiles. The growth pattern seemed to be no lag phase at the beginning of the cell growth. The cell growth curve showed a rapid period of the cell growth followed by a slow growth phase after 24 hour. The biomass concentrations were 5.56 g/L at the maximum and 4.77 g/L at the end of the fermentation that was related to the glycerol consumption profile. The low oxygen transfer at the relatively low agitation rate was shown by the rapid decrease in dissolved oxygen to zero after 24 hour of fermentation. Due to the oxygen limitation, the L-phenylalanine production was also low. L-phenylalanine was produced association with the cell growth in the fermentation broth, with the maximum concentration of 2.84 g/L at 36 hour. The L-phenylalanine concentration started to increase rapidly, from starting to 2.84 g/L at 36 hour. Then after 36 hour of

fermentation, the L-phenylalanine was slow produced to 2.53 g/L at the end of fermentation.

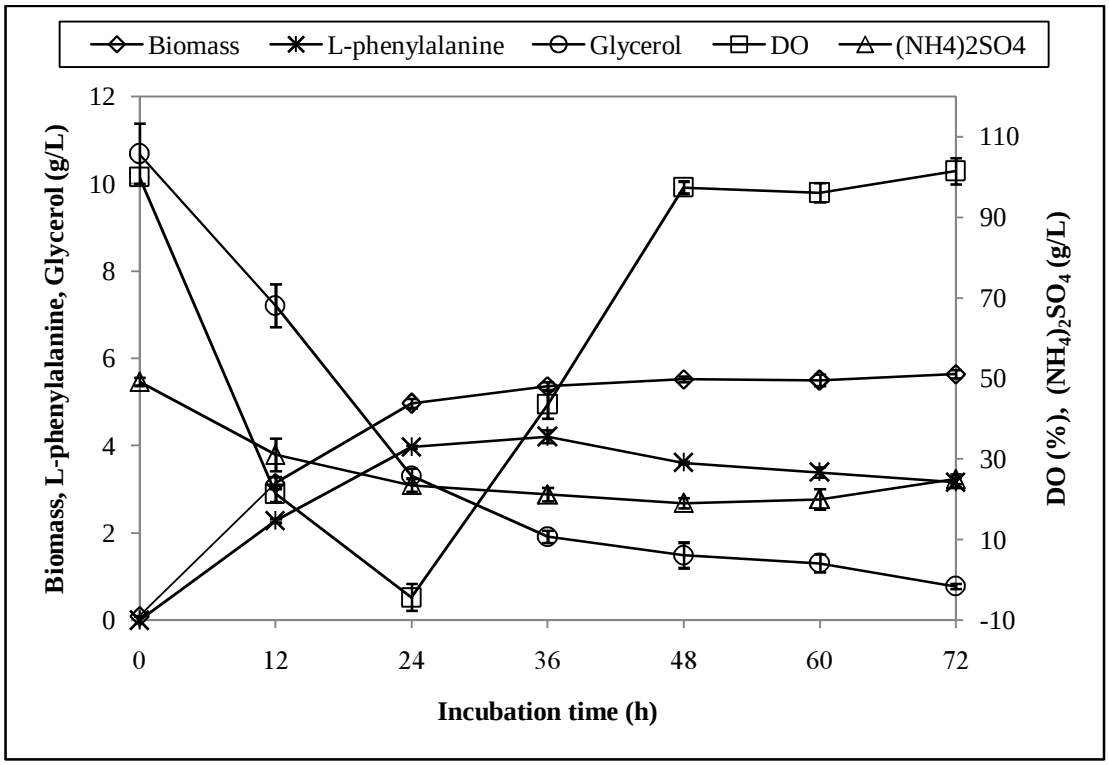

Figure 37 Biomass, L-phenylalanine, glycerol, $(NH_4)_2SO_4$ and dissolved oxygen profiles during culture of recombinant *E. coli* BL21(DE3) at the agitation rate of 300 rpm, and constant at 4.0 L/min aeration rate and pH 7.4

When the agitation rate was increased to 300 rpm, the DO profile is higher than at 200 rpm as shown in Figure 37. The optimal biomass and L-phenylalanine concentrations at 300 rpm were 5.64 g/L and 4.21 g/L respectively. This is higher than at 200 rpm agitation rate (Figure 36). It can be seen in Figure 37 that the sharply increased of the biomass concentration at the first 24 hour (the exponential growth) was associated with the improved DO level in the system. The biomass growth profile become steady after 24 hour that was related to the remaining glycerol concentration in the system. Dissolved oxygen dropped rapidly when the biomass concentration was higher. The decrease in the dissolved oxygen at 300 rpm,

was high then sharply increased comparing to the 200 rpm fermentation. Then the trend became steady until the end of fermentation. The L-phenylalanine production associated with the biomass growth at the first 36 hour then continued to decrease until 72 hour. This reduction related to low glycerol concentration in the system and the increase of ammonium sulfate concentration at the last phase of fermentation.

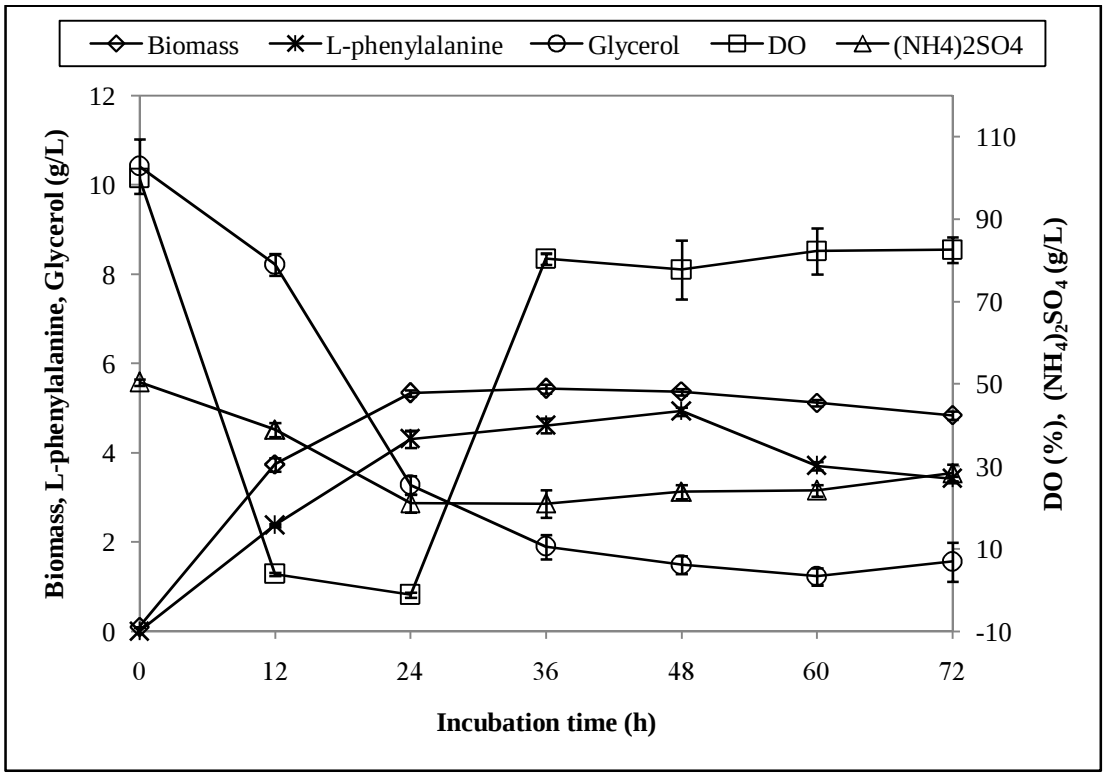

Figure 38 Biomass, L-phenylalanine, glycerol, $(NH_4)_2SO_4$ and dissolved oxygen profiles during culture of recombinant *E. coli* BL21(DE3) at the agitation rate of 400 rpm, and constant at 4.0 L/min aeration rate and pH 7.4

At the agitation rate of 400 rpm, the dissolved oxygen is increased obviously as shown in Figure 38. The optimal biomass concentration at 400 rpm was 5.44 g/L, this agitation rate gave the highest biomass concentration among 200-400 rpm. The increased biomass concentration was associated with the high dissolved oxygen level of the system. However, dissolved oxygen dropped rapidly when the

growing cell concentration was getting higher. The dissolved oxygen at the agitation rate of 400 rpm, trended to decrease like at the agitation rate at 200 and 300 rpm (Figure 36 and 37). The L-phenylalanine production increased with the increased of agitation rate to 400 rpm. The L-phenylalanine production is associated with the cell growth. Its optimal concentration was 4.93 g/L at 48 hour, which was also about 2.0 times higher than at the 200 rpm fermentation (Figure 36). Therefore, better dissolved oxygen at 400 rpm increased the L-phenylalanine production. The doubling of the protein concentration at 400 rpm fermentation comparing with at 200 and 300 rpm fermentation resulted the higher cell mass concentration.

The high agitation rate of 500 rpm fermentation was also conducted in the same reactor to investigate the effect on the biomass and L-phenylalanine productions. At this very high agitation rate, a cell density of 5.07 g/L was achieved (Figure 39). Cell growth was rapidly increased during the first 24 hours and decreased slowly to 4.2 g/L at 48 hour. The biomass concentration at 500 rpm agitation rate resulted in a lower L-phenylalanine production than at 400 rpm. The initial L-phenylalanine concentration measured at 48 hour was 1.72 g/L (Figure 39), and decreased to 1.4 g/L at the end of the fermentation.

From Figure 39, the dissolved oxygen profile showed that the DO of the high agitation rates decreased much slower than those at lower (agitation) rates. However, the increasing of the shear rate affected to decrease the biomass and L-phenylalanine productions (Figure 36-39).

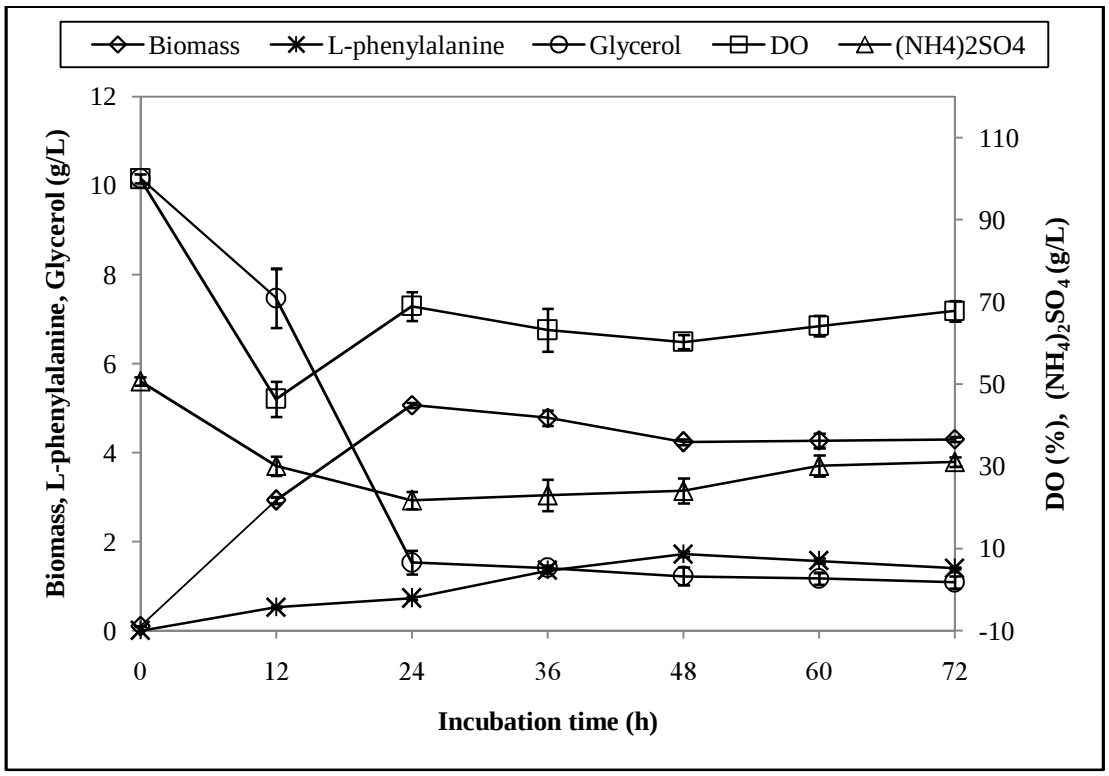

Figure 39 Biomass, L-phenylalanine, glycerol, $(NH_4)_2SO_4$ and dissolved oxygen profiles during culture of recombinant *E. coli* BL21(DE3) at the agitation rate of 500 rpm, and constant at 4.0 L/min aeration rate and pH 7.4

The effect of the agitation rate was primarily studied in the batch fermentation. The goal of the agitation study is to increase dissolved oxygen to enhance the cell growth and high production of recombinant *E. coli* BL21(DE3). Attaining this goal would lead the operating cost of this aerobic fermentation, because a large fraction of the process cost associates with the power consumption cost.

Conventionally, the agitation rate of the fermentations at 200 rpm, 300 rpm, 400 rpm and 500 rpm was conducted in the 3.3 L Bioflo III fermenter. The biomass production, L-phenylalanine production, and dissolved oxygen profile were compared among those four mentioned agitation rates systems (Figure 40-44).

Comparing of biomass productions in Figure 40, the biomass concentration at 400 rpm was 1.2-1.6 times of the biomass concentration at 200 rpm at 12-24 hour. The cell growth pattern of the fermentation at 200 rpm, 300 rpm and 400 rpm were also similar to the pattern of the fermentation at 500 rpm at the beginning of fermentation until 24 hour. Then, the growth of the cell at 500 rpm trended to decrease with a slight increase in mixing at the end of the fermentation that was indicated, the contact time between cells and oxygen molecules have influence more than concentration gradient of oxygen in the fermentation medium (Chisti, 1999).

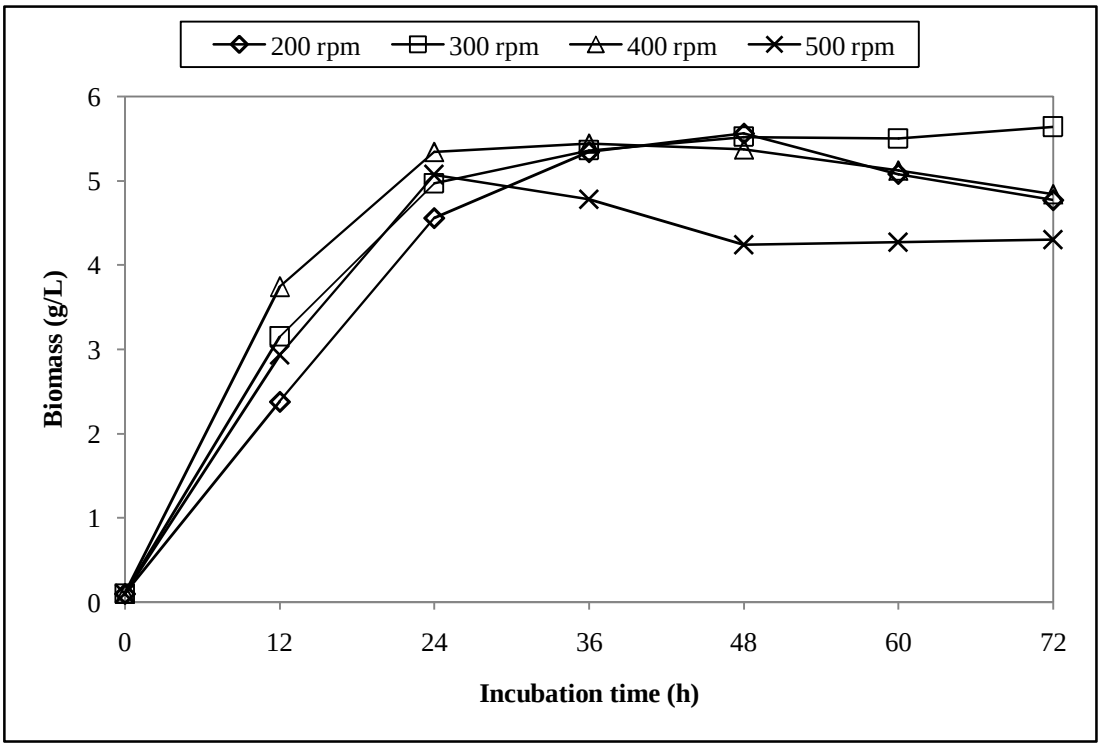

Figure 40 Comparison of biomass production during culture of recombinant *E. coli* BL21(DE3) at different agitation rates of 200 rpm, 300 rpm, 400 rpm and 500 rpm, and constant at 4.0 L/min aeration rate and pH 7.4

Production of L-phenylalanine was associated with the cell growth pattern. Its trend was similar to the cell growth's. L-phenylalanine production in the

fermentation at 200 rpm and 300 rpm were not considerably different from at the 400 rpm at 12 hour of the fermentation. L-phenylalanine concentrations at the optimal value of the fermentation run were 2.84 g/L, 4.21 g/L and 4.93 g/L at 200 rpm, 300 rpm and 400 rpm, respectively (Figure 41). While L-phenylalanine concentration at 500 rpm was comparable low.

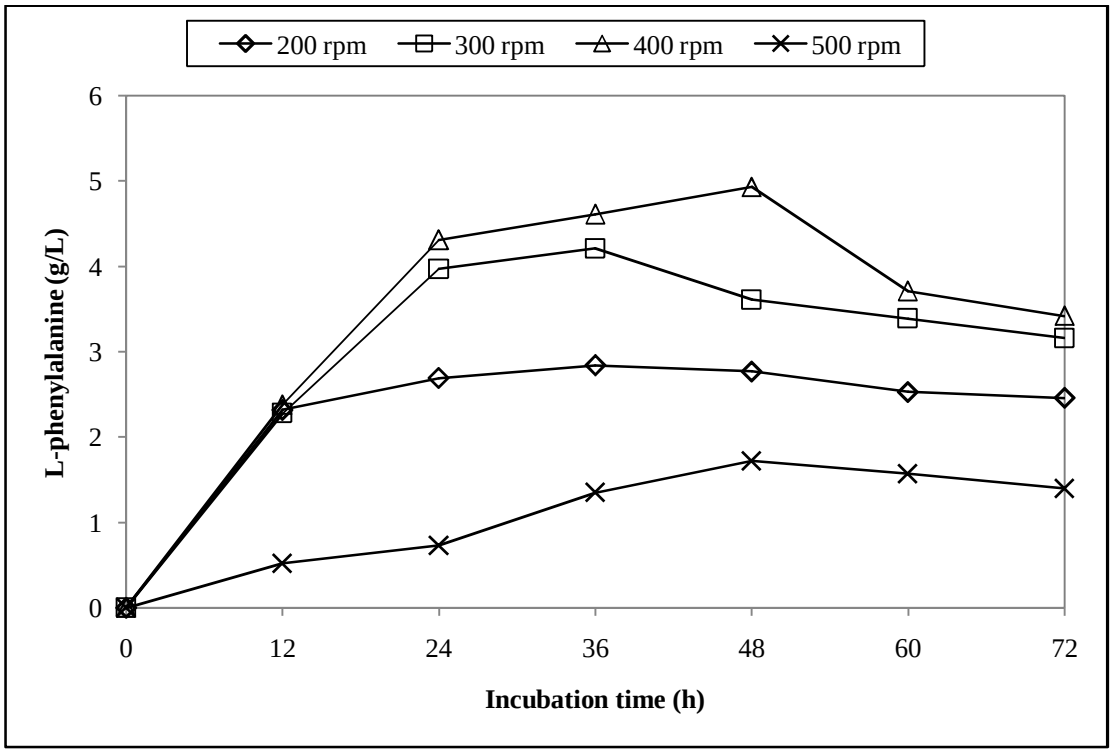

Figure 41 Comparison of L-phenylalanine production during culture of recombinant *E. coli* BL21(DE3) at different agitation rates of 200 rpm, 300 rpm, 400 rpm and 500 rpm, and constant at 4.0 L/min aeration rate and pH 7.4

It is trace in Figure 42 that dissolved oxygen (DO) profile at the high agitation rate would increase the dissolved oxygen efficiency (Figure 42). DO levels at 300 rpm, 400 rpm, and 500 rpm were increased rapidly to the critical DO level until the end of the fermentation. For the system of 200 rpm, 300 rpm and 400 rpm, the dissolved oxygen decreased to almost near zero at 24 hour. This condition was severe oxygen limitation in the system. The fermentation condition at 400 rpm also showed

oxygen limitation with DO decreasing below the critical value at 24 hour. However, the DO at 400 rpm fermentation was recovered rapidly than the DO at 200 rpm and 300 rpm agitation rates.

Therefore, the comparison of the biomass, L-phenylalanine productions, and dissolved oxygen profile of four systems are performed. The biomass productions are shown the similar pattern while the L-phenylalanine productions at 400 rpm showed higher values than at 300 rpm, 200 rpm and 500 rpm, respectively. The final concentration of DO represents the consumption of oxygen by the viable cells in the fermenter and by the oxidation of organic waste in the medium (McNeil and Harvey, 2008).

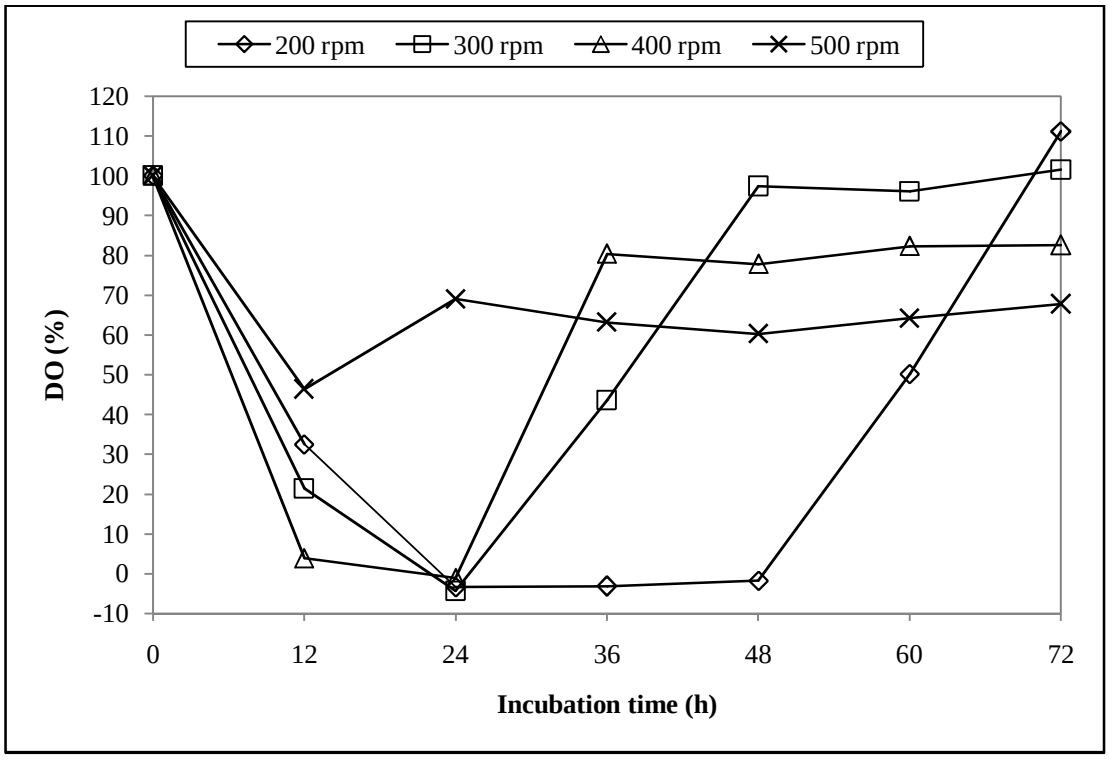

Figure 42 Comparison of dissolved oxygen during culture of recombinant *E. coli* BL21(DE3) at different agitation rates of 200 rpm, 300 rpm, 400 rpm and 500 rpm, and constant at 4.0 L/min aeration rate and pH 7.4

Volumetric productivity is expressed as a gram of the product per liter per hour and is a measure of the overall performance of a process. In the continuous or the fed-batch fermentation processes, the maximum productivity does not necessarily occur at a dilution rate corresponding to the maximum yield or conversion of substrate to cells. Moreover, the maximum biomass productivity may not occur at the same fermentation time as the appearance of the maximal productivity. In Figure 43-44, the biomass productivities and L-phenylalanine productivities were compared at various agitation rates.

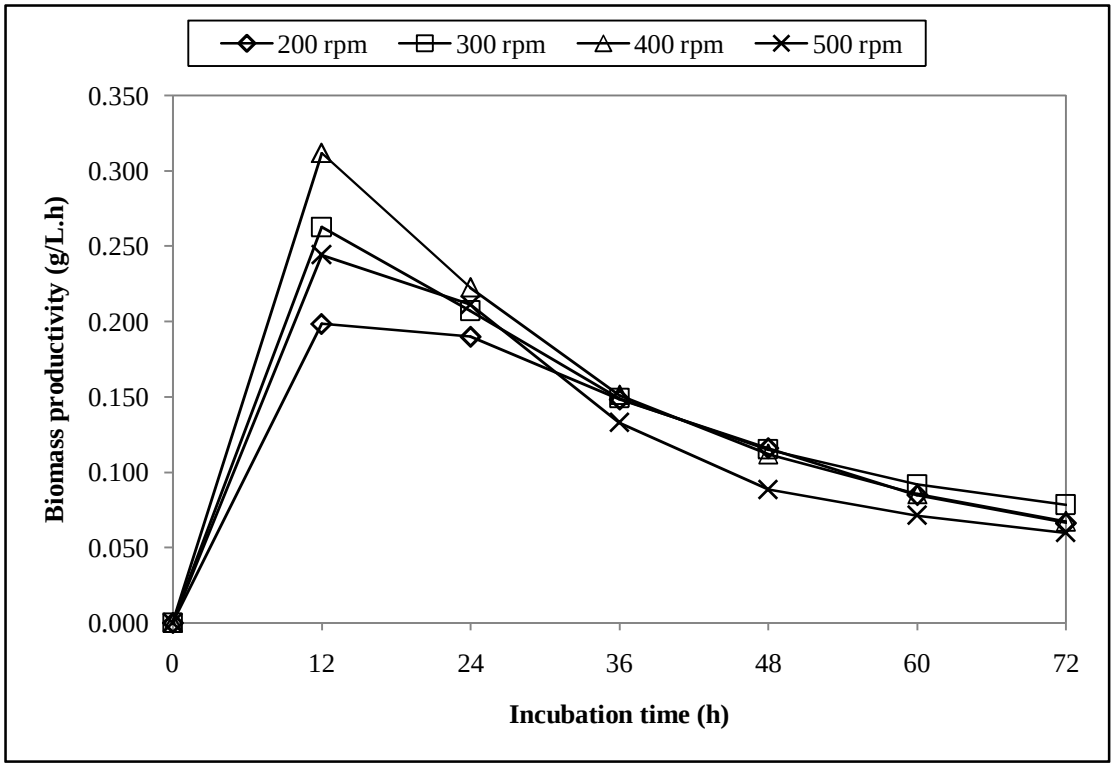

Figure 43 Comparison of biomass productivities during culture of recombinant *E. coli* BL21(DE3) at different agitation rates of 200 rpm, 300 rpm, 400 rpm and 500 rpm, and constant at 4.0 L/min aeration rate and pH 7.4

Biomass productivities at different agitation rates are shown in Figure 43. The apparent maximum attaining of the biomass productivity was attributed to the

glycerol high consumption rate. While the glycerol concentration in the fermentation broth decreased, the biomass productivity decreased. Biomass productivities at all agitation rates were the highest rate at 12 hour, then decreased gradually till 72 hour. It demonstrated that high oxygen transfer and high glycerol concentration led to high cell mass productivity in this fermentation process. The maximum productivity value (0.312 g/L.h) occurred after 12 hour of fermentation at the 400 rpm agitation rate. In addition, at the 500 rpm agitation rate had a similar pattern to the one of 300 rpm agitation rate to 24 hour of the fermentation process, the shear rate at high cell concentration was affected to decrease biomass productivity.

The L-phenylalanine productivities at the 200 rpm, 300 rpm, 400 rpm and 500 rpm are shown in Figure 44. It can be seen that the L-phenylalanine production associated with the cell growth at the beginning of fermentation. The L-phenylalanine productivity patterns at 200 rpm, 300 rpm and 400 rpm were very similar, increased very rapidly from 0 hour to 12 hour and then slowed down. The maximum protein productivities for 200 rpm, 300 rpm and 400 rpm were about 0.19 g/L.h. The L-phenylalanine productivity in the 500 rpm agitation rate was very low; attained the highest level of only 0.043 g/L.h at 12 hour and decreased slowly till 72 hour. The reason for this phenomenon was still not clear. It might be possible that the high shear force from the high agitation rate stresses the cell and affect the L-phenylalanine production or bacterial secretion process.

From the biomass and L-phenylalanine productivities, it could be concluded that at the biomass and L-phenylalanine productivities reached it’s highest level at 12 hour of fermentation. After 12 h both biomass and L-phenylalanine productivities went down till the end of the fermentation.

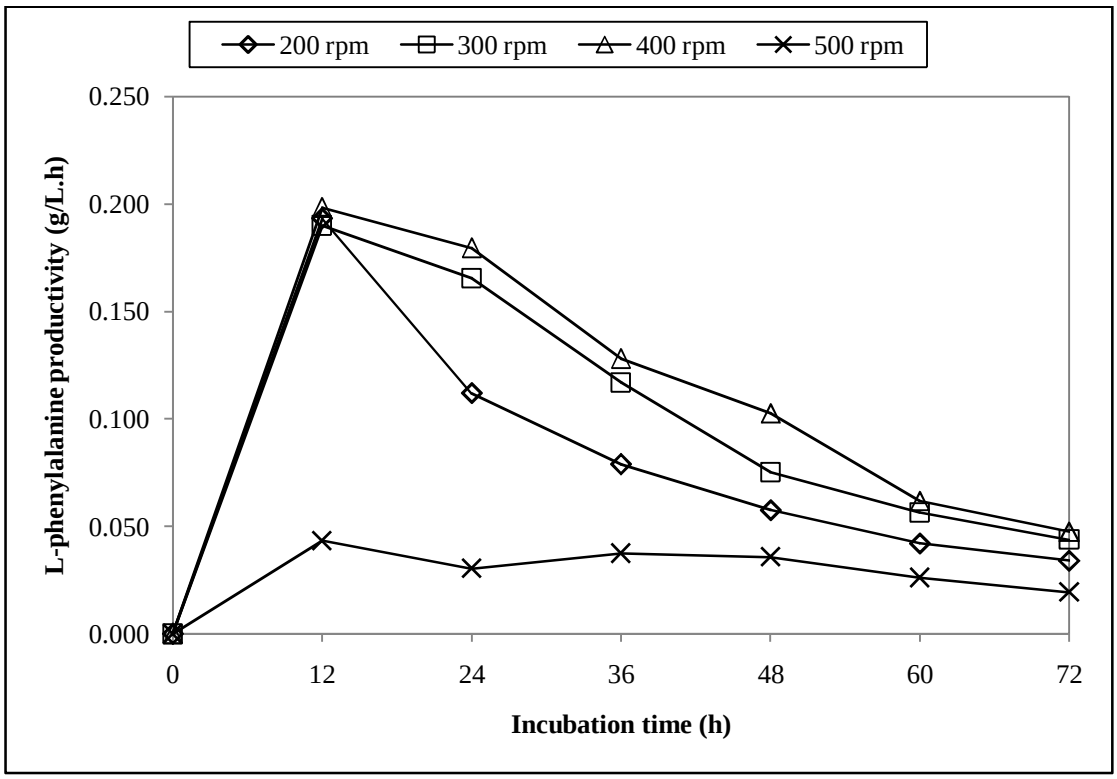

Figure 44 Comparison of L-phenylalanine productivities during culture of recombinant *E. coli* BL21(DE3) at different agitation rates of 200 rpm, 300 rpm, 400 rpm and 500 rpm, and constant at 4.0 L/min aeration rate and 7.4 pH

The specific growth rates calculated using the data from the Figure 40, are shown in Figure 45. Increasing the agitation speed to 400 rpm increased the specific growth rate of the biomass because of increasing of the oxygen supply. However, the growth rate declined while further increasing the agitation speed was made. This decline was attributed to a possible shear sensitivity of the recombinant *E. coli*. Many recombinant bacteria are known to be sensitive to excessive turbulence and high shear rates compared to the equivalent wild type strains (Gehmlich *et al.*, 1996; Belo and Mota, 1998; Chisti, 1999). The maximum observed specific growth rate was 0.3021/h. Clearly, at an aeration rate of 4 L/min, an impeller agitation speed of 400 rpm was the most suitable condition for obtaining a rapid cell growth.

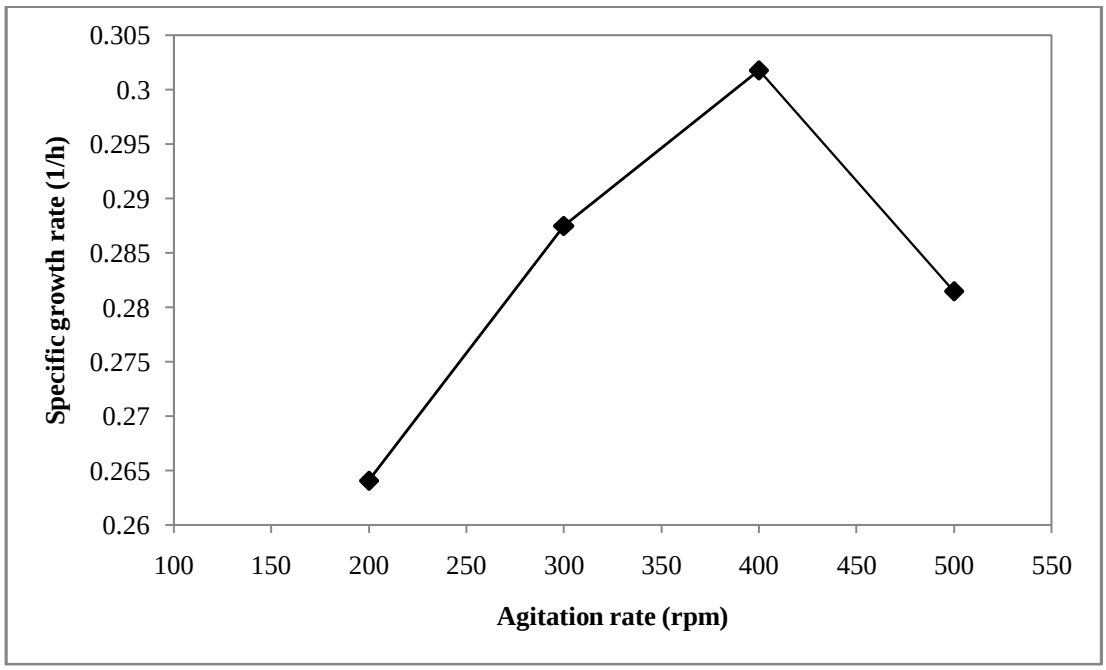

Figure 45 Specific growth rate of cell at various impeller agitation rates at a fixed aeration rate of 4.0 L/min

3.2 Aeration rate

The changes of the biomass, L-phenylalanine concentrations, DO and $(NH_4)_2SO_4$ concentration during the incubation time of 2.0, 4.0, 6.0 and 8.0 was shown in Figure 46 to 49.

The effect of aeration capacity was shown in the 2.0 L/min aeration rate (Figure 46). The cell concentration at the optimal plot of the fermentation was 4.9 g/L at 24 hour. However, the cell concentration was reduced slowly to 3.56 g/L at 72 hour that was related to the pattern of glycerol concentration in the broth which was rapidly decreased at during 24 to 72 hour. The low aeration rate at the 2.0 L/min caused the cell concentration decreased to zero after 24 hour. However, the DO was increased till the end of the fermentation. Due to the oxygen limitation, L-phenylalanine production was also poor. L-phenylalanine was produced in association with the cell growth, with the maximum concentration of 4.9 g/L at 24 hour. L-phenylalanine concentration was

increased slowly, from origin point to 2.05 g/L at the first 24 hour. During 24-48 hour of fermentation, the L-phenylalanine production was appeared to be stable and slowly decreased to 1.4 g/L at the end of the fermentation.

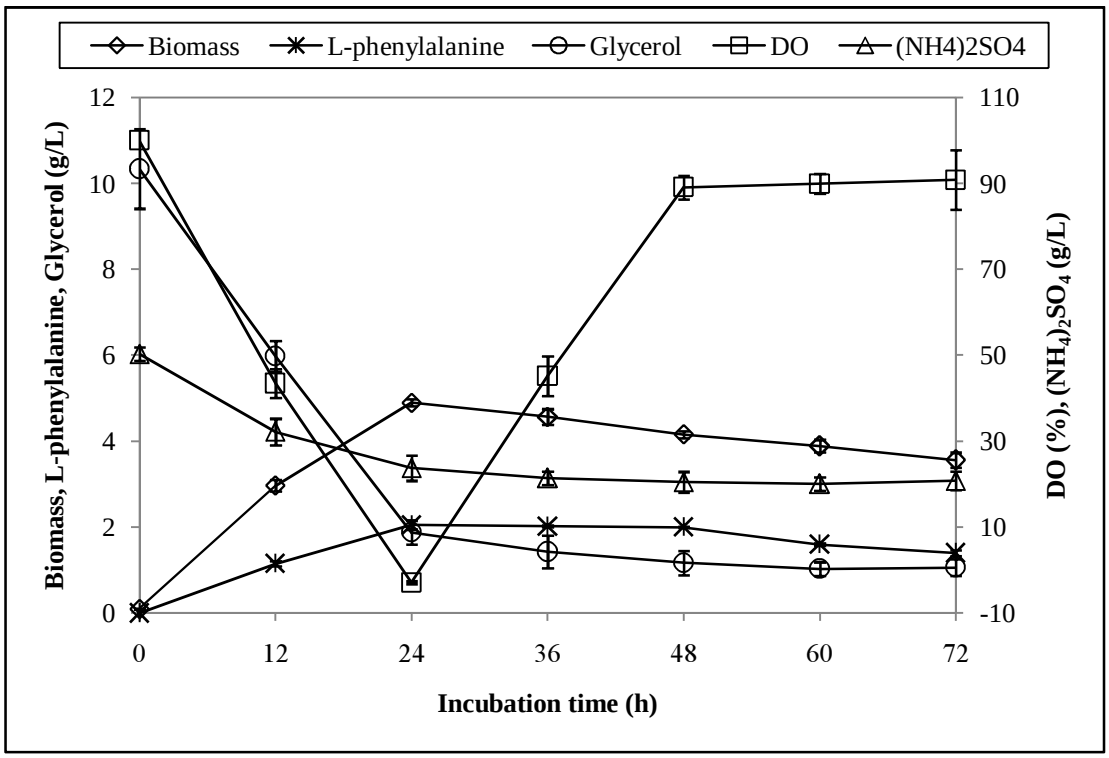

Figure 46 Biomass, L-phenylalanine, glycerol, $(NH_4)_2SO_4$ and dissolved oxygen profiles during the culture of recombinant *E. coli* BL21(DE3) at 2.0 L/min aeration rate, and constant at 400 rpm agitation rate and pH 7.4

When the aeration rate was increased to 4.0 L/min, it increased the oxygen hold up in the system as shown in Figure 47. The optimal biomass and L-phenylalanine concentrations at 4.0 L/min were 5.64 g/L and 4.85 g/L at 24 hour and 48 hour respectively, which was higher than at 2.0 L/min aeration rate (Figure 46). The increased of the biomass concentration was associated with the DO level improvement. Dissolved oxygen dropped rapidly as the cell growing. The dissolved oxygen at 4.0 L/min aeration dropped sharply to zero at 24 hour then rose to 55 %

rapidly at 36 hour. After that, it remained steady from 36 hour to the end of the fermentation.

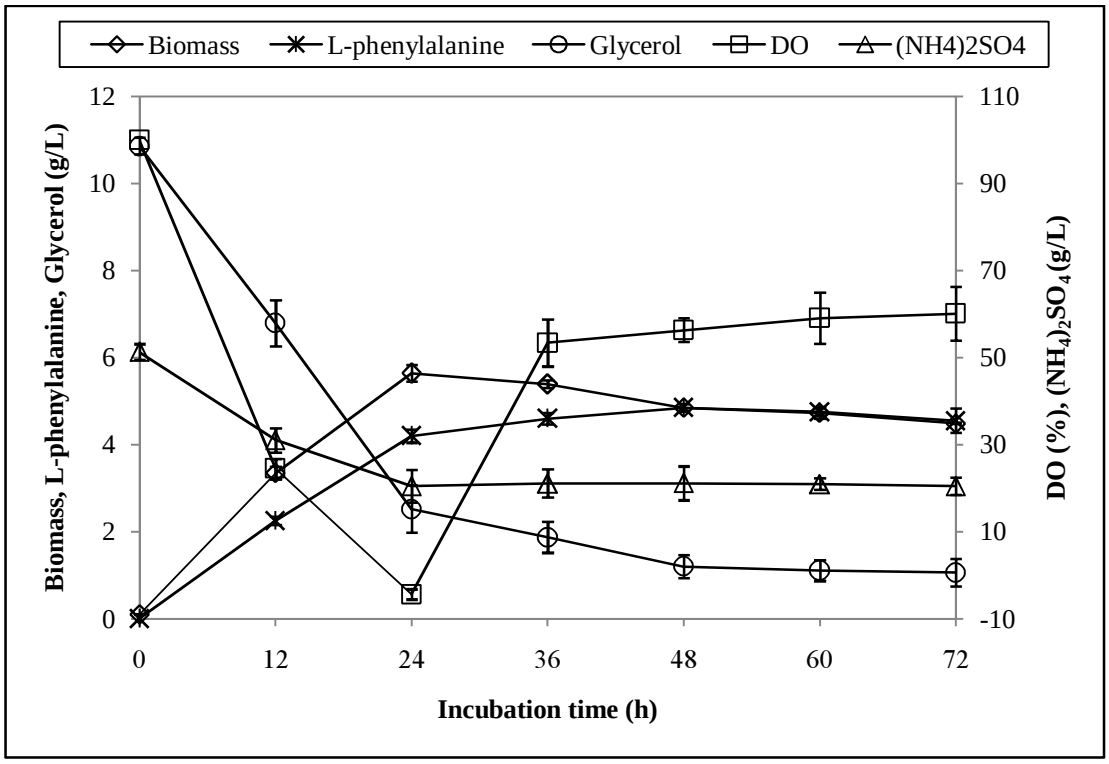

Figure 47 Biomass, L-phenylalanine, glycerol, $(NH_4)_2SO_4$ and dissolved oxygen profiles during the culture of recombinant *E. coli* BL21(DE3) at 4.0 L/min aeration rate, and constant at 400 rpm agitation rate and pH 7.4

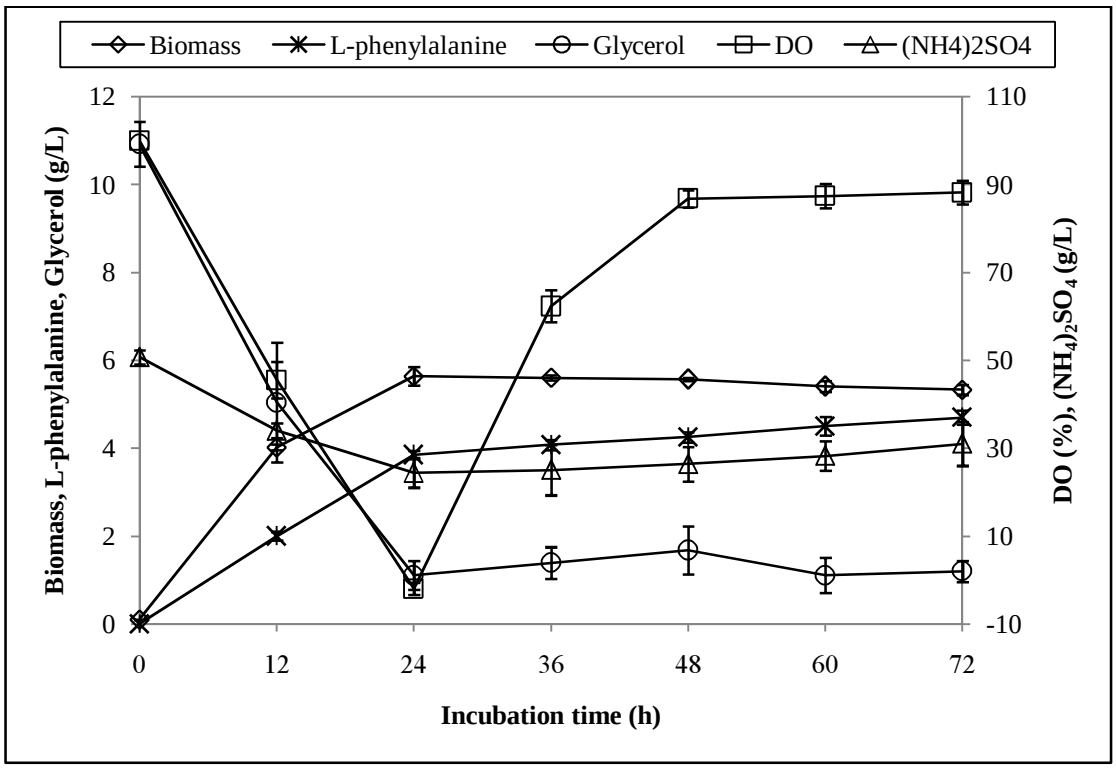

Figure 48 Biomass, L-phenylalanine, glycerol, $(NH_4)_2SO_4$ and dissolved oxygen profiles during the culture of recombinant *E. coli* BL21(DE3) at 6.0 L/min aeration rate, and constant at 400 rpm agitation rate and pH 7.4

While the aeration rate was increased to 6.0 L/min (Figure 48), the optimal biomass concentration was 5.64 g/L at 24 hour that associated with the glycerol consumption rate. This value was higher than those attained at 2.0 and 4.0 L/min aeration rate. The increased biomass concentration was associated with the high DO level of the system. Dissolved oxygen dropped rapidly as the growing cell concentration was increased. The decrease in the dissolved oxygen in the 6.0 L/min aeration rate was similar trend as in the 2.0 L/min aeration rate till 24 hour and was increased rapidly after 24 hour of the fermentation process. With the increase in oxygen feeding of 6.0 L/min aeration rate, the L-phenylalanine production was higher than at 2.0 L/min aeration rate, but lower than at 4.0 L/min aeration rate. L-phenylalanine started to be produced according to the cell growth, and the optimal concentration was 4.7 g/L at 72 hour. Therefore, not only better oxygen dissolvability

at 6.0 L/min improved biomass production but also affect the repression of L-phenylalanine production.

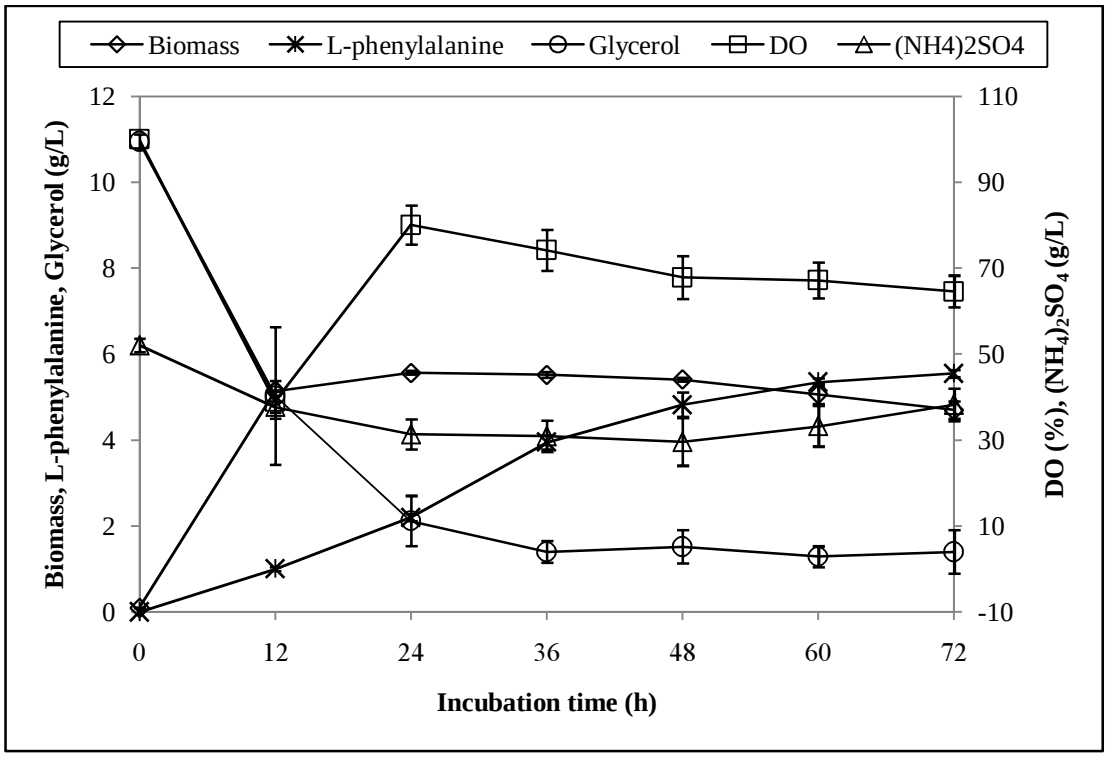

Figure 49 Biomass, L-phenylalanine, glycerol, $(NH_4)_2SO_4$ and dissolved oxygen profiles during the culture of recombinant *E. coli* BL21(DE3) at 8.0 L/min aeration rate, and constant at 400 rpm agitation rate and pH 7.4

High aeration rate of 8.0 L/min was conducted in the fermentation system to observe, the effect of more efficient oxygen feed rate on the biomass and L-phenylalanine productions. At this very high aeration rate, a optimal cell density of 5.57 g/L at 24 hour was achieved due to high oxygen solubility in the fermentation medium (Figure 49). The cell growth was rapid increased during the first 12 hours to 24 hour and remained stable after 24 hour to 36 hour till decreasing slowly to 4.7 g/L at 72 hour. The aeration rate of 8.0 L/min resulted in a low L-phenylalanine production and low cell concentration at 0 hour to 48 hour. However, it showed high L-phenylalanine production after 48 hour. The maximum L-phenylalanine

concentration at high cell concentration condition measured at 60 hour was 5.35 g/L at 5.55 g/L at the end of fermentation process.

The dissolved oxygen profile showed that the DO was increased much higher than those at higher aeration rates. However, the increasing of DO resulted the increase of the biomass production. Furthermore, at the very high DO decreased the L-phenylalanine production (Figure 46-49).

The comparison between the biomass concentrations at 4.0 L/min and 6.0 L/min aeration rate were the same. While, the biomass concentration at 8.0 L/min aeration rate was about 2 times greater than at 2.0 L/min at 12 hour (Figure 50). The cell growth pattern at 2.0, 4.0 and 6.0 L/min were also similar to at 8.0 L/min aeration rates at 24 hour forward the end of the fermentation.

Figure 51, the production of L-phenylalanine related to the cell growth pattern, and thus it showed a similar trend to the cell growth's. The L-phenylalanine production in the fermentation at 4.0 L/min aeration rate showed the highest value (4.85 g/L) at 48 hour that was same pattern of 6.0 L/min aeration rate. The trend of L-phenylalanine concentrations at very high cell concentration reversed, the 8.0 L/min aeration rate showed optimal value of 5.35 g/L at 60 hour and 5.55 g/L at the end of process. While the L-phenylalanine production at 2.0 L/min was very low comparing to other conditions.

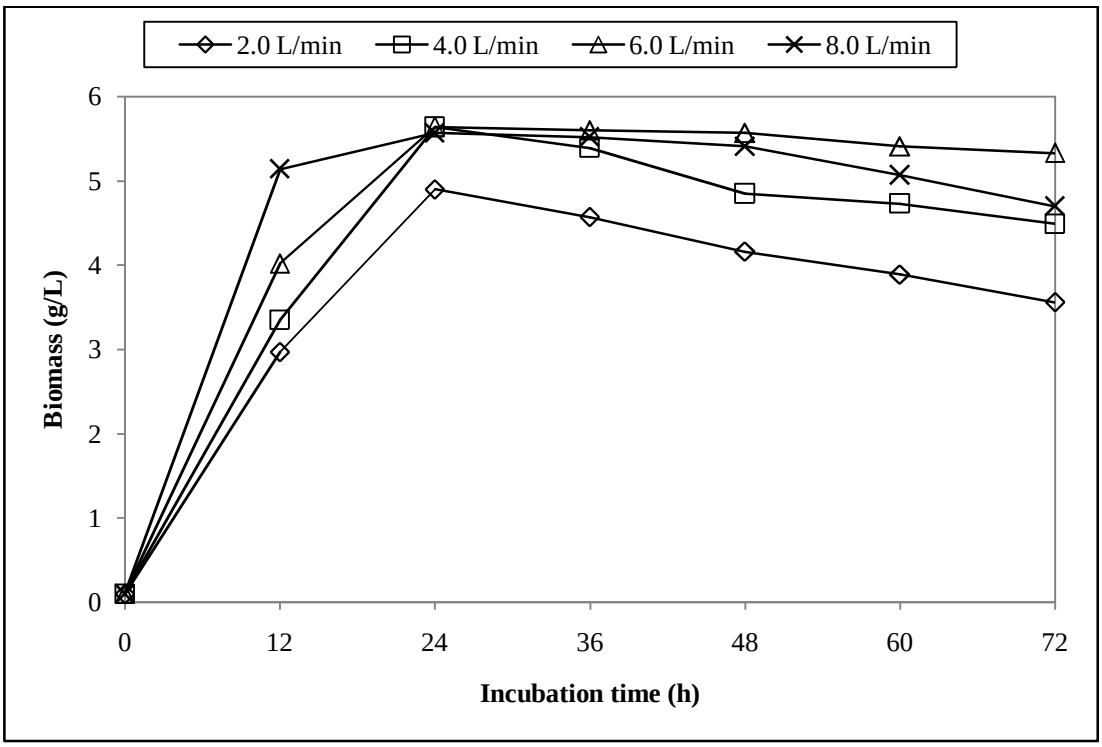

Figure 50 Comparison of biomass production during culture of recombinant *E. coli* BL21(DE3) at different aeration rates of 2.0L/min, 4.0L/min, 6.0L/min and 8.0L/min and at constant 400 rpm agitation rate and pH 7.4

Dissolved oxygen (DO) profile also showed that the high aeration rate increased the oxygen dissolve in the broth and was more rapid recovery than lower aeration rate (Figure 52). For the system of 2.0 L/min, 4.0 L/min and 6.0 L/min, the dissolved oxygen decreased to almost near zero at 24 hour, showing severe oxygen limitation of the system. The fermentation condition at 8.0 L/min showed very high oxygen solubility above the critical value throughout the process. However, the L-phenylalanine production was suppressed at 8.0 L/min aeration rate comparing with other conditions.

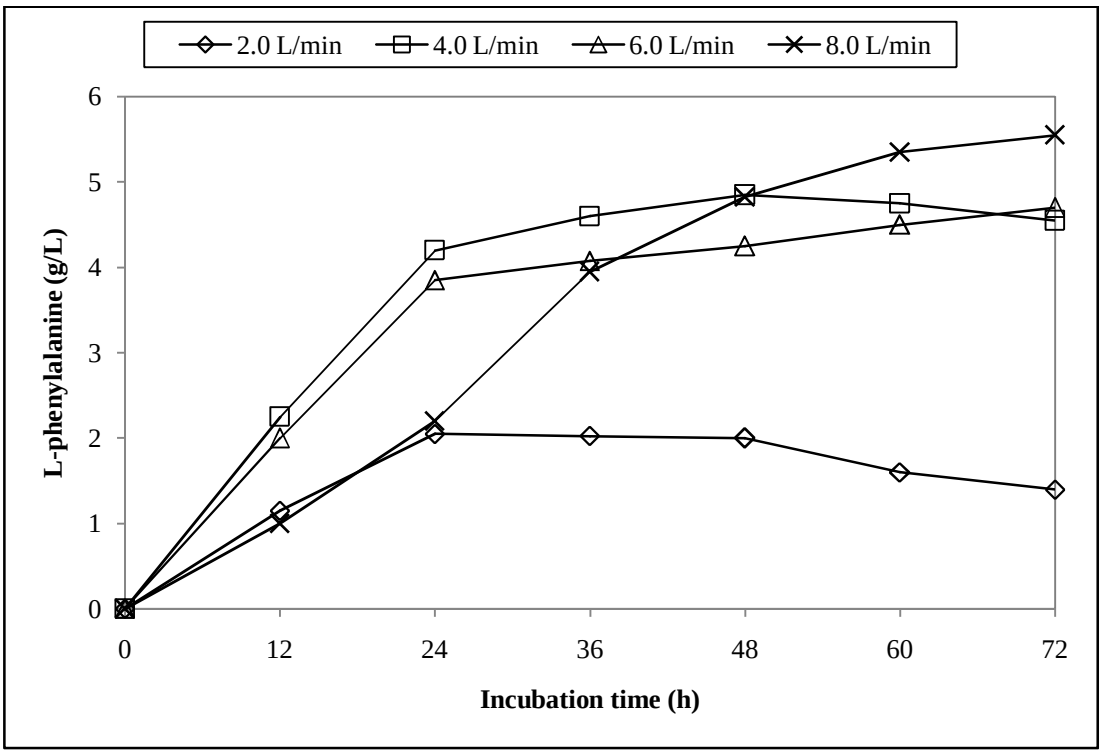

Figure 51 Comparison of L-phenylalanine production during culture of recombinant *E. coli* BL21(DE3) at different aeration rates of 2.0L/min, 4.0L/min, 6.0L/min and 8.0L/min and constant at 400 rpm agitation rate and pH 7.4

Therefore, the comparison of the biomass, L-phenylalanine productions, and dissolved oxygen profile of four systems at low cell concentration, 4.0 L/min aeration rate gave the highest value of L-phenylalanine production. However, the high oxygen dissolved at 8.0 L/min aeration rate, at high cell concentration was induced to enhance the L-phenylalanine production.

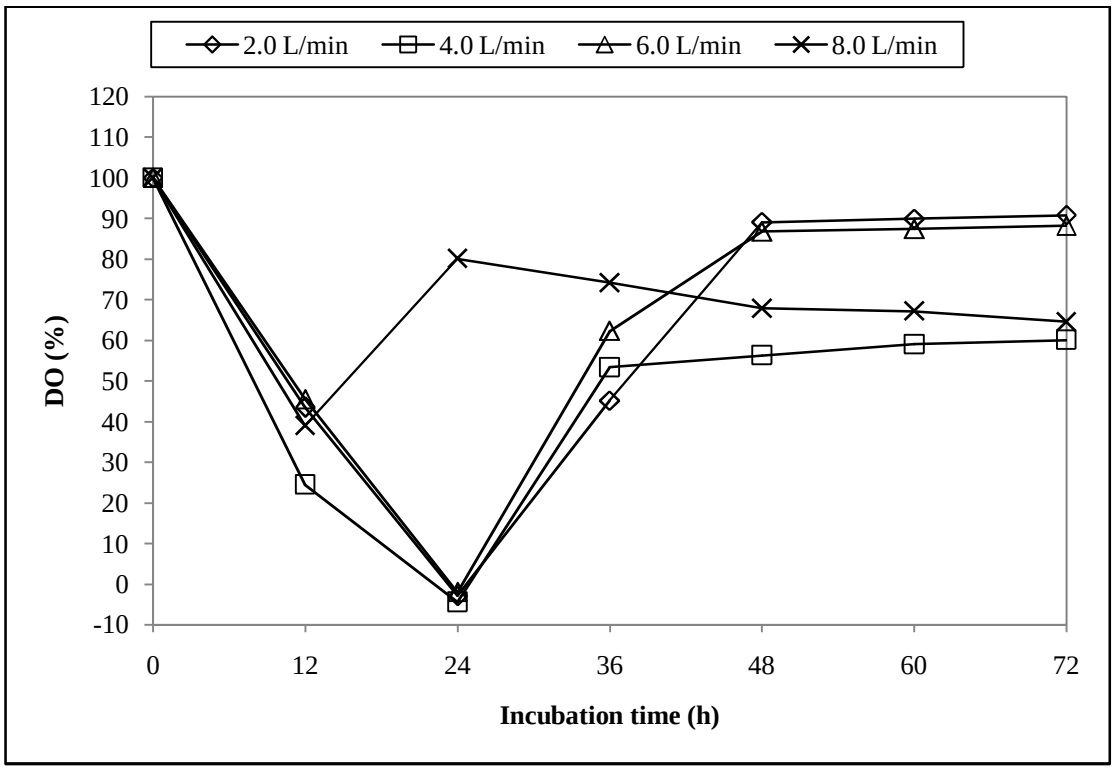

Figure 52 Comparison of dissolved oxygen during culture of recombinant *E. coli* BL21(DE3) at different aeration rates of 2.0L/min, 4.0L/min, 6.0L/min and 8.0L/min and constant at 400 rpm agitation rate and pH 7.4

The biomass productivities at different aeration rates are shown in Figure 53. The apparent maximum biomass productivity attained was attributed to the glycerol high consumption rate and high aeration rate. The biomass productivities at all agitation rates reached the highest value at 12 hour, and then decreased gradually till 72 hours of fermentation. At this high oxygen solubility and high glycerol consumption led to the high cell mass productivity in this fermentation process. The maximum productivity value (0.428 g/L.h) occurred at 12 hour at the 8.0 L/min aeration rate and the value of biomass productivity was similar to all other aeration rates at 24 hour till the end of fermentation process.

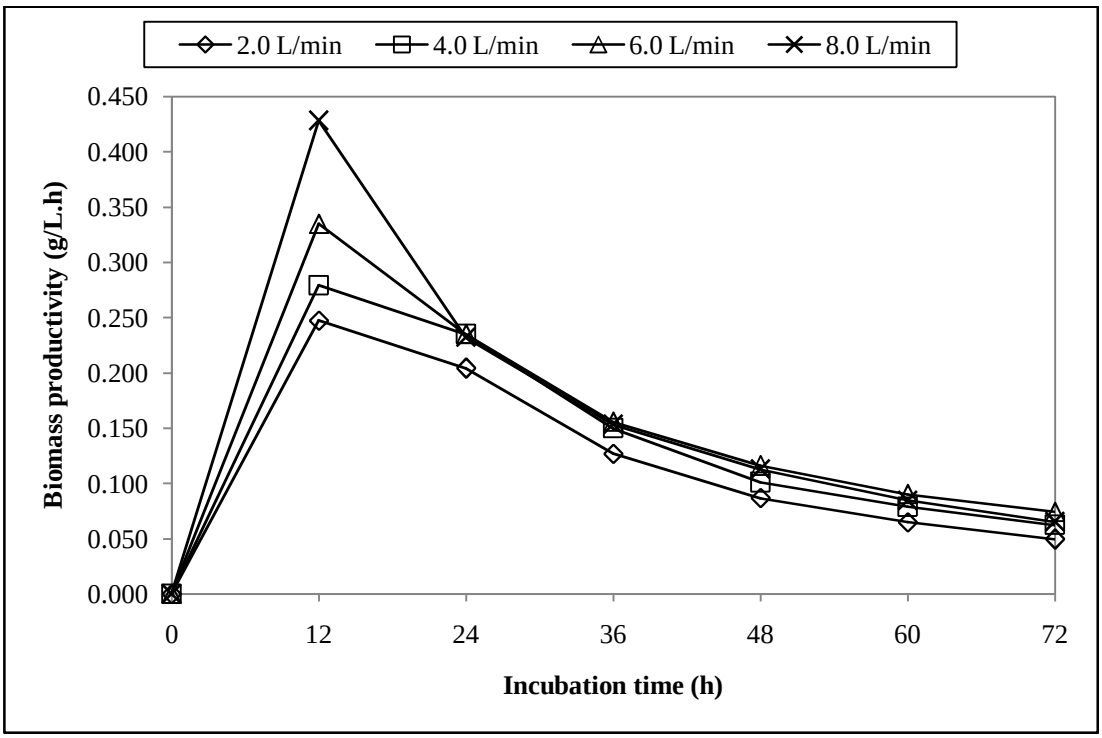

Figure 53 Comparison of biomass productivities during culture of recombinant *E. coli* BL21(DE3) at different aeration rates of 2.0L/min, 4.0L/min, 6.0L/min and 8.0L/min and constant at 400 rpm agitation rate and pH 7.4

The L-phenylalanine productivity at the 2.0 L/min, 4.0 L/min, 6.0 L/min and 8.0 L/min are shown in Figure 54. It can be seen that the L-phenylalanine production associated with the cell growth at the beginning of the fermentation. The L-phenylalanine productivity patterns at 4.0 L/min and 6.0 L/min were very similar; increased very rapidly from 0 hour to 12 hours; and then slowed down. The maximum L-phenylalanine productivities for 2.0 L/min, 4.0 L/min and 6.0 L/min were 0.188 g/L.h, 0.167 g/L.h and 0.096 g/L.h, respectively. The L-phenylalanine productivity at the 8.0 L/min aeration rate was low and attained the highest level of only 0.083 g/L.h at 12 hour and then increase slowly to the maximum value of 0.11 at 36 hours with the high cell concentration in the system. The reason for this phenomenon was probably because the sufficient oxygen dissolve attend the high cell concentration condition to increases the L-phenylalanine production.

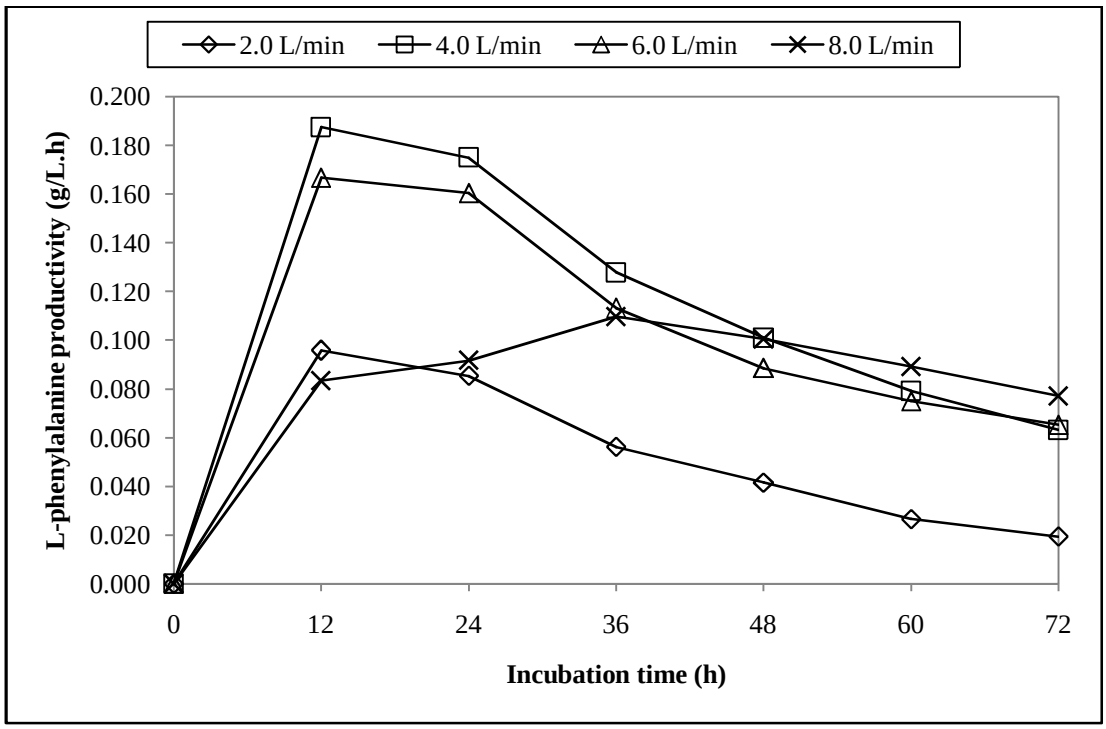

Figure 54 Comparison of L-phenylalanine productivities during culture of recombinant *E. coli* BL21(DE3) at different aeration rates of 2.0L/min, 4.0L/min, 6.0L/min and 8.0L/min and constant at 400 rpm agitation rate and pH 7.4

From the biomass and L-phenylalanine productivities, the biomass and L-phenylalanine productivities reached their highest level at 12 hours of fermentation. After 12 hours; both biomass and the L-phenylalanine productivities were slowed down till the end of the fermentation.

The calculated specific growth rates using the data in Figure 50 were shown in Figure 55. Increasing the aeration rate from 2.0 to 8.0 L/min increased the specific growth rate of the biomass because of great improvement of oxygen solubility. This increase was attributed to a possible high oxygen concentration enhancing to the *E. coli* growth. Oxygen is an important substrate for aerobic organisms since the cellular production of metabolic energy directly relates to the oxygenation rate. Moreover, oxygen concentration is very strongly coupled to the cell

growth rate that typically depends on the dissolved oxygen concentration (Hochfeld, 2006). The maximum observed specific growth rate was 0.328 h^{-1}. Clearly, at the aeration rate of 8.0 L/min, an impeller agitation speed of 400 rpm was the best condition to obtain a rapid growth of biomass.

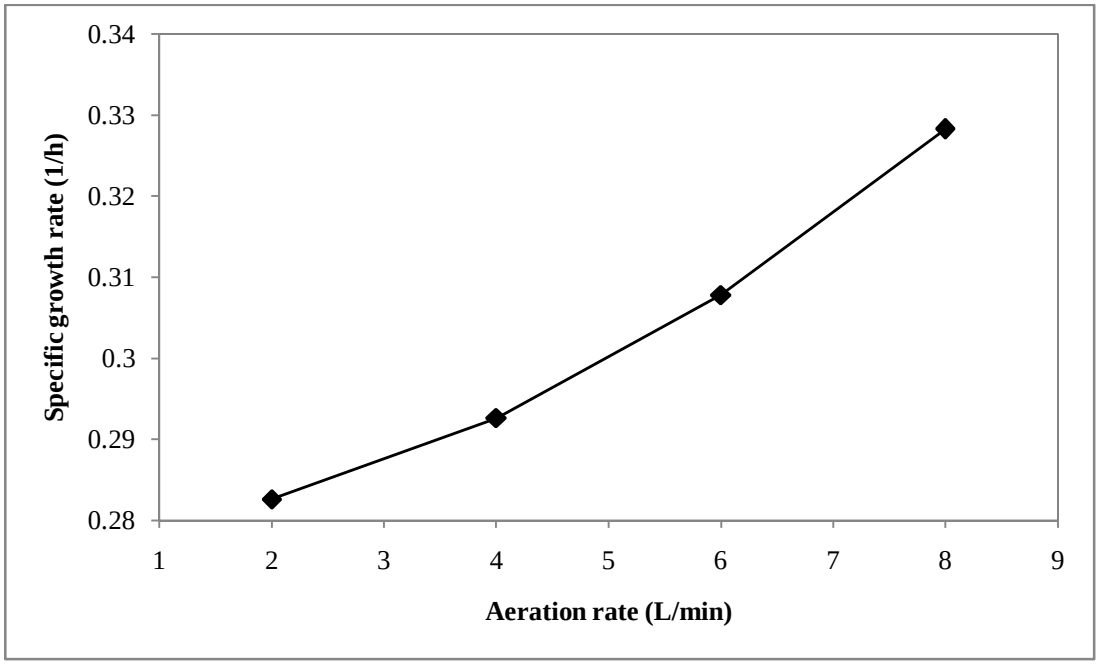

Figure 55 Specific growth rate of biomass at various aeration rates. All data were obtained at a fixed agitation rate of 400 L/min

4. The study of fed-batch fermentation

The fed-batch process with non-constant volume is the potential operation to obtain high L-phenylalanine concentration. The patterns of biomass, L-phenylalanine, glycerol, $(NH_4)_2SO_4$ and dissolved oxygen profiles are shown in Figure 56. At the batch fermentation phase (0-12 hour), the cells grew very fast and increased rapidly to 5.17 g/L. It related to the glycerol consumption while the L-phenylalanine was produced 0.6 g/L at 12.5 hour. Dissolved oxygen dropped gradually to 51 percentages as the cell concentration was higher. After 12 hours, the fermentation system changed to the fed-batch fermentation. The biomass production appeared to slow cells growth

after 12 hours (start feeding $(NH_4)_2SO_4$ and glycerol) to 48 hours while the L-phenylalanine production increased rapidly from 12 hour to 24 hour that related to the high concentration of ammonium sulfate and then increased slowly to the maximum point (6.5 g/L) at 60 hour and dropped to 5.83 g/L at 72 hour. The reason for this phenomenon might be the negative effect of rapid increase of $(NH_4)_2SO_4$ concentration. During the fed-batch fermentation phase (12-72 hours), dissolved oxygen level was stable till the end of the fermentation. The biomass production during at 48 hour to 72 hours was increased to 11.33 g/L at 72 hour. This might be the effect of increased of aeration rate to 8.0 L/min of cells adaptation in the last fermentation processes. $(NH_4)_2SO_4$ consumption rate decreased rapidly from 12 to 36 hours then appeared to slow increase till 72 hours. For ammonium sulfate (~5 g/L) at 12-36 hours was used for the L-phenylalanine production and some part was reacted with intermediate organic molecules in the fermentation medium to give the ammonia gas and lost to the air. The trend of ammonium sulfate to increase during 36-72 hours might possibly be produced from ammonium ion reduced by cells and/or the decomposition of L-phenylalanine in the medium (Vogel, 1997). The glycerol concentration profile was related to the pulse feeding (every 12 hour) and was consumed by *E. coli* for the biomass and L-phenylalanine production. The graph of glycerol showing high glycerol accumulation in the fermentation medium resulted from the decreasing of liquid medium volume during by sampling and Nevertheless, the carried over was obvious at very high aeration rate condition (~ 30 mL/24h. at 8.0 L/min aeration rate).

The biomass productivity of the fed-batch fermentation is shown in Figure 57. The biomass productivity at the batch fermentation phase (0-12 hours) in the fed-batch fermentation system showed the high rate of biomass productivity. While the L-phenylalanine productivity increased slightly. It was demonstrated that high aeration rate and good medium formula led to high biomass productivity in this fermentation process. The maximum biomass productivity of 0.414 g/L.h, occurred at 12 hours in the batch fermentation phase that less than the optimum value of the batch fermentation (0.428 g/L.h). Although the biomass productivity of the fed-batch fermentation phase (12-72 hours) decreased rapidly to 48 hours, the biomass

productivity maintained at that level for 48 to 60 hour and slightly increased at the end of fermentation. The L-phenylalanine productivity showed the similar graph pattern to the biomass productivity, by the optimum value of L-phenylalanine productivity represented at 24 hour then decreased rapidly to the end of process. It was demonstrated that the proper condition and medium formula led to high L-phenylalanine productivity at the maximum value of 0.218 g/L.h that more than the optimum value of the batch fermentation (0.198 g/L.h).

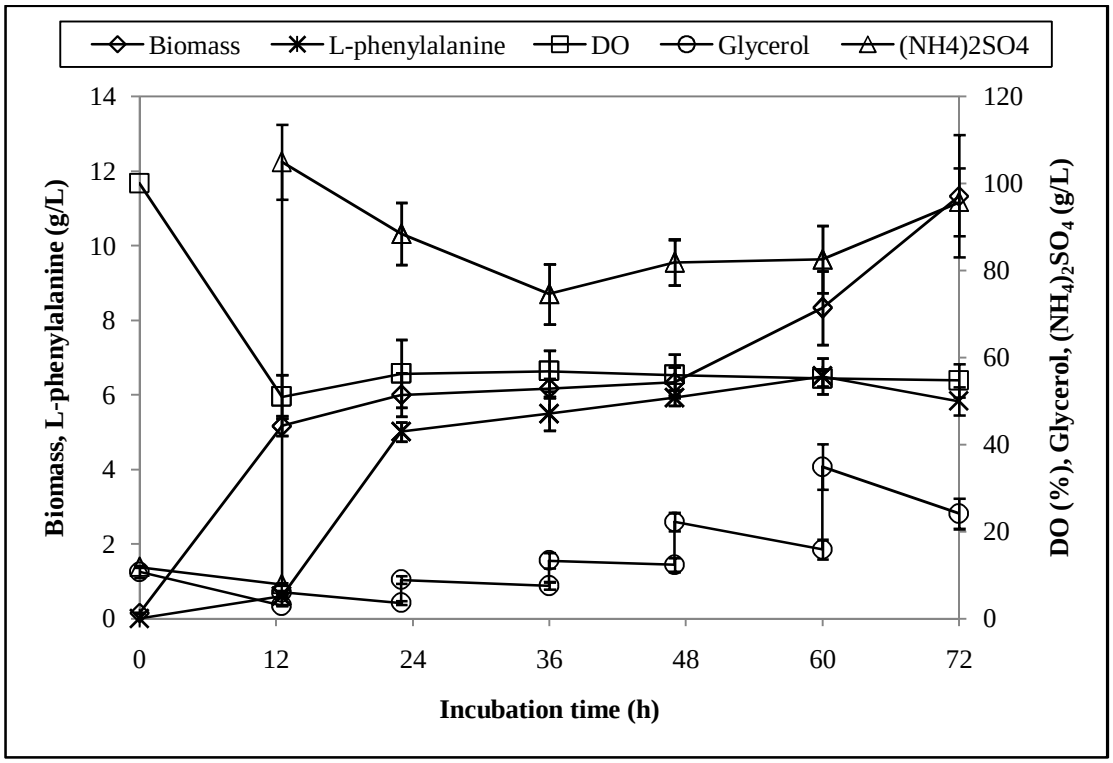

Figure 56 Biomass, L-phenylalanine, glycerol, $(NH_4)_2SO_4$ and dissolved oxygen profiles during fed-batch fermentation of recombinant *E. coli* BL21(DE3) at aeration rates of 8.0 L/min (0-12 h and 60-72 h) and 4.0 L/min (12-60 h), and constant at 400 rpm agitation rate and pH 7.4

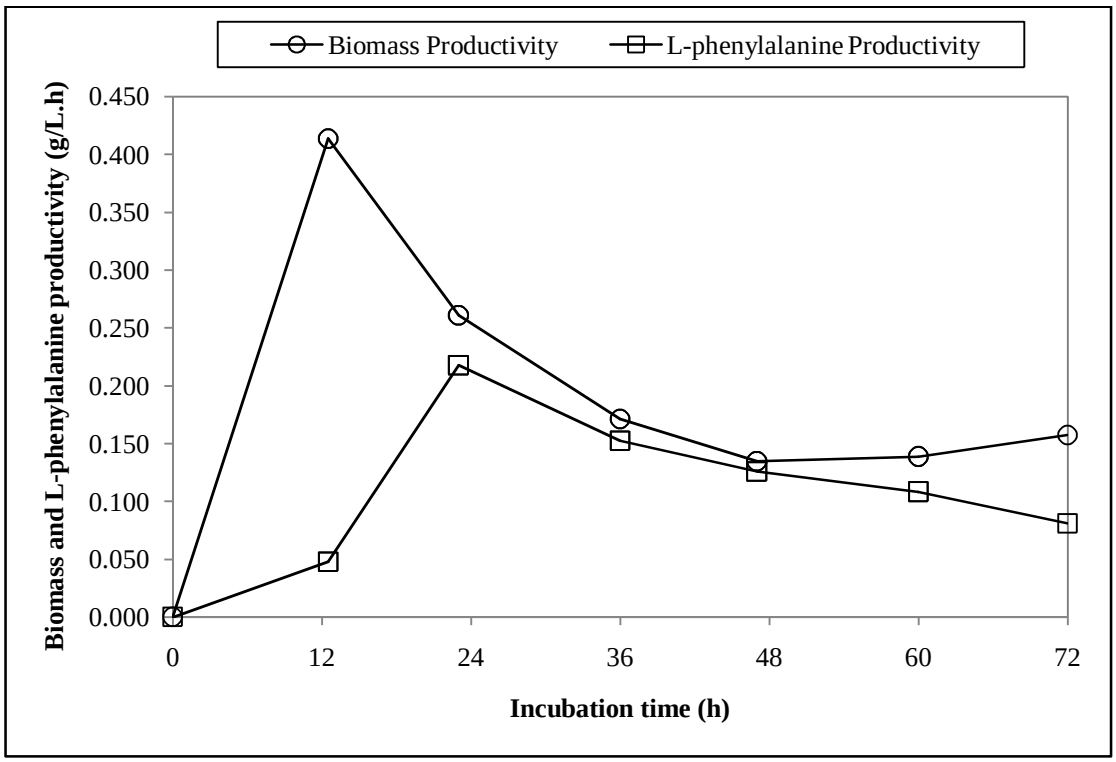

Figure 57 Patterns of biomass and L-phenylalanine productivities during fed-batch fermentation of recombinant *E. coli* BL21(DE3) at aeration rate of 8.0 L/min (0-12 h and 60-72 h) and 4.0 L/min (12-60 h), and constant at 400 rpm agitation rate and pH 7.4

CONCLUSION AND RECOMMENDATION

The present study using the RSM with CCD enables to determine the optimal medium constituents of the fermentation medium for the productions of the biomass and L-phenylalanine. The validity of the model was proved by fitting the values of the variables in the second order polynomial equation and the experimental data of the biomass and L-phenylalanine production with four independent variables, glycerol, $(NH_4)_2SO_4$, salts and vitamin concentration. Among four variables tested for the correlation between their concentrations and the productions of the biomass and L-phenylalanine, all four variables showed the significant influence on both productions. The maximum amount of the biomass and L-phenylalanine produced from glycerol predicted to be 5.00 g/L and 6.20 g/L, respectively when the optimized medium constituents of the biomass fermentation medium were set as follows: glycerol 10 g/L, $(NH_4)_2SO_4$ 10 g/L, salts 0.6867 g/L, vitamins 0.0966 g/L and glycerol 10 g/L, $(NH_4)_2SO_4$ 100 g/L, salts 0.4456 g/L and vitamins 0.0905 g/L, respectively.

The effects of the agitation and aeration rates on the L-phenylalanine and biomass productions were revealed the intricacies involved in the operation of the L-phenylalanine and biomass productions. Optimal biomass, L-phenylalanine productions and specific growth rate were also observed at 400 rpm agitation rate (5.37 g/L, 4.93 g/L and 0.302 1/h, respectively). The 8.0 L/min aeration rate showed the positive effect for the highest biomass concentration, biomass productivity and specific growth rate as 5.57 g/L, 0.428 g/L.h and 0.328 1/h, respectively while at 4.0 L/min aeration rate represented the highest L-phenylalanine productivity of 0.188 g/L.h. Under the best conditions (400 rpm, 8 L/min aeration rate), the yield of product on substrate ($Y_{P/S}$), in this case, was impressive as high as 0.58 g/g. A combination of high yield and inexpensive substrate is required for minimizing the cost of the L-phenylalanine production. Comparing the yield in this work to other research, the highest reported yield for commercial production of L-phenylalanine on sucrose is

about 0.25 g/g (Leuchtenberger *et al*., 2005), or less than 45% of the yield we obtained.

The fed-batch fermentation showed the improvement of the L-phenylalanine productivity. The L-phenylalanine productivity increased rapidly in the fed-batch fermentation phase (at 24 hour) to 0.218 g/L.h while the maximum biomass productivity was 0.414 g/L.h.

Future work would be the investigation of the plasmid stability in the batch and fed-batch cultures of recombinant *E. coli* BL21(DE3) in non-selective fermentation media. In addition, the improvement of the biomass and L-phenylalanine productions should also be further investigated in the fed-batch and continuous fermentation while sampling time was adjusted to more frequent during the exponential growth phase (9-18 hours).

LITERATURE CITED

Abbad-Andaloussi, S., C. Manginot-Dürr, J. Amine, E. Petitdemange and H. Petitdemange. 1995. Isolation and characterization of *Clostridium butyricum* DSM 5431 mutants with increased resistance to 1,3-propanediol and altered production of acids. **Appl. Env. Microbiol.** 61: 4413–4417.

Ahrens, K., K. Menzel, A. P. Zeng and W. D. Deckwer. 1998. Kinetic, dynamic, and pathway studies of glycerol metabolism by *Klebsiella pneumoniae* in anaerobic continuous culture: III. Enzymes and fluxes of glycerol dissimilation and 1,3-propanediol formation. **Biotechnol. Bioeng.** 59: 544–552.

Akesson, M., E. N. Karlsson, P. Hagander, J. P. Axelsson, and A. Tocaj. 1999. On-line detection of acetate formation in *Escherichia coli* cultures using dissolved oxygen responses to feed transients. **Biotechnol. Bioeng.** 64: 590-598.

Akesson, M., P. Hagander, and J. P. Axelsson. 2001. Avoiding acetate accumulation in *Escherichia coli* cultures using feedback control of glucose feeding. **Biotechnol. Bioeng.** 73: 223-230.

Akashi, Y., H. Shibai and Y. Hirose. 1979. Effect of oxygen on L-phenylalanine, L-proline, L-glutamine and L-arginine fermentation. **J. Ferment. Technol.** 57: 317-320.

Banks, G. T. 1979. Scale-up of fermentatin processes. **Topics in Enzyme and Fermentation Biotechnology.** 3: 170-267.

Barbirato, F. and A. Bories. 1997. Relationship between the physiology of *Enterobacter agglomerans* CNCM 1210 grown anaerobically on glycerol and the culture conditions. **Res. Microbiol.** 148: 475-484.

Barbiorato, F., D. Chedaille and A. Bories. 1997. Propionic acid fermentation from glycerol: Comparison with conventional substrates. **Appl. Microbiol. Biotechnol.** 47: 441-446.

Barbirato, F., P. Soucaille and A. Bories. 1996. Physiologic mechanisms involved in accumulation of 3-hydroxypropionaldehyde during fermentation of glycerol by *Enterobacter agglomerans*. **Appl. Env. Microbiol.** 62: 4405-4409.

Bartholomew, W. H. 1960. Scale-up of submerged fermentations. **Adv. App. Micro.** 2: 289-300.

Bennett, T. P. and E. Frieden. 1967. **Modern topics in biochemistry.** The MacMillan Company, New York.

Berberich, R., M. Kaback and E. Freese. 1968. D-amino acids as inducers of L-alanine dehydrogenase in *Bacillus subtilis.* **J. Biol. Chem.** 243: 1006-1011.

Belo, I., and M. Mota. 1998. Batch and fed-batch cultures of *E. coli* TB1 at different oxygen transfer rates. effect of stirring and oxygen partial pressures on cell growth and cytochrome b5 production. **Bioprocess Eng.** 18: 451–455.

Biebl, H. 2001. Fermentation of glycerol by *Clostridium pasteurianum* batch and continuous culture studies. **J. Ind. Microbiol. Biotech.** 27: 18–26.

Biebl, H, A. P. Zeng, K. Menzel and W. D. Deckwer. 1998. Fermentation of glycerol to 1,3-propanediol and 2,3-butanediol by *Klebsiella pneumoniae*. **Appl. Microbiol. Biotechnol.** 50: 24–29.

Biebl, H., S. Marten, H, Hippe and W. D. Deckwer. 1992. Glycerol conversion to 1,3-propanediol by newly isolated clostridia. **Appl. Microbiol. Biotech.** 36: 592-597.

Biebl, H. 1991. Glycerol fermentation of 1,3-propanediol by *Clostridium butyricum*. Measurement of product inhibition by use of a pH-auxostat. **Appl. Microbiol. Biotech.** 35: 701–705.

Bongaerts, J., M. Kramer, U. Muller, L. Raeven and M. Wubbolts. 2001. Metabolic engineering for microbial production of aromatic amino acids and derived compounds. **Metab. Eng.** 3: 289–300.

Boodhoo, K. V. K., M. Vicevic, C. D. Cartwright, T. Ndlovu and E. C. Toogood. 2008. Intensification of gas-liquid mass transfer using a rotating bed of porous packing for application to an *E. coli* batch fermentation process. **Chem. Eng. J.** 135: 141-150.

Bories, A., C. Claret and P. Soucaille. 1991. Kinetic study and optimisation of the production of dihydroxyacetone from glycerol using *Gluconobacter oxydans*. **Process Biochem.** 26: 243-248.

Box, G. E. P. and N. R. Draper. 2007. **Response Surface, Mixture, and Ridge Analyses.** 2nd ed. John Wiley and Sons, Inc., Hoboken, New Jersey.

Braun T, A. Philippsen, S. Wirtz, M. J. Borgnia, P. Agre and W. Kühlbrandt. 2000. The 3.7 Å projection map of the glycerol facilitator GlpF: a variant of the aquaporin tetramer. **EMBO Rep.** 11: 183-189.

Buckland, B. C., K. Gbewonyo, D. JAIN, K. Glazomitsky, G. Hunt and S. W. Drew. 1988. Oxygen transfer efficiency of hydrofoil impellers in both 800L and 1900L fermenters, pp. 1-16. **The International Conference on Bioreactor Fluid Dynamics 2nd**. Cambridge University, England.

Busca, P., F. Paradisi, E. Moynihan, M A. R. aguire and P. C. Engel. 2004. Enantioselective synthesis of non-natural amino acids using phenylalanine dehydrogenase modified by site-directed mutagenesis. **Org. Biomol. Chem.** 2: 2684-2691.

Calton, G. J., L. L. Wood, M. H. Updick, L. Lantz and J. P. Hammen. 1986. The production of L-phenylalanine by polyazetidine immobilized microbes. **Bio. Technology.** 4: 317-320.

Chao, Y. P., T. E. Lo and N. S. Luo. 2000. Selective production of L-aspartic acid and L-phenylalanine by coupling reaction of aspartase and aminotransferase in *Escherichia coli*. **Enzyme Microb. Technol.** 27: 19-25.

Chisti, Y. 1999. **Encyclopedia of Bioprocess Technology: Fermentation, Biocatalysis, and Bioseparation vol. 5**, Flickinger, M. C., Drew, S. W., Wiley, New York.

Claret, C., J. M. Salmon, C. Romieu and A. Bories. 1994. Physiology of *Gluconobacter oxydans* during dihydroxyacetone production from glycerol. **Appl. Environ. Microbiol.** 41: 359-365.

Clark, D. P. 2002. **Biochemistry and physiology of microorganism.** Available Source: http://www.science.siu.edu/microbiology/micr425/425Notes/04-C&Energy.html, October 23, 2002.

Colin, T., A. Bories, C. Lavigne and G. Moulin. 2001. Effects of acetate and butyrate during glycerol fermentation by *Clostridium butyricum*. **Curr. Microbiol.** 43: 238–243.

Cooney, C. L. 1979. Conversion yields in penicillin production: Theory versus practice. **Process Biochem.** 14 (5): 31-33.

Daniel, R., K. Stuertz and G. Gottschalk. 1995. Biochemical and molecular characterization of the oxidative branch of glycerol utilization by *Citrobacter freundii*. **J. Bacteriol.** 177: 4392–4401.

Darbon E., K. Ito, H. S. Huang, T. Yoshimoto, S. Poncet and J. Deutscher. 1999. Glycerol transport and phosphoenolpyruvate-dependent enzyme I- and Hpr-catalyzed phosphorylation of glycerol kinase in *Thermus flavus*. **Microbiology.** 145: 3205–3212.

Darlington, W. A. 1964. Aerobic hydrocarbon fermentation: A practical evaluation. **Biotech. Bioeng.** 6 (2): 241-242.

Deckwer, W. D. 1995. Microbial conversion of glycerol to 1,3-propanediol. **FEMS Microbiol. Rev.** 16: 143-149.

DeLisa, M. P., J. Li, R. Govind, A. W. William, and E. B. William. 1999. Monitoring GFP-operon fusion protein expression during high cell density cultivation of *Escherichia coli* using an on-line optical sensor. **Biotechnol. Bioeng.** 65: 54-64.

Dharmadi, Y. A. Murarka and R. Gonzalez. 2006. Anaerobic fermentation of glycerol by *Escherichia coli*: a new platform for metabolic engineering. **Biotechnol. Bioeng.** 94: 821-829.

Doran, P. M. 1995. **Bioprocess engineering principles**. Academic Press, San Diego.

Ensari, S. and J. H. Kim. 2003. Unstructured model for L-lysine fermentation under controlled dissolved oxygen. **Biotechnol. Prog.** 19: 1387-1390.

Forage, R. G. and A. M. Foster. 1982. Glycerol fermentation in *Klebsiella pneumoniae*: functions of the coenzyme B12-dependent glycerol and diol dehydratases. **J. Bacteriol.** 149: 413–419.

Forage, R. G. and C. C. Lin. 1982. DHA system mediating aerobic and anaerobic dissimilation of glycerol in *Klebsiella pneumoniae* NCIB 418. **J. Bacteriol.** 151: 591–599.

Fu, D., A. Libson, L. J. W. Miercke, C. Weitzman, P. Nollert and J. Krucinski. 2000. Structure of a glycerolconducting channel and the basis for its selectivity. **Science.** 290: 481-486.

Gehmlich, I., H. D. Pohl and W. A. Knorre. 1996. Cell harvesting of shear-sensitive genetically engineered *Escherichia coli* with a rotational shear split filter. **Chem. Ing. Tech.** 68: 546–550.

González-Pajuelo, M., I. Meynial-Salles, F. Mendes, P. Soucaille and I. Vasconcelos. 2006. Microbial conversion of glycerol to 1,3-propanediol: physiological comparison of a natural producer, *Clostridium butyricum* VPI 3266 and an engineered strain, *Clostridium acetobutylicum* DG1 (pSPD5). **Appl. Env. Microbiol.** 72: 96-101.

González-Pajuelo, M., J. C. Andrade and I. Vasconcelos. 2005a. Production of 1,3-propanediol by *Clostridium butyricum* VPI 3266 in continuous cultures with high yield and productivity. **J. Ind. Microbiol. Biotech.** 32: 391-396.

González-Pajuelo, M., I. Meynial-Salles, F. Mendes, J. C. Andrade, I. Vasconcelos and P. Soucaille. 2005b. Metabolic engineering of *Clostridium butyricum* for the industrial production of 1,3-propanediol from glycerol. **Metab. Eng.** 7: 329-336.

González-Pajuelo, M., J. C. Andrade and I. Vasconcelos. 2004. Production of 1,3-propanediol by *Clostridium butyricum* VPI 3266 using a synthetic medium and raw glycerol. **J. Ind. Microbiol. Biotech.** 31: 6-442.

Gu, K. F., and T. M. Chang. 1990. Conversion of ammonia or urea into essential amino acids, L-leucine, L-valine, and L-isoleucine using artificial cells containing an immobilized multienzyme system and dextran-NAD L-lactic dehydrogenase for coenzyme recycling. **Appl. Biochem. Biotechnol.** 26: 115-124.

Heller, K. B., E. C. C. Lin and T. H. Wilson. 1980. Substrate specificity and transport properties of the glycerol facilitator of *Escherichia coli*. **J. Bacteriol.** 144: 274-278.

Himmi, E. H., A. Bories and F. Barbirato. 1999. Nutrient requirements for glycerol conversion to 1,3- propanediol by *Clostridium butyricum*. **Bioresour. Technol.** 67: 123–128.

Hirose, Y. and H. Shibai. 1980. Amino acid fermentation. **Biotechnol. Bioeng.** 22: 111-125.

Hochfeld, W. L. 2006. **Producing biomolecular substances with fermentors, bioreactor, and biomolecular synthesizers.** Taylor & Francis, New Jersey.

Holum, J. R. 1982. **Fundamental of general, organic and biological chemistry,** 2nd ed. John Wiley & Sons, Inc., Hoboken, New Jersey.

Homann, T., C. Tag, H. Biebl., W. D. Deckwer and B. Schink. 1990. Fermentation of glycerol to 1,3-propanediol by Klebsiella and Citrobacter strains. **Appl. Microbiol. Biotech.** 33:121–126.

Hou, C. T. and J. F. Shaw. 2008. **Biocatalysis and bioenergy.** John Wiley & Sons, Inc., Hoboken, New Jersey.

Huanga, W. C., S. J. Chenb and T. L. Chena. 2006. The role of dissolved oxygen and function of agitation in hyaluronic acid fermentation. **Biochem. Eng. J.** 32: 239-243.

Hua, Q. and K. Shimizu. 1999. Effect of dissolved oxygen concentration on the intercellular flux distribution for pyruvate fermentation. **J. Biotechnol.** 68: 135-147.

Hua, Q., P. C. Fu and K. Shimizu. 1998. Microaerobic lysine fermentation and metabolic flux analysis. **Biochem. Eng. J.** 2: 89-100.

Hummel, W., H. Schutte, E. Schmidt, C. Wandrey, and M. R. Kula. 1987. Isolation of L-phenylalanine dehydrogenase from *Rhodococcus* sp. M4 and its application for the production of L-phenylalanine. **Appl. Microbiol. Biotechnol.** 26: 409-416.

Hummel, W., and M. R. Kula. 1989. Dehydrogenases for the synthesis of chiral compounds. **Eur. J. Biochem**. 184: 1-13.

Imandi, S. B., V. V. R. Bandaru, S. R. Somalanka and H. R. Garapati. 2006. Optimization of medium constituents for the production of citric acid from byproduct glycerol using Doehlert experimental design. **Enzyme and Microb. Technol.** 40: 1367-1372.

Ito, T., Y. Nakashimada, K. Senba, T. Matsui and N. Nishio. 2005. Hydrogen and ethanol production from glycerol-containing wastes discharged after biodiesel manufacturing process. **J. Biosci. Bioeng.** 100: 260–265.

Jeffery, G. H., J. Basset, J. Mendham and R. C. Denney. 1989. **Vogel's textbook of quantitative chemical analysis,** 5th ed. Longman Scientific & Technical, Longman Group UK Limited, England.

Johnson, M. J. 1964. Utilization of hydrocarbons by microorganisms. **Chem. Ind.** 36: 1532-1537.

Jensen, E. B., and S. Carlsen. 1990. Production of recombinant human growth hormone in *Escherichia coli* expression of different precursors and physiological-effects of glucose, acetate, and salts. **Biotechnol. Bioeng.** 36: 1-11.

Kamphuis, J., E. M. Meijer, W. H. Boesten, T. Sonke, W. J. van den Tweel and H. E. Schoemaker. 1992. New developments in the synthesis of natural and unnatural amino acids. **Ann. NY Acad. Sci.** 672: 510-527.

Kaster, J. A., D. J. Michelsen, and W. H. Velander. 1990. Increased oxygen transfer in a yeast fermentation using a microbubble dispersion. **Appl. Biochem. Biotechnol.** 24 (25): 469-484.

Kwak, K. O., S. J. Jung, S. Y. Chung, C. M. Kang, Y. I. Huh and S. O. Bae. 2006. Optimization of culture conditions for CO_2 fixation by a chemoautotrophic microorganism, strain YN-1 using factorial design. **Biochem. Eng. J.** 31: 1-7.

Lazic, Z. R. 2004. **Design of experiments in chemical engineering: A Practical Guide.** Wiley-Vch Verlag GmbH & Co. KGaA, U.S.A.

Lee, S. Y. 1996. High cell density culture of *Escherichia coli*. **Trends Biotechnol.** 14: 98-105.

Leuchtenberger, W., K. Huthmacher and K. Drauz. 2005. Biotechnological production of amino acids and derivatives: current status and prospects. **Appl. Microbiol. Biotechnol.** 69: 1-8.

Luers, F., M. Seyfried, R. Daniel and G. Gottschalk. 1997. Glycerol conversion to 1,3-propanediol by *Clostridium pasteurianum*: cloning and expression of the gene encoding 1,3- propanediol dehydrogenase. **FEMS Microbiol. Lett.** 154: 337-345.

Luli, G. W. 1988. **The Influence of Glucose Metabolism on High Cell Density Fermentation.** Ph.D. Thesis, Ohio State University.

Macis, L., R. Daniel and G. Gottschalk. 1998. Properties and sequence of the coenzyme B12- dependent glycerol dehydratase of *Clostridium pasteurianum*. **FEMS Microbiol. Lett.** 164: 21-28.

Malaoui, H and R. Marczak. 2001. Separation and characterization of the 1,3-propanediol and glycerol dehydrogenase activities from *Clostridium butyricum* E5 wild-type and mutant D. **J. Appl. Microbiol.** 90: 1006-1014.

Marchetti, J. M., V. U. Miguel and A. F. Errazu. 2007. Possible methods for biodiesel production. **Renewable and Sustainable Energy Reviews.** 11: 1300-1311.

Mateles, R. I. 1971. Calcullation of the oxygen required for cell production. **Biotechnol. Bioeng.** 13: 581-582.

McNeil, B. and L. M. Harvey. 2008. **Practical fermentation technology.** John Wiley & Sons, Inc., Hoboken, New Jersey.

Menzel, K., A. P. Zeng and W. D. Deckwer. 1997. Enzymatic evidence for an involvement of pyruvate dehydrogenase in the anaerobic glycerol metabolism of *Klebsiella pneumoniae*. **J. Biotechnol.** 56: 135–142.

Mizutani, S., H. Mori, S. Shimizu, K. Sakaguchi, and T. Kobayashi. 1986. Effect of amino acid supplement on cell yield and gene product in *Escherichia coli* harboring plasmid. **Biotechnol. Bioeng.** 28: 204-209.

Motarjemi, M., and G. J. Jameson. 1978. Mass transfer from very small bubbles-the optimum bubble size for aeration. **Chem. Eng. Sci**. 33 (11): 1415-1423.

Mu, Y., H. Teng, D. J. Zhang, W. Wang and Z. L. Xiu. 2006. Microbial production of 1,3-propanediol by *Klebsiella pneumoniae* using crude glycerol biodiesel preparations. **Biotechnol. Lett.** 28: 9-1755.

Myers, R. H. and D. C. Montgomery. 2002. **Response surface methodology: Process and product optimization using designed experiment.** 2nd ed. John Wiley and Sons, Inc., New Jersey.

Najafpour, G. D. 2007. **Biochemical engineering and biotechnology.** Elsevier, Amsterdam, Netherland.

Nakamichi, K., K. Nabe, Y. Nishida and T. Tosa. 1989. Production of L-phenylalanine from phenylpyruvate by *Paracoccus denitrificans* containing aminotransferase activity. **Appl. Microbiol. Biotechnol.** 30: 243-246.

Naviglio, D., R. Romano, F. Pizzolongo, A. Santini, A. D. Vito, L. Schiavo, G. Nota and S.S. Musso. 2007. Rapid determination of esterified glycerol and glycerides in triglyceride fats and oils by means of periodate method after transesterrification. **Food Chem.** 102: 399-405.

Németh, A., B. Kupcsulik and B. Sevella. 2003. 1,3-Propanediol oxidoreductase production with *Klebsiella pneumoniae* DSM2026. **World J. Microbiol. Biotechnol.** 19: 659–663.

Nikerel, I. E., E. Oner, B. Kirdar and R. Yildirim. 2006. Optimization of medium composition for biomass production of recombinant *Escherichia coli* cells using response surface methodology. **Biochem. Eng. J.** 32: 1-6.

Ohshima, T. and K. Soda. 1989. Thermostable amino acid dehydrogenases: applications and gene cloning Trends. **Biotechnology.** 7: 210-214.

Packdibamrung, K., S. Sittipraneed, S. Nagata and H. Misono. 2007. Amino acid dehydrogenases from thermotolerant bacteria, pp. 75-76. **Summary Book: JSPS-NRCT Core University Program (1998-2008) on development of thermotolerant microbial resources and their applications**. Bangkok.

Papanikolaou, S., L. Muniglia, I. Chevalot, G. Aggelis and I. Marc. 2002. *Yarrowia lipolytica* as a potential producer of citric acid from raw glycerol. **J. Appl. Microbiol.** 92: 44-737.

Park, Y. S., K. Kai, S. J. Lijima, and T. Kobayashi. 1992. Enhanced β-Galactosidase Production by High Cell-Density Culture of Recombinant *Bacillus subtilis* with Glucose Concentration Control. **Biotechnol. Bioeng.** 40: 686-696.

Paula da Silva, G., M. Mack and J. Contiero. 2009. Glycerol: A promising and abundant carbon source for industrial microbiology. **Biotechnology Advance.** 27: 30-39.

Prakash, G. V. S. B., V. Padmaja and R. R. S. Kiran. 2007. Statistical optimization of process variables for the large-scale production of *Metarhizium anisopliae* conidiospores in solid-state fermentation. **Bioresource Technol.** 99: 1530-1537.

Rao, D. G. 2005. **Introduction to biochemical engineering**. Tata McGrew-Hell Publishing Limited, New Delhi, India.

Raynaud, C., P. Sarçabal, I. Meynial-Salles, C. Croux and P. Soucaille. 2003. Molecular characterization of the 1,3-propanediol (1,3-PD) operon of *Clostridium butyricum*. **Proc. Natl. Acad. Sci.** 100: 5010–5015.

Righelato, R. C., A. P. J. Trinci, S. J. Pirt and A. Peat. 1968. Influence of maintenance energy and growth rate on the metabolic activity, morphology and conidiation of *Penicillium chrysogenum*. **J. Gen. Micro.** 50(1): 394-412.

Robbins, J. W., and K. B. Taylor. 1989. Optimization of *Escherichia coli* Growth by Controlled Addition of Glucose. **Biotechnol. Bioeng.** 34: 1289-1294.

Ruch, F. E., J. Lengeler and C. C. Lin. 1974. Regulation of glycerol catabolism in *Klebsiella aerogenes*. **J. Bacteriol.** 119: 50-56.

Saint-Amans, S., L. Girbal, J. Andrade, K. Ahrens and P. Soucaille. 2001. Regulation of carbon and electron flow in *Clostridium butyricum* VPI 3266 grown on glucose-glycerol mixtures. **J. Bacteriol.** 183: 1748–1754.

Seifert, C., S. Bowien, G. Gottschalk and R. Daniel. 2001. Identification and expression of the genes and purification and characterization of the genes products involved in reactivation of coenzyme B12-dependent glycerol dehydratase of *Citrobacter freundii*. **Eur. J. Biochem.** 268: 2369-2378.

Sitthai, P. 2004. **Cloning and expression of phenylalanine dehydrogenase gene from *Acinetobacter lwoffii* and the possibility for amino acid production.** M.S. Thesis, Chulalongkorn University.

Skraly, F. A., B. L. Lytle and D. C. Cameron. 1998. Construction and characterization of a 1,3-propanediol operon. **Appl. Env. Microbiol.** 64: 98-105.

Snay, J., J. W. Jeong, and M. M. Ataai. 1989. Effects of growth conditions on carbon utilization and organic by-product formation in *B. subtilis*. **Biotechnol. Progr.** 5: 63-69.

Stanbury, P. F., A. Whitaker and S. J. Hall. 1999. **Principles of fermentation technology.** 2nd ed. MPG Book Ltd., Bodmin, Cornwall, UK.

Stanier, R. Y., M. Doudoroff and E. A. Adelberg. 1976. Adelberg. **The Microbial World.** 3th ed. Prentice Hall, Englewood Cliffs, New Jersey.

Stocchi, V., L. Cucchiarini, G. Piccoli and M. Magnani. 1985. Complete high-performance liquid chromatographic separation of 4-N,N-dimethylaminoazobenzene-4'-thiohydantoin and 4-dimethylaminoazobenzene-4'-sulphonyl chloride amino acids utilizing the same reversed-phase column at room temperature. **J. Chromatography.** 349: 77-82.

Suye, S. I., M. Kawagoe and S. Inuta. 1992. Enzymatic production of L-alanine malic acid with malic enzyme and alanine dehydrogenase with coenzyme regeneration. **Can. J. Biochem. Eng.** 34: 306-312.

Talarico, T. L., L. T. Axelsson, J. Novotny, M. Fiuzat and W. J. Dobrogosz. 1990. Utilization of glycerol as a hydrogen acceptor by *Lactobacillus reuteri*: purification of 1,3-propanediol:NAD+ oxidoreductase. **Appl. Env. Microbiol.** 56: 943-948.

Tang, Y. J. and J. J. Zhong. 2003. Role of oxygen supply in submerged fermentation of *Ganoderma lucidium* for production of Ganoderma poly saccharide and ganoderic acid. **Enzyme Microb. Technol.** 32: 478-484.

Taylor P. P., D. P. Pantaleone, R. F. Senkpeil, and I. G. Fotheringham. 1998. Novel biosynthetic approaches to the production of unnatural amino acids using aminotransferase. **Trends Biotechnol.** 16: 412–418.

The Department of Alternative Energy Development and Efficiency (DEDE). 2009. **Biodiesel**. Available Source: http://www.dede.go.th/dede/index.php?id=351, January 27, 2009.

The National Energy Policy Office (NEPO). 2001. Thailand's Energy Situation 2001. **NEPO Journal**. 53: 53-113.

Thomson, B. G., M. Kole, and D. F. Gerson. 1985. Control of ammonium concentration in *Escherichia coli* fermentation. **Biotechnol. Bioeng.** 27: 818-824.

Tong, I. T., H. H. Liao and D. C. Cameron. 1991. 1,3-propanediol production by *Escherichia coli* expressing genes from the *Klebsiella pneumoniae* dha regulon. **Appl. Env. Microbiol.** 57: 3541–3546.

Toraya, T., S. Honda, S. Kuno and S. Fukui. 1980. Distribution of coenzyme B12-dependent diol dehydratase and glycerol dehydratase in selected genera of Enterobacteriaceae and Propionibacteriaceae. **J. Bacteriol.** 141: 1439-1442.

Toraya, T., S. Honda, S. Kuno and S. Fukui. 1978. Coenzyme B12-dependent diol dehydratase: Regulation of apoenzyme synthesis in *Klebsiella pneumoniae* (*Aerobacter aerogenes*) ATCC 8724. **J. Bacteriol.** 135: 726-729.

Unden, G. and J. Bongaerts. 1997. Alternative respiratory pathways of *Escherichia coli*: energetic and transcriptional regulation in response to electron acceptors. **Biochem. Biophys. Acta.** 1320: 217-234.

vande Walle, M., and J. Shiloach. 1998. Proposed mechanism of acetate accumulation in two recombinant *Escherichia coli* strains during high density fermentation. **Biotechnol. Bioeng.** 57: 71-78.

Van't Riet, K. and S. Van. 1992. Foaming, mass transfer and mixing: Interrelations in large scale fermentations. pp. 189-192. **Harnessing Biotechnology for the 21st Century**. American Chemical Society, U.S.A.

Van't Riet, K. 1979. Review of measuring methods and results in non-viscous gas-liquid mass transfer in stirred vessels. **Ind. Eng. Chem. Process Des. Dev.** 18 (3): 357-360.

Veiga da Cunha, M. and M. A. Foster. 1992. 1,3-propanediol: NAD+ oxidoreductases of *Lactobacillus brevis* and *Lactobacillus buchneri*. **Appl. Env. Microbiol.** 58: 2005-2010.

Vogel, H. C. 1997. **Fermentation and Biochemical Engineering Handbook**, 2nd ed. Noyes Publications, Park Ridge, New Jersey.

Voegele, R. T., G. D. Sweet and W. Boos. 1993. Glycerol kinase of *Escherichia coli* is activated by interaction with the glycerol facilitator. **J. Bacteriol.** 175: 1087-1094.

Vuolanto, A., N. von Weymarn, J. Kerovuo, H. Ojamo, and M. Leisola. 2001. Phytase production by high cell density culture of recombinant *Bacillus subtilis*. **Biotechnol. Lett.** 23: 761-766.

Wang, Y. and Y. Inoue. 2001. Effect of dissolved oxygen concentration in the fermentation medium on transformation of the carbon source during the biosynthesis of poly(3-hydroxybuty rate-co-3-hydroxypropionate) by *Alcaligenes latus*. **Int. J. Biol. Macromol.** 28: 235-243.

Wang, Z. X., J. Zhuge, H. Fang and B. A. Prior. 2001. Glycerol production by microbial fermentation: a review. **Biotechnol. Adv.** 19: 201–223.

Went, R. C. 1979. **Handbook of chemistry and physics**, 60th ed. CRC Press, Boca Raton, Florida.

Willke, T. H. and K. D. Vorlop. 2004. Industrial bioconversion of renewable resources as an alternative to conventional chemistry. **Appl. Microbiol. Biotechnol.** 66: 131-142.

Yamada, S., K. Nabe, N. Izuo, K. Nakamichi and I. Chibata. 1981. Production of L-phenylalanine from *trans*-cinnamic acid with *Rhodotorula glutinis* containing L-phenylalanine ammonialyase activity. **Appl. and Env. Micro.** 42 (5): 773-778.

Yamamoto, K., T. Tosa and I. Chibata. 1980. Continuous production of L-alanine using *Pseudomonas dacungae* immobilization carrageenan. **Biotech. Bioeng.** 22: 2045-2054.

Yee, L., and H. W. Blanch. 1993a. Defined media optimization for growth of recombinant *Escherichia coli* X90. **Biotechnol. Bioeng.** 41: 221-230.

Yee, L., and H. W. Blanch. 1993b. Recombinant trypsin production in high cell density fed-batch cultures in *Escherichia coli*. **Biotechnol. Bioeng.** 41: 781-790.

Yuste, A. J. and M. P. Dorado. 2006. A neural network approach to simulate biodiesel production from waste olive oil. **Energy and Fuels**. 20: 399-402.

Zain, W. S. W. M., R. M. Illias, M. M. Salleh, O. Hassan, R. A. Rahman and A. A. Hamid. 2007. Production of cyclodextrin glucanotransferase from alkalophilic *Bacillus* sp. TS1-1: optimization of carbon and nitrogen concentration in feed medium using central composite design. **Biochem. Eng. J.** 33: 26-33.

Zheng, Z. M., Q. L. Hu, J. Hao, F. Xu, N. N. Guo, Y. Sun and D. H. Liu. 2008. Statistical optimization of culture conditions for 1,3-propanediol by *Klebsiella pneumonia* AC 15 via central composite design. **Bioresource Technol.** 99: 1052-1056.

Zhu, M. M., P. D. Lawman and D. C. Cameron. 2002. Improving 1.3-propanediol production from glycerol in a metabolically engineered *Escherichia coli* by reducing accumulation of sn-glycerol-3-phosphate. **Biotechnol. Prog.** 18: 694-699.

APPENDICES

Appendix A
Media formula

Appendix Table A1 Luria-Bertani (LB) medium

Components	Amount
Peptone	10 g/L
NaCl	10 g/L
Yeast extract	5.0 g/L

* Add deionized water to make solution 1 liter and adjust pH to 7.4 with NaOH. For agar plates, the medium was supplemented with 10-15 g/L agar.

Appendix Table A2 Basal salts, Trace salts and Vitamins solution

Components	Amount
KH_2PO_4	1.0 g/L
K_2HPO_4	1.0 g/L
$MgCl_2$	1.0 g/L
$FeSO_4$	0.002 g/L
$MnSO_4$	0.002 g/L
$CaCl_2$	0.05 g/L
$ZnSO_4$	0.01 g/L
Yeast extract	1.0 g/L
Thiamine-HCl	0.1 g/L

* Add deionized water to make solution 1 liter

Appendix Table A3 Biomass fermentation medium

Components	Amount
Glycerol (99 %)	10.0 g/L
$(NH_4)_2SO_4$	10.0 g/L
KH_2PO_4	2.94 g/L
K_2HPO_4	2.94 g/L
$MgCl_2$	0.98 g/L
$FeSO_4$	0.002 g/L
$MnSO_4$	0.002 g/L
$CaCl_2$	0.05 g/L
$ZnSO_4$	0.01 g/L
Yeast extract	0.878 g/L
Thiamine-HCl	0.0878 g/L

*Add deionized water to make solution 1 liter

Appendix Table A4 L-phenylalanine fermentation medium

Components	Amount
Glycerol (99 %)	10.0 g/L
$(NH_4)_2SO_4$	100.0 g/L
KH_2PO_4	1.91 g/L
K_2HPO_4	1.91 g/L
$MgCl_2$	0.64 g/L
$FeSO_4$	0.002 g/L
$MnSO_4$	0.002 g/L
$CaCl_2$	0.05 g/L
$ZnSO_4$	0.01 g/L
Yeast extract	0.823 g/L
Thiamine-HCl	0.0823 g/L

* Add deionized water to make solution 1 liter

Appendix B
Assay methods

1. L-phenylalanine derivatization method (Stocchi *et al*., 1985)

DASB-Cl derivatives are prepared by adding 50 µl of 1.5M $NaHCO_3$ (pH 9.0), followed by 100 µl of 2 mg/mL dabsyl-chloride in acetone, to each 110 µl aliquot of amino acid standard. The mix was vortexed then heated at 70 °C for 10 minutes. After drying under vacuum, the aliquot is resuspended in 200 µl of 70 % ethanol, centrifuged for 2 minutes at 14000 x g, and transferred to a low volume vial.

2. Glycerol concentration determination method (Naviglio *et al*., 2007)

Reagents, 1. Periodate reagent: dissolve 65 mg of $NaIO_4$ in 90 mL DW, add 10 mL acetic acid, mix and add 7.7 g of ammonium acetate and mix. 2. Acetylacetone reagent: add 2.5 mL of acetylacetone to 245.5 mL of isopropanol, mix and store in the dark.

Procedure, add 1 mL of periodate reagent to the samples and keep 5 minutes at room temperature. Add 2.5 mL acetylacetone reagent, mix and warm 20 minutes at 50 °C. Cool and read absorbance at 410 nm against a reagent blank. Calibrate with known amounts of glycerol (2-50 mg/tube).

Comments, not that glucose and other hexoses give the same color reaction. If glycoside-containing acylglycerols are present, a hydrolysis step with 2M HCl at 100 °C during 1 hour is necessary to cleave glycosidic bond before glycerol analysis.

2. Determination of ammonia (NH_3) in an ammonium salt (Jeffery *et al*., 1989)

In the indirect method, the ammonium salt is boiled with a known excess of standard sodium hydroxide solution. The boiling is continued until on more ammonium escapes with the steam. The excess of sodium hydroxide is titrated with standard acid, using methyl red as indicator.

$$OH^- + NH_4^+ \longrightarrow NH_3 + H_2O$$

Method: Ammonium salt sample solution 10 mL (0.1-0.2 g/L) into a 250 Pyrex flask, and add 10 mL 0.1 M sodium hydroxide and boil the mixture until a piece of filter paper moistened with mercury (I) nitrate solution and held in the escaping steam no longer turned black. Cool the solution, add a few drop of methyl red, and titrate with standard 0.1 M hydrochloric acid. Repeat the determination.

Appendix C
Standard graphs

Appendix Table C1 Biomass concentration calibration data

OD (600 nm)	Biomass concentration (g/L)
0.141	0.180
0.316	0.540
0.605	0.899
0.925	1.439
1.156	1.979

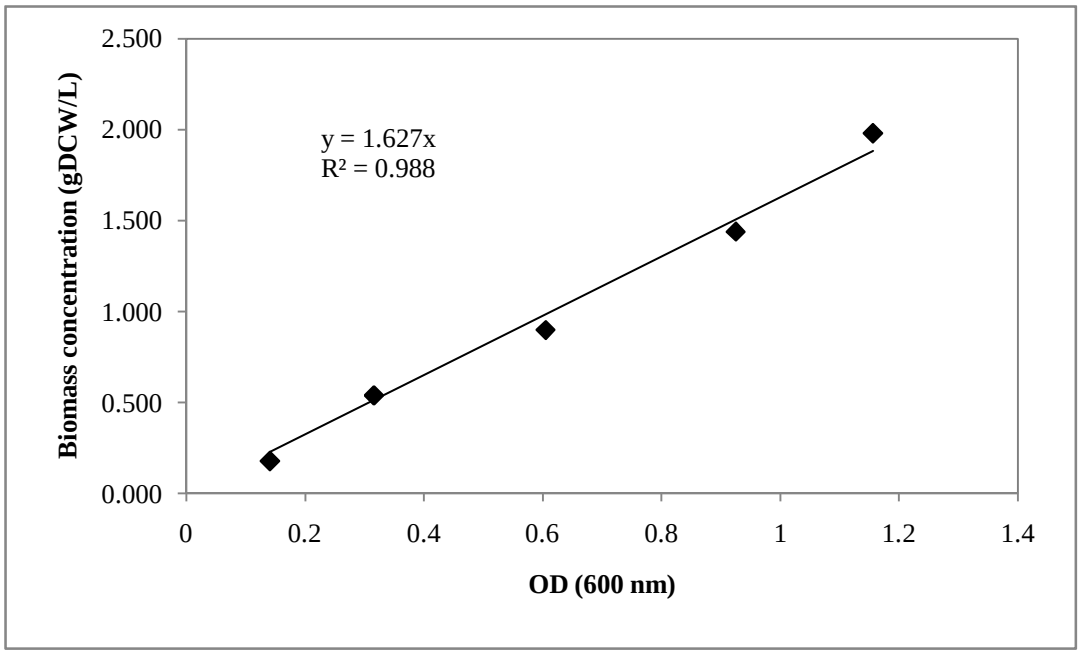

Appendix Figure C1 Biomass concentration calibration curve

Appendix Table C2 L-phenylalanine concentration calibration data

Peak area (x 10^{-5})	L-phenylalanien concentration (g/L)
0	0.000
2.29660	0.125
15.39549	0.250
23.32039	0.750
44.63100	1.000

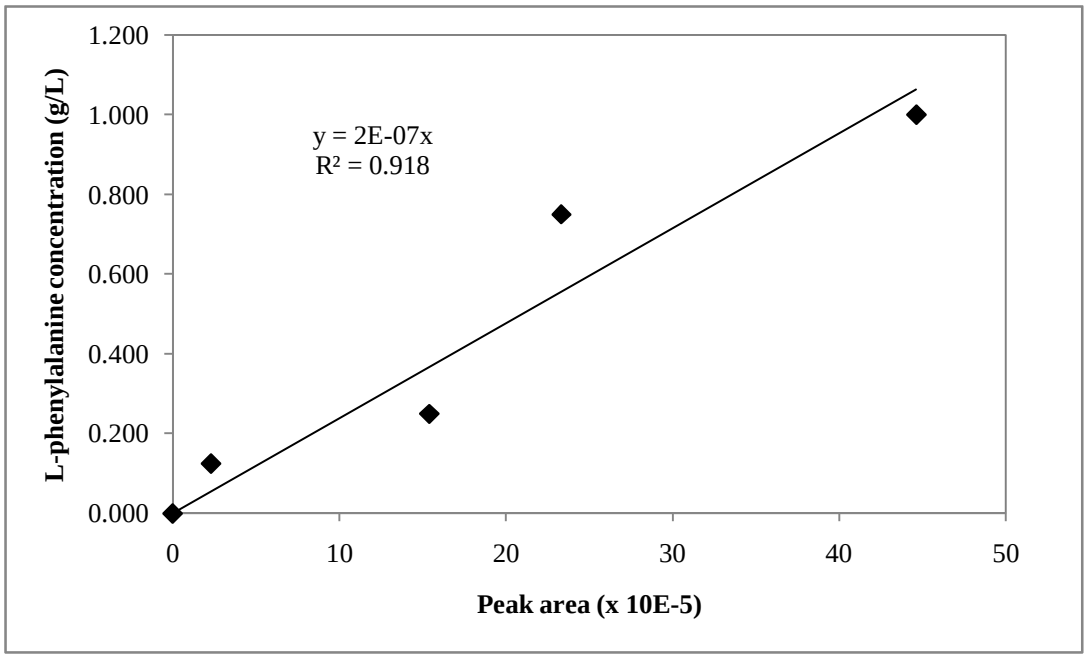

Appendix Figure C2 L-phenylalanine concentration calibration curve

Appendix Table C3 Glycerol concentration calibration data

DO (410 nm)	Glycerol concentration (g/L)
0	0
0.130	0.0075
0.273	0.0150
0.403	0.0225
0.612	0.0300
0.770	0.0375
0.979	0.0450
1.176	0.0525
1.352	0.0600

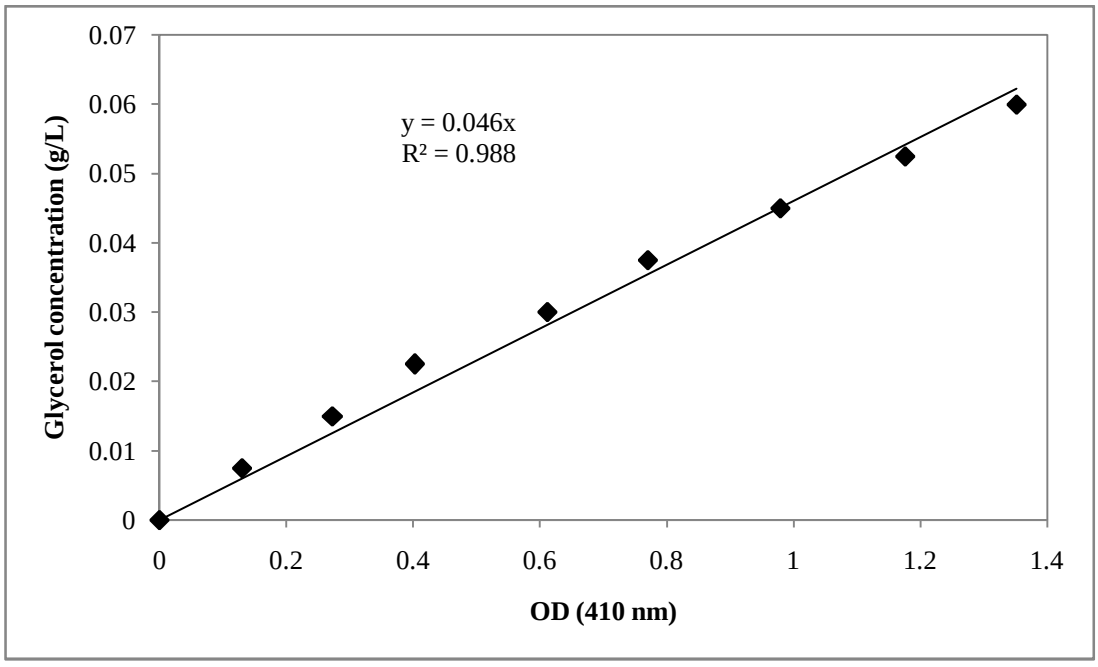

Appendix Figure C3 Glycerol concentration calibration curve

Appendix D

HPLC chromatogram of the L-phenylalanine

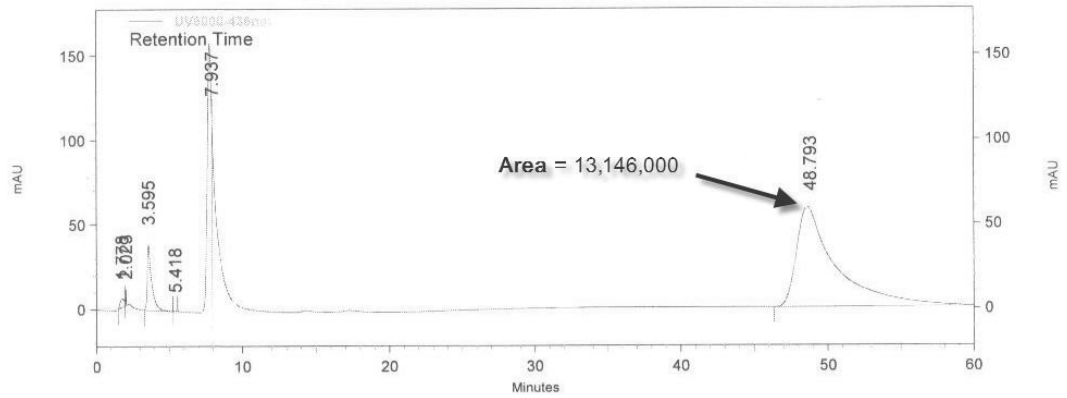

Appendix Figure D1 HPLC chromatogram of the L-phenylalanine production from *E. coli* BL21(DE3) at 0.7 mL/min flow rate and 5 µl injection volume

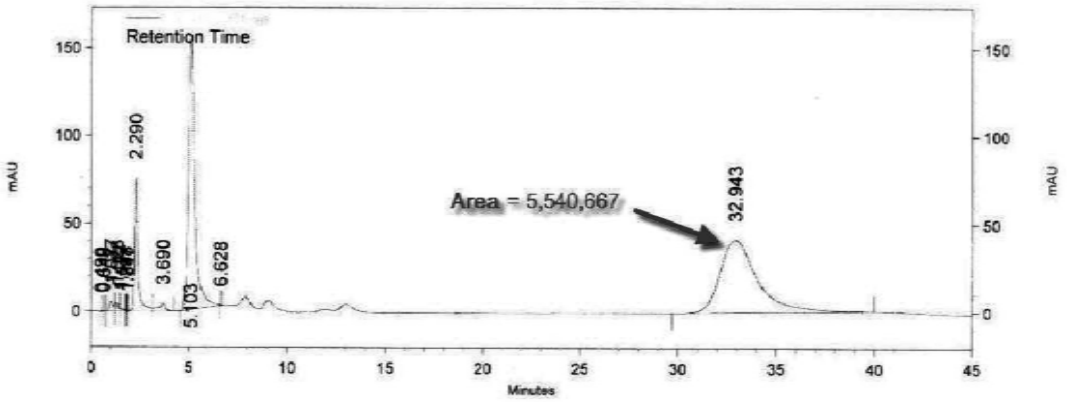

Appendix Figure D2 HPLC chromatogram of the L-phenylalanine production from *E. coli* BL21(DE3) at 1.0 mL/min flow rate and 5 µl injection volume

Appendix E
Bioreactor and instruments

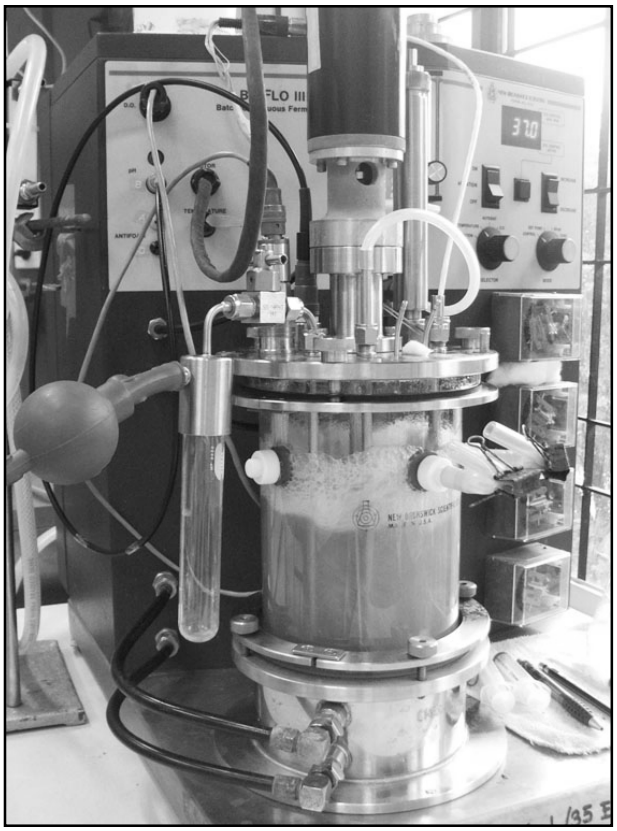

Appendix Figure E1 3.3 L BioFio III reactor (New Brunswick Scientific, USA) with controller

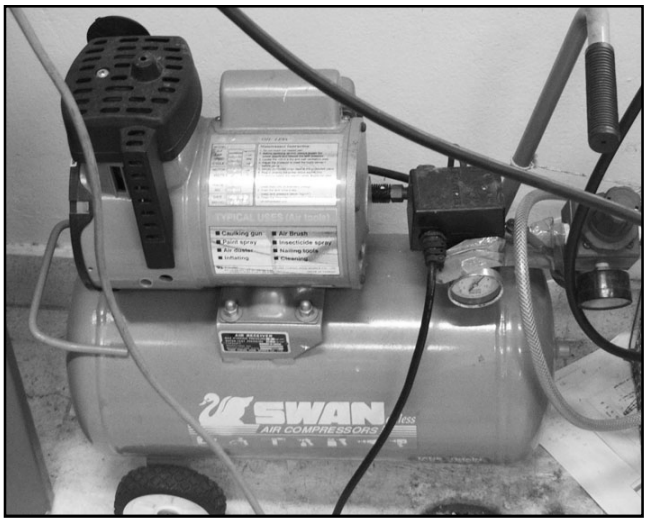

Appendix Figure E2 Air pump

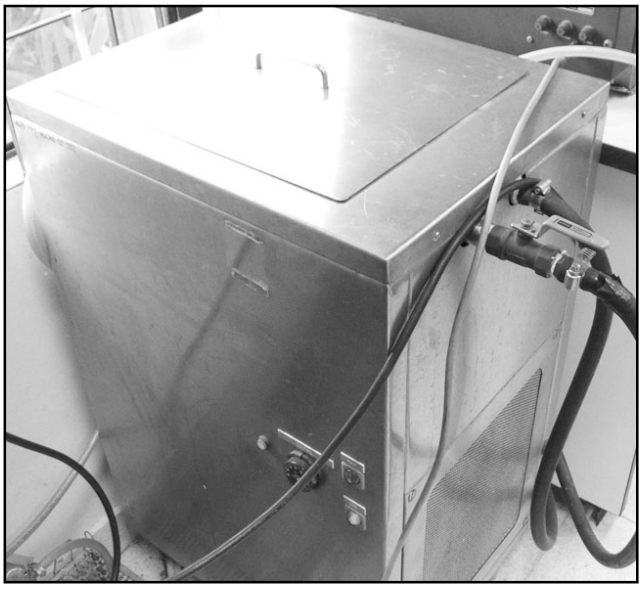

Appendix Figure E3 Water cooler

Appendix F
Raw data

Appendix Table F1 Raw data of screening experiments by one-factor-at -a-time technique (Effect of glycerol concentration)

Glycerol (x10, g/L)	Biomass			Mean (g/L)
	Exp. 1 (g/L)	Exp. 2 (g/L)	Exp. 3 (g/L)	
1.0	0.460	0.450	0.470	0.460
2.0	0.470	0.490	0.495	0.485
3.0	0.610	0.580	0.655	0.615
4.0	0.730	0.760	0.700	0.730
5.0	0.790	0.810	0.725	0.775
6.0	0.800	0.860	0.890	0.850
7.0	0.910	0.940	0.865	0.905
8.0	0.960	1.010	0.871	0.947
9.0	0.700	0.670	0.715	0.695
10.0	0.420	0.430	0.470	0.440

Appendix Table F2 Raw data of screening experiments by one-factor-at -a-time technique (Effect of $(NH4)_2SO_4$ concentration)

$(NH4)_2SO_4$ ($x10^{-1}$ g/L)	Biomass			Mean (g/L)
	Exp. 1 (g/L)	Exp. 2 (g/L)	Exp. 3 (g/L)	
1.0	0.867	0.790	0.855	0.837
2.0	0.895	0.844	0.916	0.885
3.0	1.011	0.995	0.980	0.995
4.0	1.423	1.322	1.284	1.343
5.0	1.454	1.428	1.479	1.454
6.0	1.508	1.596	1.588	1.564
7.0	1.785	1.707	1.626	1.706
8.0	1.817	1.785	1.754	1.785
9.0	0.853	0.903	0.948	0.901
10.0	0.083	0.086	0.092	0.087

Appendix Table F3 Raw data of screening experiments by one-factor-at -a-time technique (Effect of pH)

No.	pH	Biomass			Mean
		Exp. 1 (g/L)	Exp. 2 (g/L)	Exp. 3 (g/L)	(g/L)
1	6.0	1.230	1.190	1.195	1.205
2	6.5	1.370	1.276	1.209	1.285
3	7.0	1.550	1.640	1.427	1.539
4	7.4	1.680	1.790	1.675	1.715
5	8.0	1.600	1.720	1.465	1.595

Appendix Table F4 Raw data of screening experiments by one-factor-at -a-time technique (Effect of temparature)

Temparature	Biomass			Mean
(°C)	Exp. 1 (g/L)	Exp. 2 (g/L)	Exp. 3 (g/L)	(g/L)
30	1.080	1.100	1.015	1.065
37	1.650	1.760	1.645	1.685
45	0.017	0.022	0.018	0.019

Appendix Table F5 Raw data of optimization of fermentation media by RSM

Runs	Biomass (g/L)				L-Phenylalanine (g/L)			
	Exp. 1	Exp. 2	Exp. 3	Mean	Exp. 1	Exp. 2	Exp. 3	Mean
1	4.262	4.418	4.383	4.35	0.997	1.043	1.019	1.02
2	4.538	4.400	4.435	4.445	3.371	3.468	3.559	3.466
3	4.366	4.228	4.280	4.305	2.963	3.525	3.257	3.248
4	5.004	4.832	4.849	4.897	4.152	3.831	4.287	4.09
5	4.659	4.711	4.607	4.659	5.318	6.431	6.189	5.979
6	4.452	4.556	4.521	4.504	2.704	2.525	2.398	2.542
7	4.521	4.538	4.469	4.504	3.827	3.906	3.598	3.777
8	4.746	4.832	4.815	4.798	5.165	5.318	4.538	5.007
9	4.038	4.090	3.969	4.038	5.894	6.283	5.016	5.731
10	4.815	4.746	4.849	4.794	2.048	2.033	2.426	2.169
11	4.383	4.418	4.400	4.397	2.953	3.087	3.382	3.141
12	4.400	4.504	4.418	4.44	3.963	4.525	4.053	4.18
13	4.418	4.521	4.435	4.452	3.863	3.325	3.028	3.405
14	4.435	4.418	4.521	4.452	3.207	3.625	3.573	3.468
15	4.487	4.504	4.469	4.487	0.980	0.843	0.970	0.931
16	4.055	4.073	4.107	4.073	3.547	3.059	3.354	3.32
17	4.297	4.383	4.211	4.288	3.360	3.676	3.548	3.528
18	4.418	4.349	4.366	4.383	2.217	2.144	2.473	2.278
19	4.297	4.366	4.314	4.34	4.271	4.525	4.671	4.489
20	4.366	4.418	4.331	4.366	3.963	3.525	4.462	3.983
21	4.452	4.487	4.452	4.469	5.366	6.328	5.202	5.632
22	4.418	4.366	4.349	4.383	3.627	3.525	3.957	3.703
23	5.022	4.953	4.970	4.987	5.401	6.431	5.796	5.876
24	4.383	4.331	4.314	4.357	1.859	1.968	1.616	1.814
25	5.160	5.056	5.073	5.082	1.846	1.330	1.816	1.664
26	4.901	4.918	4.953	4.92	3.809	3.307	3.420	3.512
27	4.659	4.625	4.521	4.607	1.967	1.598	1.422	1.662
28	4.314	4.159	4.245	4.245	1.885	1.660	1.964	1.836
29	4.642	4.538	4.625	4.604	2.972	3.518	2.908	3.133
30	4.659	4.487	4.607	4.589	3.963	3.525	4.345	3.944
31	4.073	4.004	4.038	4.031	3.547	3.399	3.641	3.529

Appendix Table F6 Raw data of optimization for agitation rate in batch fermentation (Aeration rate was fixed at 4.0 L/min.)

Agitation rate was fixed at 200 rpm.															
Time	Biomass (g/L)			L-phenylalanine (g/L)			Glycerol (g/L)			$(NH_4)_2SO_4$ (g/L)			Dissolved Oxygen (DO; %)		
(h)	exp. 1	exp. 2	exp. 3	exp. 1	exp. 2	exp. 3	exp. 1	exp. 2	exp. 3	exp. 1	exp. 2	exp. 3	exp. 1	exp. 2	exp. 3
0	0.097	0.099	0.103	0.000	0.000	0.000	11.050	10.470	10.610	50.050	49.540	48.910	100.000	100.000	100.000
12	2.440	2.379	2.321	2.297	2.290	2.373	8.770	8.350	8.590	37.880	33.000	27.880	32.000	30.500	35.000
24	4.588	4.497	4.595	2.670	2.691	2.709	7.840	7.440	8.390	30.510	25.090	17.870	-4.200	-2.000	-4.000
36	5.290	5.350	5.380	2.870	2.779	2.871	4.160	4.090	3.810	27.150	23.900	25.480	-2.200	-3.700	-3.550
48	5.600	5.570	5.510	2.801	2.762	2.747	1.100	1.050	0.910	26.890	27.950	27.030	-2.000	-1.000	-2.300
60	5.041	5.110	5.089	2.520	2.611	2.459	0.970	1.020	0.800	27.050	28.770	28.210	50.400	46.940	53.260
72	4.704	4.810	4.796	2.461	2.522	2.397	0.990	1.070	1.240	28.000	29.750	29.370	109.400	110.600	113.600
Agitation rate was fixed at 300 rpm.															
Time	Biomass (g/L)			L-phenylalanine (g/L)			Glycerol (g/L)			$(NH_4)_2SO_4$ (g/L)			Dissolved Oxygen (DO; %)		
(h)	exp. 1	exp. 2	exp. 3	exp. 1	exp. 2	exp. 3	exp. 1	exp. 2	exp. 3	exp. 1	exp. 2	exp. 3	exp. 1	exp. 2	exp. 3
0	0.098	0.101	0.100	0.000	0.000	0.000	10.220	10.780	11.070	49.000	49.870	48.850	100.000	100.000	100.000
12	3.071	3.201	3.178	2.260	2.302	2.278	7.050	7.500	7.080	31.840	33.420	28.040	21.700	20.000	22.500
24	4.900	4.990	5.020	3.990	3.974	3.946	3.330	3.420	3.180	24.520	23.040	23.210	-2.700	-3.400	-6.800
36	5.390	5.402	5.288	4.191	4.311	4.128	1.850	1.990	1.920	20.300	21.000	22.540	41.500	44.700	44.600
48	5.490	5.554	5.516	3.600	3.594	3.636	1.320	1.590	1.560	19.110	20.040	18.150	98.440	97.500	96.260
60	5.590	5.477	5.433	3.422	3.442	3.306	1.220	1.420	1.290	21.050	20.980	18.180	97.000	97.000	94.300
72	5.647	5.700	5.573	3.110	3.222	3.148	0.800	0.750	0.790	25.870	24.860	24.510	103.400	100.400	100.700

Appendix Table F6 (Continued)

Agitation rate was fixed at 400 rpm.

Time	Biomass (g/L)			L-phenylalanine (g/L)			Glycerol (g/L)			$(NH_4)_2SO_4$ (g/L)			Dissolved Oxygen (DO; %)		
(h)	exp. 1	exp. 2	exp. 3	exp. 1	exp. 2	exp. 3	exp. 1	exp. 2	exp. 3	exp. 1	exp. 2	exp. 3	exp. 1	exp. 2	exp. 3
0	0.098	0.101	0.099	0.000	0.000	0.000	10.090	10.290	10.880	50.790	50.050	50.630	100.000	100.000	100.000
12	3.831	3.690	3.699	2.370	2.400	2.370	8.150	8.370	8.140	40.040	38.560	38.220	4.140	3.940	3.620
24	5.297	5.364	5.359	4.350	4.411	4.169	3.420	3.250	3.170	21.000	19.600	22.760	-1.510	-1.000	-0.790
36	5.495	5.402	5.423	4.570	4.710	4.550	2.100	1.890	1.710	20.500	19.000	23.530	79.770	80.000	81.430
48	5.400	5.330	5.380	4.910	4.880	5.000	1.590	1.390	1.490	23.400	23.030	25.180	78.000	83.000	72.400
60	5.160	5.091	5.109	3.692	3.771	3.667	1.100	1.220	1.370	25.000	24.550	23.170	80.000	80.400	86.500
72	4.823	4.900	4.797	3.440	3.390	3.430	1.320	1.470	1.890	29.860	27.990	27.290	81.900	80.990	84.910

Agitation rate was fixed at 500 rpm.

Time	Biomass (g/L)			L-phenylalanine (g/L)			Glycerol (g/L)			$(NH_4)_2SO_4$ (g/L)			Dissolved Oxygen (DO; %)		
(h)	exp. 1	exp. 2	exp. 3	exp. 1	exp. 2	exp. 3	exp. 1	exp. 2	exp. 3	exp. 1	exp. 2	exp. 3	exp. 1	exp. 2	exp. 3
0	0.098	0.100	0.102	0.000	0.000	0.000	10.210	10.110	10.160	49.990	50.830	51.250	100.000	100.000	100.000
12	2.960	2.891	2.939	0.530	0.510	0.520	7.010	7.550	7.850	31.750	30.000	28.520	47.000	49.000	43.200
24	5.073	5.110	5.027	0.730	0.705	0.755	1.680	1.430	1.480	21.550	20.400	23.300	66.940	70.110	69.950
36	4.810	4.880	4.650	1.390	1.330	1.330	1.440	1.390	1.400	22.990	20.080	25.840	67.000	63.000	59.600
48	4.251	4.199	4.270	1.691	1.754	1.715	1.320	1.120	1.220	24.500	25.900	21.750	61.460	60.100	59.340
60	4.240	4.179	4.391	1.552	1.606	1.552	1.210	1.090	1.210	29.950	32.000	28.500	64.060	66.000	62.540
72	4.340	4.300	4.260	1.412	1.390	1.398	1.110	1.000	1.160	30.420	31.500	31.290	69.010	68.440	65.950

Appendix Table F7 Raw data of optimization for aeration rate in batch fermentation (Agitation rate was fixed at 400 rpm.)

Aeration rate was fixed at 2.0 L/min.															
Time	Biomass (g/L)			L-phenylalanine (g/L)			Glycerol (g/L)			$(NH_4)_2SO_4$ (g/L)			Dissolved Oxygen (DO; %)		
(h)	exp. 1	exp. 2	exp. 3	exp. 1	exp. 2	exp. 3	exp. 1	exp. 2	exp. 3	exp. 1	exp. 2	exp. 3	exp. 1	exp. 2	exp. 3
0	0.098	0.100	0.092	0.000	0.000	0.000	10.050	10.890	10.080	50.770	51.000	49.100	100.000	100.000	100.000
12	2.990	2.880	3.040	1.144	1.190	1.116	6.010	5.730	6.200	34.500	32.200	29.870	41.700	44.900	43.900
24	4.860	4.940	4.900	2.040	2.120	1.990	1.670	1.880	2.090	24.770	22.070	24.440	-2.800	-3.100	-2.800
36	4.500	4.670	4.540	2.020	2.012	2.043	1.300	1.650	1.340	22.040	21.990	20.260	43.900	48.000	43.700
48	4.182	4.110	4.188	2.010	2.000	1.990	1.000	1.250	1.260	21.250	21.500	18.630	87.510	90.040	89.750
60	3.790	3.880	4.000	1.610	1.580	1.610	0.920	1.050	1.120	20.650	19.220	20.430	89.040	91.200	89.520
72	3.554	3.690	3.436	1.400	1.350	1.450	0.960	1.150	1.070	20.890	19.200	22.280	91.000	95.800	85.600
Aeration rate was fixed at 4.0 L/min.															
Time	Biomass (g/L)			L-phenylalanine (g/L)			Glycerol (g/L)			$(NH_4)_2SO_4$ (g/L)			Dissolved Oxygen (DO; %)		
(h)	exp. 1	exp. 2	exp. 3	exp. 1	exp. 2	exp. 3	exp. 1	exp. 2	exp. 3	exp. 1	exp. 2	exp. 3	exp. 1	exp. 2	exp. 3
0	0.098	0.100	0.097	0.000	0.000	0.000	11.000	10.850	10.730	50.050	51.550	52.240	100.000	100.000	100.000
12	3.440	3.310	3.300	2.220	2.210	2.320	7.010	6.500	6.860	30.840	33.020	29.200	24.220	26.000	23.280
24	5.643	5.500	5.777	4.090	4.210	4.300	2.700	2.200	2.660	23.200	20.500	17.680	-3.910	-4.000	-5.290
36	5.340	5.420	5.410	4.640	4.660	4.500	2.050	1.700	1.860	21.300	18.750	23.160	49.900	54.550	55.750
48	4.849	4.790	4.911	4.880	4.800	4.870	1.260	1.030	1.310	20.270	19.040	24.050	55.400	57.900	55.600
60	4.700	4.660	4.830	4.770	4.690	4.790	1.090	0.950	1.290	21.000	19.980	21.810	57.900	62.900	56.410
72	4.486	4.500	4.484	4.370	4.610	4.670	0.980	0.900	1.300	21.870	20.560	18.950	61.700	63.100	55.500

Appendix Table F7 (Continued)

Aeration rate was fixed at 6.0 L/min.

Time (h)	Biomass (g/L)			L-phenylalanine (g/L)			Glycerol (g/L)			$(NH_4)_2SO_4$ (g/L)			Dissolved Oxygen (DO; %)		
	exp. 1	exp. 2	exp. 3	exp. 1	exp. 2	exp. 3	exp. 1	exp. 2	exp. 3	exp. 1	exp. 2	exp. 3	exp. 1	exp. 2	exp. 3
0	0.100	0.099	0.095	0.000	0.000	0.000	11.000	10.580	11.180	51.600	50.050	50.600	100.000	100.000	100.000
12	4.020	3.971	4.069	2.070	1.990	1.940	6.050	5.050	4.020	33.330	34.950	33.750	42.740	46.200	47.560
24	5.700	5.510	5.710	3.881	3.796	3.873	1.300	1.000	1.030	25.000	22.190	26.070	-2.100	-1.000	-2.900
36	5.640	5.592	5.568	3.999	4.100	4.126	1.550	1.200	1.420	27.800	26.520	20.740	63.600	60.220	63.080
48	5.556	5.555	5.599	4.277	4.310	4.163	2.020	1.540	1.480	28.770	27.000	23.430	87.000	85.400	88.000
60	5.401	5.500	5.329	4.377	4.571	4.552	1.350	1.170	0.810	26.520	27.500	30.790	89.200	86.900	86.100
72	5.322	5.410	5.258	4.590	4.688	4.822	1.300	1.070	1.230	28.380	29.900	34.780	90.000	87.710	86.890

Aeration rate was fixed at 8.0 L/min.

Time (h)	Biomass (g/L)			L-phenylalanine (g/L)			Glycerol (g/L)			$(NH_4)_2SO_4$ (g/L)			Dissolved Oxygen (DO; %)		
	exp. 1	exp. 2	exp. 3	exp. 1	exp. 2	exp. 3	exp. 1	exp. 2	exp. 3	exp. 1	exp. 2	exp. 3	exp. 1	exp. 2	exp. 3
0	0.099	0.096	0.100	0.000	0.000	0.000	11.050	10.900	10.900	52.220	51.000	52.990	100.000	100.000	100.000
12	4.990	5.200	5.230	1.000	0.969	1.031	5.300	5.960	3.830	39.570	37.470	36.090	40.900	39.060	37.040
24	5.592	5.550	5.568	2.200	2.140	2.260	1.900	2.450	2.010	33.000	32.300	28.720	83.040	79.100	78.160
36	5.490	5.500	5.570	4.054	3.972	3.824	1.550	1.440	1.210	30.400	28.750	33.610	77.200	73.000	72.400
48	5.407	5.440	5.383	4.930	4.666	4.879	1.400	1.350	1.810	28.550	26.500	33.750	70.000	65.200	68.500
60	5.210	5.000	5.000	5.387	5.302	5.361	1.180	1.220	1.470	30.950	32.000	36.770	68.300	64.600	68.700
72	4.740	4.810	4.550	5.601	5.521	5.528	1.090	1.540	1.570	35.610	38.610	40.620	62.410	64.000	67.390

Appendix Table F8 Raw data comparison of biomass and L-phenylalanine production during batch fermentation under optimized medium by RSM and basal medium

Time (h)	Basal medium						RSM							
	Biomass (g/L)			L-phenylalanine (g/L)			Biomass (g/L)				L-phenylalanine (g/L)			
	Ex.1	Ex.2	Mean	Ex.1	Ex.2	Mean	Ex.1	Ex.2	Ex.3	Mean	Ex.1	Ex.2	Ex.3	Mean
0	0.010	0.009	0.010	0.000	0.000	0.000	0.097	0.099	0.103	0.100	0.000	0.000	0.000	0.000
12	1.340	1.380	1.360	0.110	0.150	0.120	2.440	2.379	2.321	2.380	2.297	2.290	2.373	2.320
24	2.090	2.290	2.190	0.410	0.320	0.370	4.588	4.497	4.595	4.560	2.670	2.691	2.709	2.690
36	2.780	2.900	2.840	0.750	0.870	0.890	5.290	5.350	5.380	5.340	2.870	2.779	2.871	2.840
48	2.950	2.870	2.910	0.940	1.000	1.050	5.600	5.570	5.510	5.560	2.801	2.762	2.747	2.770
60	2.900	2.960	2.930	0.900	0.890	0.980	5.041	5.110	5.089	5.080	2.520	2.611	2.459	2.530
72	2.920	2.960	2.940	0.780	0.630	0.770	4.704	4.810	4.796	4.770	2.461	2.522	2.397	2.460

Appendix Table F9 Raw data of fed-batch fermentation

Time	sequence	Biomass (g/L)			L-phenylalanine (g/L)			Glycerol (g/L)			$(NH_4)_2SO_4$ (g/L)			Dissolved Oxygen (DO; %)		
(h)		exp. 1	exp. 2	exp. 3	exp. 1	exp. 2	exp. 3	exp. 1	exp. 2	exp. 3	exp. 1	exp. 2	exp. 3	exp. 1	exp. 2	exp. 3
0	-	0.160	0.150	0.140	0.000	0.000	0.000	10.857	9.757	11.657	11.780	11.900	11.960	100.000	100.000	100.000
12.5	Befor	4.990	5.200	5.320	0.580	0.620	0.600	2.927	2.957	3.107	7.720	7.900	8.140	48.000	52.500	52.500
12.5	After	4.990	5.200	5.320	0.580	0.620	0.600	6.214	5.874	5.954	109.500	101.200	104.120	48.000	52.500	52.500
23	Befor	5.650	6.180	6.170	4.900	5.150	4.980	3.525	3.925	3.425	83.880	90.100	91.340	51.220	57.760	59.920
23	After	5.650	6.180	6.170	4.900	5.150	4.980	8.335	9.035	9.435	83.880	90.100	91.340	51.220	57.760	59.920
36	Befor	6.120	6.340	6.050	5.330	5.750	5.390	8.166	7.466	7.066	70.500	73.490	79.750	54.000	58.200	58.500
36	After	6.120	6.340	6.050	5.330	5.750	5.390	13.955	12.355	13.755	70.500	73.490	79.750	54.000	58.200	58.500
47	Befor	6.200	6.570	6.220	5.810	6.010	5.940	12.000	11.522	13.534	78.300	82.670	84.550	53.110	55.320	59.570
47	After	6.200	6.570	6.220	5.810	6.010	5.940	22.871	20.971	22.818	78.300	82.670	84.550	53.110	55.320	59.570
60	Befor	7.800	8.750	8.440	6.280	6.750	6.470	17.218	16.218	14.174	81.220	87.650	78.630	55.050	56.500	54.050
60	After	7.800	8.750	8.440	6.280	6.750	6.470	32.119	37.119	35.433	81.220	87.650	78.630	55.050	56.500	54.050
72	-	11.12	12.450	10.420	5.750	6.070	5.670	21.895	24.895	25.571	90.750	97.550	98.800	56.000	52.450	55.650

CIRRICULUM VITAE

NAME **:** Mr. Methee Khamduang

BIRTH DATE **:** June 19, 1979

BIRTH PLACE : Ang Thong, Thailand

EDUCATION : YEAR	**INSTITUTE**	**DEGREE/DIPLOMA**
2001	Chulalongkorn Univ.	B.Sc. (Genetics)
2004	Chulalongkorn Univ.	M.Sc. (Biotechnology)
2009	Kasetsart Univ.	D.Eng. (Chemical Engineering)